Functional analysis of human hyaluronan synthase 3 splicing variant 2

Inaugural-Dissertation

zur
Erlangung des Doktorgrades
Dr. rer. nat.

des Fachbereichs
Biologie und Geografie
an der

Universität Duisburg-Essen
vorgelegt von

Guang Dai

aus Liaoning, China
2009

1. Gutachter: Prof. Dr. Jens Fischer
2. Gutachter: Prof. Dr. Michael Ehrmann
Vorsitzender: Prof. Dr. Helmut Esche

Datum der Disputation: 16.12.2009

1. *When a distinguished but elderly scientist states that something is possible, he is almost certainly right. When he states that something is impossible, he is very probably wrong.*
2. *The only way of discovering the limits of the possible is to venture a little way past them into the impossible.*
3. *Any sufficiently advanced technology is indistinguishable from magic.*

Clarke's three laws

to my family

Contents

List of Figures

List of Tables

Chapter 1

Introduction

1.1 Hyaluronan (HA)

Hyaluronan (HA) was first described in 1934 by Mayer and Palmer as a polysaccharide found in vitreous body of bovine eye [Meyer and Palmer 1934]. Hyaluronan belongs to the family of glucosaminoglycans (GAGs). The GAG family is defined by linear carbohydrate polymers consisting of disaccharide units. In proteoglycans, protein cores are posttranslationally modified by glycosyltransferases in the Golgi apparatus, where GAGs are added to protein cores. In contrast to the other GAGs, hyaluronan is not sulfated, lacks the protein core and is synthesized on the plasma membrane [Fraser et al. 1997]. Hyaluronan is synthesized by addition of alternating N-acetylglucosamine and D-glucuronic acid linked by $\beta(1-4)$ and $\beta(1-3)$ bonds (Figure 1.1). In average, hyaluronan consists of approximately 25,000 disaccharide units, which is corresponding to 10 μm extended length [Fessler and Fessler 1966]. Hyaluronan can range in size from 5 to 20,000 kDa *in vivo*.

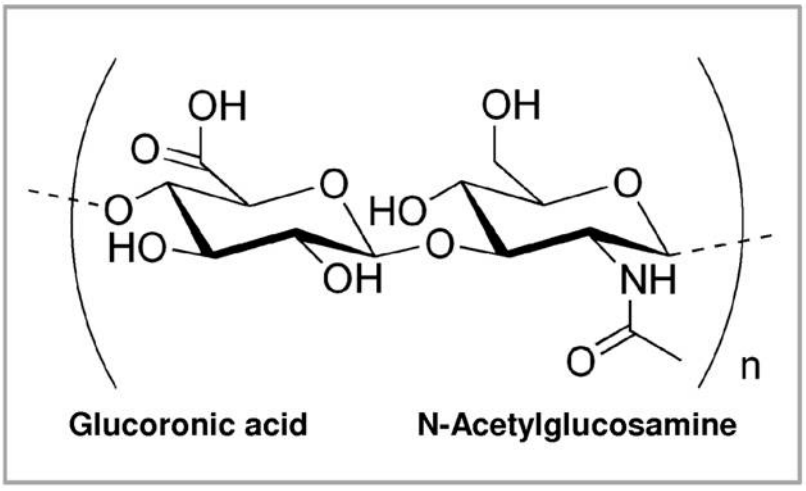

Figure 1.1: **Structure of Hyaluronan**

1.2 HA Metabolism

HA is synthesized by enzymes named hyaluronan synthases and degraded by hyaluronidases. The turnover of HA in the human body occurs rapidly. Arround one third of hyaluronan in the human body is turned over each day.

1.2.1 Hyaluronan synthases (HAS)

The mammalian hyaluronan synthases were cloned in 1996 and 1997. The first cloned HAS was the murine HAS1, which was highly expressed in brain and to a lesser extent in liver, skeletal muscle and pancreas [Itano and Kimata 1996a]. Later the same year, human HAS1 was isolated through screening of a human cDNA library in an attempt to find cDNA clones that encode proteins, which could bind to a T-cell lymphoma cell line [Shyjan et al. 1996]. Human HAS1 is the homologue of mouse HAS1 that shared 96% amino acid homology, and developed from the same original gene. Northern blot experiments showed that the human HAS1 mRNA is highly expressed in ovary [Shyjan et al. 1996].

In the same year, human and murine HAS2 were isolated by Spicer and colleagues. The murine HAS2 is highly expressed in the mouse embryo and in adult tissues such as brain, spleen and lung. Northern blot analysis showed two bands at 3.2 kb and 4.8 kb [Spicer et al. 1996]. This indicates that there are two transcriptional splicing variants for HAS2. However, no annotation for the shorter splicing variant of HAS2 was entered to the Genbank database.

In 1997, Spicer and colleagues reported that the third HAS gene was detected in both human and mouse named HAS3 [Spicer et al. 1997a]. They also showed that there were two transcriptional splicing variants (6.5kb and 4kb) of

mouse HAS3 by northern blot. In 2002, it was revealed that human HAS3 also has two splicing variants [Sayo et al. 2002; Monslow et al. 2003]. Northern blot analysis showed two bands of 4.8 kb and 2 kb.

In human and mouse, the three HAS genes are localized on different chromosomes [Spicer et al. 1997b] and evidence indicates that gene duplication induced the three HAS isoforms by evolution. After the first gene duplication, HAS1 and HAS2 genes were formed. Then, the HAS1 gene was duplicated to generate HAS1 pseudogene (found in *Xenopus laevis*, xHas-rs) and the HAS3 gene is formed by HAS2 duplication, respectively [Spicer and McDonald 1998]. The HAS1 pseudogene could not yet be detected in mammals [DeAngelis 1999]. Disruption of HAS2 causes embryonic lethality at E9.5 in mice, whereas deletion of HAS1 and HAS3 showed no obvious phenotype during embryonic development [Camenisch et al. 2002].

Topology of HAS isoforms

As in Figure 1.2, the HAS enzymes are localized in the plasma membrane and the topological prediction shows that they span the membrane seven times with the active site presumably located in the large cytoplasmic loop [Weigel et al. 1997]. Studies on raw membrane preparations showed that the sugars were added to the reducing end of the chain [Weigel et al. 1997; Asplund et al. 1998; Itano and Kimata 1996b]. The enzymatic activity of hyaluronan synthases is refered to the glycosyltransferase of both glucoronic acid and acetylglucosamine. Site directed mutagenesis experiments showed that the active center of HAS likely resides in the large intracellular loop between the second and the third transmembrane domain [Yoshida et al. 2000]. Polymerization of HA is thought to occur at the cytoplasmic active center of HAS and the growing polymer is

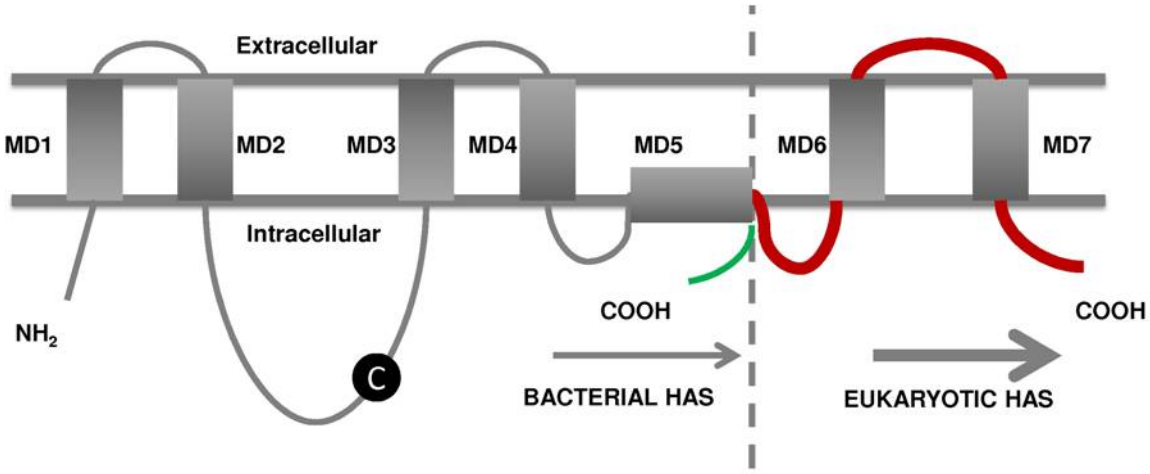

Figure 1.2: **Predicted topological structure of eukaryotic and bacterial hyaluronan synthases.**

Very similar hydropathy plots and primary structure (28 - 71 % identity) among all the HAS isozymes suggest that they are similarly organized within the membrane. The scheme depicts the N- and C-termini and the large central domain, between MD2 and MD3, inside the cell. The larger eukaryotic HASs (red line) have additional amino acids in all regions compared to the bacterial HASs (green line), except for the highly conserved 178 amino acids carboxyl terminal of the central domain and MD1-MD5. In particular, the carboxyl terminal $\sim$25 % of the eukaryotic HASs has two additional predicted membrane domains (MD6 and MD7), missing in the bacterial proteins. The conserved Cys is indicated by the *circled C*. MD5 can be modeled as an amphipathic helix, which orients the C terminus of all HAS members inside. (Modified from [Weigel et al. 1997])

extruded to the outside of the cell during elongation. HA is exported to the extracellular matrix either by the HAS enzyme itself or through one of the ABC transporters or the combination of both [DeAngelis and Weigel 1994; DeAngelis and Achyuthan 1996; Schulz et al. 2007; Prehm and Schumacher 2004].

Activity of HAS isoforms

All three HAS isoforms catalyze the same reaction. Even though, each HAS isoform produces HA of different length with different enzymatic kinetics [Itano et al. 1999a]. HAS1 and HAS2 produce high molecular weight (HMW) HA with the average size of 2×10^6 Da, wherease the product of HAS3 is about 2×10^5 Da in size [Spicer et al. 1997a; Itano et al. 1999a; Brinck and Heldin 1999]. *In vitro* study indicated that HAS enzyme could polymerize 10 - 100 UDP sugar precursors per second [DeAngelis 1999]. Thus, it takes a HAS enzyme 5 - 10 minutes to produce HA chain with 1 - 10 $\times$ 10^6 Da in length *in vitro*.

Splicing variants of HAS3

Two splicing variants of human HAS3 were discovered, namely HAS3v1 and HAS3v2. Figure 1.3 A shows the genomic structure of human HAS3 gene annotated in the Genbank. HAS3v2 spreads longer on the genome than HAS3v1. Thus, HAS3v1 consists of 553 AA while HAS3v2 is only 281 AA in length. This is due to the fact that the coding sequence on the last exon of HAS3v2 is shorter. The difference in the 5' UTR (untranslated region) between HAS3v1 and HAS3v2 indicates the diverse transcriptional regulation. HAS3v1 and HAS3v2 share the first two coding exons, which causes that the first 246 amino acid from HAS3v1 and HAS3v2 are identical. Homology analysis reveals that HAS3v2 is

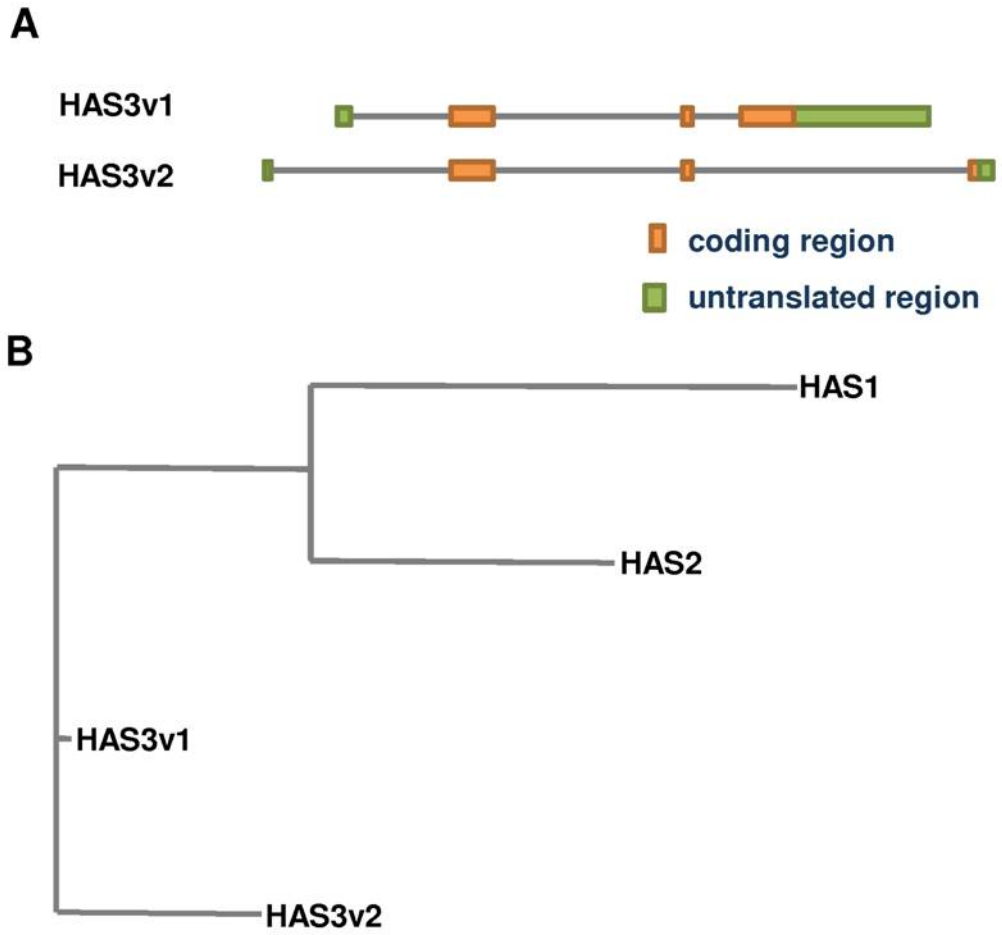

Figure 1.3: **HAS3v1 and HAS3v2 are close related**

(**A**): Genomic structure of HAS3 splicing variants; (**B**): Homology analysis of HAS isoforms.

closer related to HAS3v1 than HAS2 and HAS1(figure 1.3 B). No report has yet addressed human HAS3v2 except the first detection [Sayo et al. 2002; Monslow et al. 2003].

1.2.2 Hyaluronidases (HYAL)

Enzymes that are capable to degrade hyaluronan are known as hyaluronidases. There are six genes in mammals that encode hyaluronidases. These six hyaluronidase

Chromosomal cluster	Gene	Protein	Degradation product of HA	physiological expression pattern	Optimal PH
3p21.3	Hyal1	Hyal1	tetra-& hexa-saccharides	serum, liver, kidney, heart	3-4
	Hyal2	Hyal2	20kDa	liver, kidney, heart, placenta	4
	Hyal3	Hyal3	n.d.	bone marrow, testis	n.d.
7p31.3	Hyal4	Hyal4	-	n.d.	n.d.
	SPAM1	PH20	tetra-& hexa-saccharides	Testis	4.5, 7.5
	HyalP1	None	-	-	-

Table 1.1: **The six hyaluronidase paralogues in human genome**

n.d.-not determined

genes are localized to two gene clusters on the chromosomes 3p21 and 7q31 in human.

Hyaluronidase 1 (HYAL1) is originally isolated from serum [Frost et al. 1997]. The molecular weight of human Hyal1 is 45 kDa after translation, and 8 kDa is added by the post-translational glycosylation. The enzymatic activity of HYAL1 is optimal at an acidic pH. HYAL2 is approximately 40 % paralogous to HYAL1. HYAL2 can only cleave hyaluronan into an intermediate size (about 20 kDa). In mice, HYAL2 is expressed in the brain during the fetal development and silenced after birth [Strobl et al. 1998; Lepperdinger et al. 2001]. This indicates the HYAL2 plays an important role in embryonic development of brain. HYAL2 can attach to the surface of cell membrane as a GPI anchored protein, which may work as a receptor for an oncogenic virus, namely Jaagsiekte sheep retrovirus [Rai et al. 2001]. PH20 is expressed in the testis in two forms. During the fertilization, one form of PH20 is localized on the surface of the acrosomal head of the sperm to enable the sperm to penetrate the HA-rich ECM of the cumulus cells surrounding the egg. Then, the other form of PH20, which is localized in the acrosomal vesicle, is required for the sperm to degrade the surface associated HA and to bind to the surface of the egg cell [Kreil 1995]. Table 1.1 shows the known enzymatic properties of human hyaluronidases.

The mammalian hyaluronidases function as β-endo-N-acetyl-glucosaminodases, which degrade not only hyaluronan but also other GAGs such as chondroitin sulfate and dermatan sulfate [Batra et al. 1997]. To date, the HA specific hyaluronidases are only discovered in *Streptococci Pneumococcus* and *Streptomyces hyalurolyticus*.

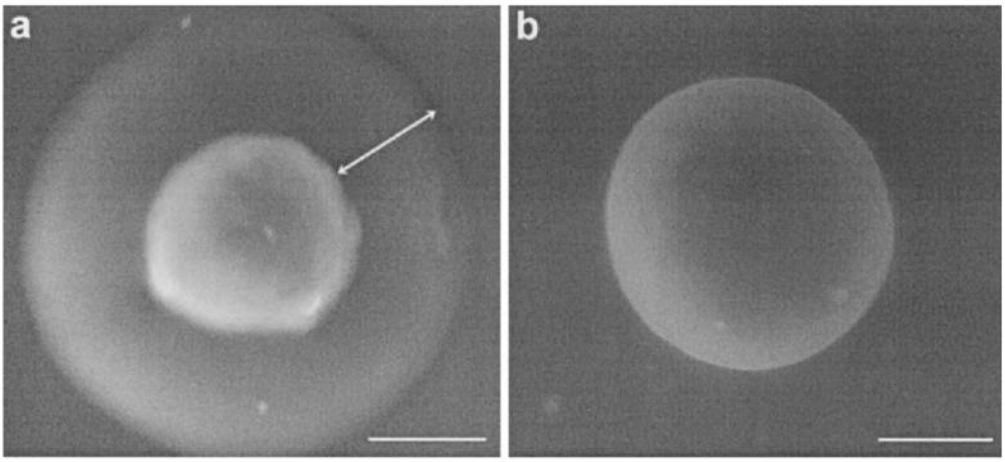

Figure 1.4: **Pericellular hyaluronan coat**
Chondrocytes were fixed and incubated with uranyl acetate in suspension, then examined using ESEM (environmental scanning electron microscopy). (**A**) Untreated cells are surrounded by a 4.4 $\pm$ 0.7-mm-thick hyaluronan coat (arrow). (**B**) Hyaluronidase removed the pericellular hyaluronan coat competely. Scale bar, 5 mm. [Zaidel-Bar et al. 2004]

1.3 Localizatioin of HA

1.3.1 Extracellular hyaluronan

Hyaluronan is a key component of the extracellular matrix (ECM). During synthesis, the growing polymer chain is extruded through the membrane into the pericellular space. After synthesis, hyaluronan can be retained on the cell surface to form a voluminous pericellular matrix (pericellular coat). Figure 1.4 shows the hyaluronan dependent pericellular matrix in Chondrocytes [Zaidel-Bar et al. 2004]. This pericellular hyaluronan matrix plays multiple roles in cell adhesion/detachment, and cell shape changes associated with proliferation and locomotion. By overexpressing the hyaluronan synthases, microvillous membrane protrusions were observed that form the scaffold of hyaluronan coats in certain cells [Rilla et al. 2005; Kultti et al. 2006]. Hyaluronan is crosslinked by

various proteins, such as aggrecan, TSG-6, inter-alpha-trypsin inhibitor, versican and brevican [Day and Prestwich 2002]. This enables hyaluronan to gain different functions such as inflamatory response.

1.3.2 Intracellular hyaluronan

In 1976, it was first reported by Margolis and colleagues that glycosaminoglycans are enriched in the rat brain nuclei and hyaluronan accounts for nearly 1/3 of the total quantity [Margolis et al. 1976]. Intense HA staining was observed in rough endoplasmic reticulum (rER) membranes (but not lumen), plasma membranes, and nuclei in all the tissues studied [Londoño and Bendayan 1988; Kan 1990; Ripellino et al. 1988; Eggli and Graber 1995]. Intracellular HA can be accumulated under hyperglycemia condition [Wang and Hascall 2009]. Evanko and Wight showed that HA accumulated intracellularly in the perinuclear region of aortic smooth muscle cells during the premitotic and mitotic stages [Evanko and Wight 1999]. However, the source of the intracellular HA is not yet clear. A recent study treated viable smooth muscle cells with hyaluronidase to remove pericellular HA to pervent the internalization. This eliminated most but not all of the intracellular HA. This supports the conclusion that a large proportion might be due to endocytosis uptake. Further, exogenous fluorescein-labeled hyaluronan was taken up into vesicles in growing cells but was localized distinctly compared to endogenous hyaluronan, suggesting that hyaluronan in cells may be derived from an intracellular source [Evanko and Wight 1999].

1.3.3 Intracellular hyaladherins

The identification of intracellular HA-binding proteins (IHABPs), including RHAMM, IHABP4, CDC37 and HABP1, lends additional support to the existance of intracellular HA [Day and Prestwich 2002; Assmann et al. 1998; Hofmann et al. 1998; Huang et al. 2000; Turley et al. 2002]. RHAMM is one of the well-studied HA receptors. The precise function of RHAMM is described in a subsequent section (see section 1.4.2). Human IHABP4 is 57 kDa in size. IHABP4 is a cytoplasmic and nuclear protein that can be phophorylated on serine and therosine residues. IHABP4 could bind to hyaluronan as well as chondroitin sulfate, heparane sulfate, and RNA though with low affinity. The IHABP4 expression is enriched in some tumor cells [Kobarg et al. 1997]. IHABP4 was shown to associate with RACK1/PKC pathway for regulating the cellular functions [Nery et al. 2004]. In 1995, Grammatikakis and colleagues showed that cell cycle control protein, CDC37, could bind to hyaluronan, chondroitin sulfate and heparin *in vitro* [Grammatikakis et al. 1995]. It still unknown whether cell division could be modified by cdc37 after binding to HA. HABP1was first isolated from rat kidney by HA sepharose affinity chromatography [Gupta et al. 1991]. The GAG binding affinity of HABP1 is restricted to hyaluronan. HABP1 coated culture plates allowed more cell to attach [Gupta and Datta 1991]. Subcellularly, HABP1 localized in the mitochondrial matrix, cytoplasma, nuclear and also on the plasma membrane [Gupta et al. 1991; Muta et al. 1997; Dedio et al. 1998; Simos and Georgatos 1994]. Activated ERK, one of the MAP kinases, can phosphorylate HABP1 [Majumdar et al. 2002]. Phorbol 12-myristate 13-acetate (PMA) can derease HABP1 in cytoplasma with parallel increase in the nucleus by activating ERK. This indicates that HABP1 contributes in part to the MAP kinase cascade implying a broad role in signaling. Furthermore, HABP1 was up-regualted at

both mRNA and protein level during cisplatin and TNF-alpha-induced apoptosis [Kamal and Datta 2006; Guo et al. 1999]. Ectopic expression of HABP1 induces apoptosis, autophagic vacuoles and mitochondrial dysfunction [Meenakshi et al. 2003; Sengupta et al. 2004; Chowdhury et al. 2008]. Overexpression of HABP1 was observed in a variety of adenocarcinomas including thyroid, colon, gastric, esophageal and lung adenocarcinoma [Rubinstein et al. 2004].

1.4 Physiological function of HA

1.4.1 Physical function of HA

HA has diverse functions despite of its unbranched simple composition. The axial hydrogen atoms create a non-polar, relatively hydrophobic core while the equatorial side chains produce a more polar, hydrophilic surface, thereby inducing a twisting ribbon structure. As a result, the hyaluronan molecule can randomly fold to coiled structure under physiological conditions and occupy a very large space [Scott et al. 1991]. HA binds a huge amount of water in the extracellular space and thus hydrates tissues and skin dermis. Hyaluronan regulates water balance, osmotic pressure and acts as an ion exchange resin. Furthermore, HA forms a thin layer in the luminal surface of blood vessel, named apical glycocalyc that excludes certain macromolecules,leukocytes and pletelets from direct interaction with the luminal surface of endothelial cells [Henry and Duling 1999]. As a lubricant and a shock absorber, hyaluronan acts as a structural molecule in the vitreous humor of the eye, in joint fluid, and in Wharton's jelly [Toole 2004].

1.4.2 HA receptors and intracellular signaling pathways.

It is now known that HA plays an important role in modulating cell behavior. Hyaluronan regulates cell motility, cell-cell and cell-matrix adhesion, cell proliferation and differentiation. It participates in fundamental processes such as embryological development and morphogenesis [Toole 1990, 2001], wound healing [Weigel et al. 1988; Longaker et al. 1991], repair and regeneration and inflammation [Noble 2002; De la Motte et al. 2003; Majors et al. 2003]. HA regulates the intracellular signaling pathways by binding to the proteins known as hyaladherins including LYVE1 (Lymphatic Vessel Endothelial Receptor 1), HARE (Hyaluronan Receptor for Endocytosis), toll-like receptors TLR and TLR4, CD44 (Cluster of Differentiation 44) and RHAMM (Receptor for Hyaluronan Mediated Motility).

RHAMM

RHAMM localizes both intracellularly and on the outer plasma membrane, although, there is no signal peptide or transmembrane domains encoded [Turley 1980]. Intracellularly, RHAMM exists in the cytoplasm, mitochondria and nucleus [Assmann et al. 1999; Crainie et al. 1999; Entwistle et al. 1996; Lynn et al. 2001]. RHAMM interacts with cytoskeleton, microtubules, centrosomes and mitotic spindle [Assmann et al. 1999; Maxwell et al. 2003]. RHAMM is engaged in different cellular functions including cell transformation and proliferation. Overexpression of RHAMM leads to ras-dependent cell transformation in fibroblasts [Hall et al. 1995]. It also influences cell mitosis by inducing the expression of cdc25 and cyclin B1, which are both involved in cell cycle regulation [Mohapatra et al. 1996]. The expression of RHAMM is also differentially regulated during

the different phases of the cell cycle [Sohr and Engeland 2008]. The mRNA and protein levels of RHAMM are elevated during the S-phase and peak during the mitotic phase (G2/M). HA accumulates during the mitosis for cell detachment [Brecht et al. 1986]. Further, RHAMM expression can be down-regulated by the tumor suppressor P53. Therefore, HA-RHAMM interaction might play an important role in cell cycle regulation and thereby RHAMM is significantly involved in cancer progression. A current model of HA-dependent RHAMM mediated signaling pathways is demonstrated in figure 1.5 [Turley et al. 2002].

The basal expression level of RHAMM is low in normal tissues [Turley et al. 2002; Evanko et al. 2007; Slevin et al. 2007]. Deficiency of RHAMM in mice showed no obvious effect on embryonic development and adult mouse homeostasis but revealed delayed wound healing [Crainie et al. 1999; Nedvetzki et al. 2004; Tolg et al. 2006]. However, up-regulation of RHAMM was reported in several advanced cancers [Giannopoulos and Schmitt 2006; Hus et al. 2008; Rein et al. 2003; Tolg et al. 2003; Yamano et al. 2008; Zlobec et al. 2008]. For example, RHAMM is defined as a breast cancer susceptibility gene [Pujana et al. 2007]. The interaction between HA and RHAMM activates multiple signaling pathways that affect the motility and progression of breast cancer cells [Turley et al. 2002]. Higher expression of RHAMM in breast cancer is associated with poorer clinical prognosis and higher risk of lymph node metastasis [Assmann et al. 2001; Wang et al. 1998].

CD44

CD44 belongs to the class 1 transmembrane glycoprotein family and functions as a ubiquitous cell surface receptor of hyaluronan. CD44 is a single copy gene and highly conserved [Screaton et al. 1992]. CD44 transcripts are subject to

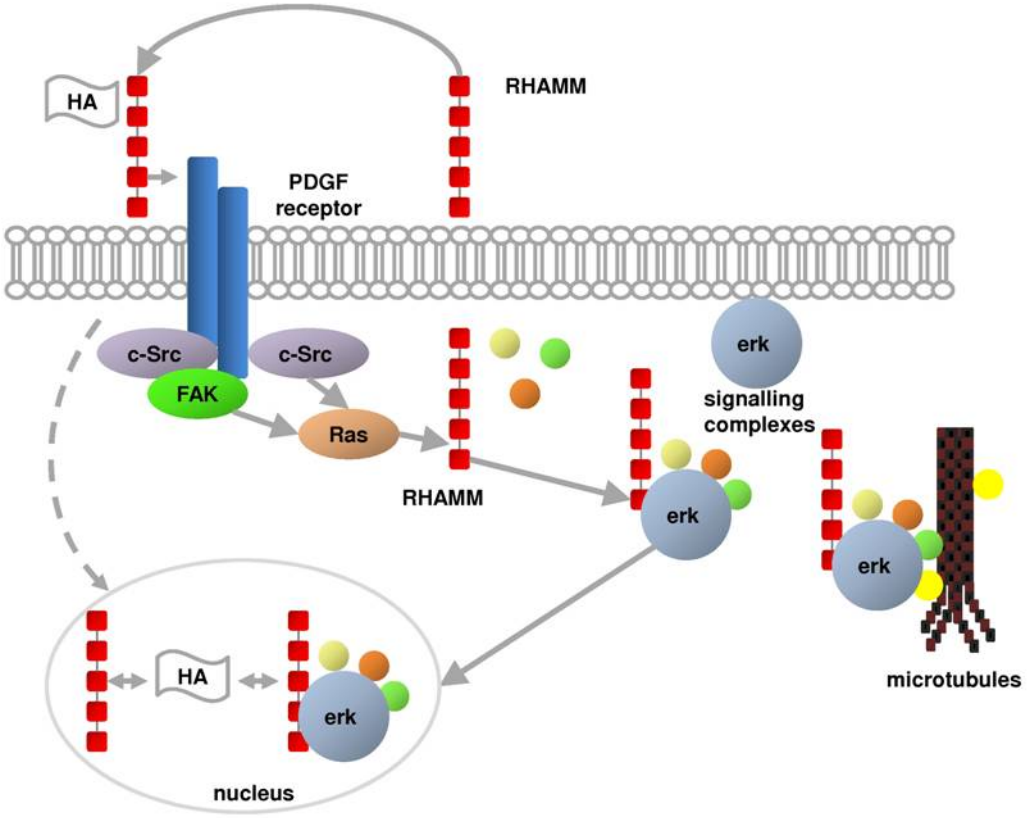

Figure 1.5: **HA-dependent RHAMM mediated signaling pathways**
RHAMM is a hyaladherin that occurs in multiple subcellular compartments and that can also be exported to the extracellular milieu where it binds to the cell surface. Cell surface RHAMM-hyaluronan interactions regulate signaling through Ras and Src. Cell surface RHAMM stimulates the PDGF receptor to activate Erk kinase, a key map kinase involved in cell motility. Intracellular RHAMM proteins encode multiple kinase docking and recognition sites, and an intracellular form of RHAMM has been shown to physically associate with Erk1 kinase. Intracellular forms also associate with the cytoskeleton, notably interphase and mitotic spindle microtubules. The ability of intracellular RHAMM to associate with multiple signaling complexes and to associate with the cytoskeleton suggest that RHAMM functions as adapter proteins like vinculin and paxillin. FAK, focal adhesion kinase. (Modified from [Turley et al. 2002])

alternative splicing, which affects predominantly the extracellular membrane-proximal nast of CD44 proteins [Stamenkovic et al. 1991; Günthert et al. 1991]. The standard isoform of CD44 consists of an N-terminal signal sequence (exon 1), a HA binding domain with homology to the link protein family of aggrecan and HA binding proteins (exons 2 and 3), a stem region of 248 amino acids (Exons 4, 5, 16, 17), a 21 amino acid transmembrane domain (exon 18), and a 72 amino acid cytoplasmic domain (exon 19). The splice variants are generated as a result of insertion of various permutations and combinations of exons 6-15 (v1-v10) into the stem region. CD44 isoforms are broadly expressed and range form 80 to 200 kDa in size. The mRNA and protein structures of CD44 splicing variants are shown in figure 1.6. The variants are most commonly expressed in epithelial cells and are upregulated under pathological conditions such as cancer [Screaton et al. 1992; Stamenkovic et al. 1991; Goldstein and Butcher 1990].

CD44 can be regulated at multiple levels: promoter methylation, transcription, post-translational modifications such as glycosylation, glycosaminoglycan interaction, and phosphorylation, ligand binding, and proteolytic processing of the extracellular domain [Lou et al. 1999; Verkaik et al. 1999; Yan et al. 2003; Borland et al. 1998; Greenfield et al. 1999; Zhang et al. 1995; Legg et al. 2002; Neame and Isacke 1992; Cichy and Puré 2003]. The binding of CD44 isoforms to hyaluronan contributes to the stimulation of aggregation, proliferation, migration, and angiogenesis [Lesley et al. 1993; Bourguignon et al. 1992, 1998; Lokeshwar et al. 1996]. The intracellular domain of CD44 isoforms selectively interacts with cytoskeletal proteins and regulates specific signalings such as PI 3 kinase pathway [Bourguignon et al. 1998]. Therefore, CD44 isoforms directly link with hyaluronan and the cytoskeleton. Figure 1.6 summarizes the signal cascades, which are regulated by hyaluronan-CD44 interaction.

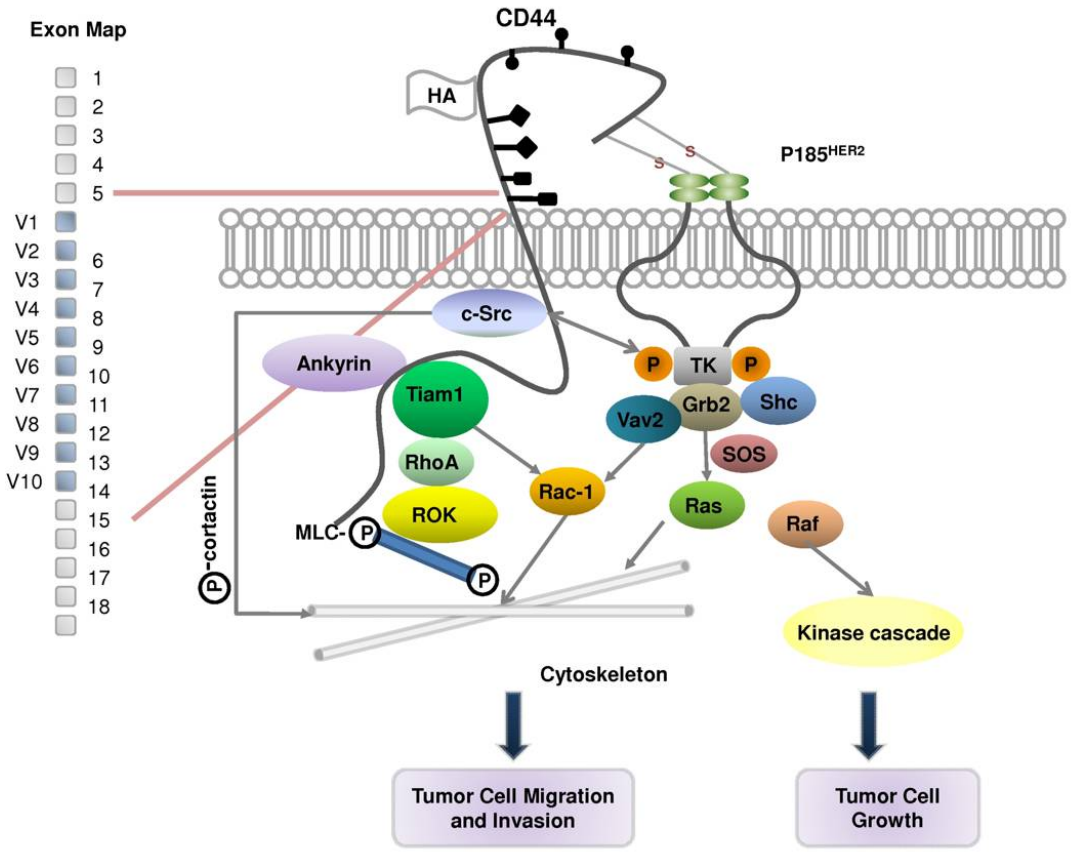

Figure 1.6: **HA-dependent CD44 mediated signaling pathways**
CD44-hyaluronan interactions promote tyrosine kinase (TK) activity of HER2 and the non-receptor kinase, Src. Src phosphorylates cortactin, which recruits it to the cell membrane. CD44-hyaluronan interactions also activate RHOA and Rac1, and CD44 binds to Tiam1 and Vav2. Hyaluronan binding also causes the association of CD44 forms with cytoskeletal proteins such as ankyrin and ERM proteins. The current model suggests that the close interactions between CD44 and its selected binding partners play a pivotal role in coordinating cross-talk among various intracellular signaling pathways (e.g. Rho/Ras signaling and receptor-linked (p185HER2)/non-receptor-linked (c-Src) tyrosine kinase pathways) leading to the concomitant onset of multiple functions such as tumor cell adhesion, proliferation/growth, migration, and invasion. MLC, myosin light chains. (Modified from [Turley et al. 2002])

1.5 Hyaluronan in cancer

Hyalronan is shown to be elevated in both the cancer epithelium and peritumoral stroma during cancer progression depending on the cancer type. Either is associated with an unfavorable outcome of the disease. Recently, it is shown that hyaluronan is not only a prognostic indicator but also a novel target of therapy [Nakazawa et al. 2006; Pályi-Krekk et al. 2007].

Tumor hyaluronan is correlated with the mRNA expression level of HAS isoforms [Pienimaki et al. 2001; Karvinen et al. 2003; Pasonen-Seppänen et al. 2003]. This indicates that transcriptional regulation may play an important role in determining the hyaluronan accumulation. HAS isoform expression is stimulated by growth factors like EGF, KGF and PDGF [Pienimaki et al. 2001; Karvinen et al. 2003; Pasonen-Seppänen et al. 2003; Jacobson et al. 2000]. Furthermore, the expression levels of both growth factors and their receptors are frequently induced in cancers. Growth factors from cancer and stromal cells may act in convert to stimulate hyaluronan synthesis [Jacobson et al. 2000]. Specifically, cancer cells may induce the stromal cells to produce a HA-enriched tissue structure, which is more appropriate for tumor growth [Knudson and Toole 1988; Edward et al. 2005]. On the other hand, growth factors from stromal cells could stimulate cancer cell migration [Karnoub et al. 2007].

The malignant transformation of cells is frequently associated with aberant HA synthesis and ECM gene expression [Weigel et al. 1997; Itano and Kimata 2002; Stern et al. 2006]. Both HAS1 and HAS2 expression are elevated in highly malignant cells transformed with v-src. This implies that HAS isoforms may be involved in different stages of malignant transformation although the HAS enzymes are not transformed by themselves [Toole 2004]. Furthermore,

overexpression of HAS2 and HAS3 genes resulted in HA over-production and increased tumorigenicity of fibrosarcoma, melanoma, and mesothelioma cells [Kosaki et al. 1999; Liu et al. 2001; Itano et al. 1999b]. The importance of HAS enzymes for tumor cell phenotypes is also supported by the finding that suppression of HAS2 or HAS3 diminished the tumorigenic potential in a variety of tumors [Koyama et al. 2007; Zoltan-Jones et al. 2003; Desmoulière et al. 2004; Löhr et al. 2001]. Elevated HAS1 expression and intronic gene splicing correlate with poor prognosis in human colon cancer, ovarian cancer, and multiple myelomas [Itano et al. 2004; Theocharis et al. 2003; Itano et al. 2002]. Although the above evidences strongly supports the pro-tumorigenic role of HAS, the tumor promoting ability of HAS up-regulation can not be generalized because HAS2 overexpression can e.g. also inhibit the tumorigenesis of glioma cells [Cheng et al. 2007].

1.5.1 Tumor cell derived hyaluronan

Hyaluronan possitive cancer cells were detected in about half of the breast and prostate tumor cases and over 80 % of ovarian, colorectal and gastric cancers showed hyaluronan positive cancer cells [Auvinen et al. 2000; Ropponen et al. 1998; Lipponen et al. 2001; Anttila et al. 2000; Setälä et al. 1999]. In most cases, hyaluronan is detected arround the plasma membrane, and it also occasionally exists in the cytoplasm and even in the nucleus [Auvinen et al. 2000; Ropponen et al. 1998]. The proportion of hyaluronan-positive cancer cells, as well as the intensity of hyaluronan staining on those cells, directly correlates with tumor grade and degrees of cell differentiation [Auvinen et al. 2000; Ropponen et al. 1998; Anttila et al. 2000; Setälä et al. 1999; Hautmann et al. 2001; Pirinen et al. 2001; Suwiwat et al. 2004]. Furthermore, cancer metastasis often derives

from primary tumors with high hyaluronan expression suggesting an active role in cancer metastasis [Anttila et al. 2000; Böhm et al. 2002]. Furthermore, high hyaluronan levels in the cancer cells associate with unfavorable outcomes, i.e. shortened overall survival (OS) time and disease free survival (DFS) time in breast, gastric and colorectal cancers [Auvinen et al. 2000; Ropponen et al. 1998; Setälä et al. 1999; Köbel et al. 2004]. However, other studies showed that accumulation of hyaluronan in tumor could serve as a favorable prognostic factor. In lung squamous cell carcinoma, de-differentiated cancer cells showed less HA staining compared to higher differentiated ones with a more promising prognosis [Pirinen et al. 1998]. Therefore, the role of hyaluronan and its association with progression and metastasis can not be generalized and needs to be studied in different cancer entities.

1.5.2 Hyaluronan in stromal tissue

Stromal hyaluronan is increased in breast tumors, and this increase was more prominent at the invasion front than in the central tumor areas [Bertrand et al. 1992; Ponting et al. 1993]. It was later confirmed that the increased stromal hyaluronan is not restricted to breast cancer but also present in prostate, ovarian, bladder, endometrial, thyroid carcinomas and lung adenocarcinomas [Auvinen et al. 2000; Lipponen et al. 2001; Anttila et al. 2000; Pirinen et al. 2001; Lokeshwar et al. 2001; Afify et al. 2005; Aaltomaa et al. 2002; Ekici et al. 2004; Posey et al. 2003; Hiltunen et al. 2002]. Stromal HA can be markedly induced in tissue with low basal HA level. For instance, the stromal HA increased up to 49 fold in grade 3 ovarian cancer [Hiltunen et al. 2002]. High grade and poorly differentiated tumors are often paralleled with intense stromal hyaluronan. Furthermore, high levels of HA in stroma are also associated with cancer

cell penetration of capsules, lymph vessels and nerves in prostate carcinomas, local lymph node infiltration in breast cancers and with distant metastasis in thyroid, ovarian and prostate cancers [Auvinen et al. 2000; Lipponen et al. 2001; Anttila et al. 2000; Böhm et al. 2002; Lokeshwar et al. 2001; Aaltomaa et al. 2002; Wernicke et al. 2003]. 50 % of the breast cancer patients with high stromal hyaluronan passed away during 5 years of follow up, while all patients with low stromal hyaluronan survived [Auvinen et al. 2000]. The corresponding survival rates in ovarian cancer were 25 % and 45 % [Anttila et al. 2000]. Concisely, tumors with intensive stromal hyaluronan are induced in proliferation and metastasis.

1.6 Esophageal cancer

Esophageal cancer is the 3^{rd} most common gastrointestinal malignancy [Blot and McLaughlin 1999] and is the 6^{th} most frequent cancer worldwide [Parkin et al. 1999]. The incidence rate of esophageal cancer dramatically varies in different geographical regions of the world [Gore 1997]. The highest incidence of the disease occurs in the Esophageal Cancer Belt which stretches from eastern Turkey to Iraq, Iran, China, India, and certain regions of South Africa [Ribeiro et al. 1996]. More than 90 % of the esophageal cancers are either squamous cell carcinomas (ESCC) or esophageal adenocarcinomas (EAC) [Blot 1995]. Although patient presentation of ESCC and EAC are similar, the epidemiology, etiology, prognosis and treatment strategy are quite different [Mariette et al. 2005; Siewert and Ott 2007]. ESCC and EAC are considered to represent two different diseases occuring in the same organ.

1.6.1 Epidemiology

Until the 1970s, ESCC was the dominent type of esophageal cancer. High incident regions of ESCC are in the Southern and Eastern Africa and a central Asian belt passing from Turkey through Iran, Iraq, Kazakhstan, Mongolei and onto Northern China. The incidence in high-risk areas can reach up to 100/10,000 per year compared to 5 -10/10,000 per year in Western countries [Holmes and Vaughan 2007]. Worldwide, the male:female ratio is 3:1. However, the distribution is more equal in the high-risk regions reflecting an equal exposure to risk factors [Wabinga et al. 2000].

During the last 30 years, there has been a decline or stabilization in the incidence of ESCC in Western contries [Keeney and Bauer 2006; Vizcaino et al. 2002; Pera 2003; Pera et al. 2005; Newnham et al. 2003a]. Over the same period, the age-standardized incidence of EAC has risen faster than any other malignancy in Western world. Though, EAC was a rare disease with the incidence $<$ 1:100,000 before the 1970s, the incidence of EAC has now exceeded that of ESCC [Pohl and Welch 2005; Shaheen 2005; Lagergren 2005]. The incident rise is most significant in the white male population. It reaches 5 / 100,000 for white male in US and 8 -12 / 100,000 in the highest incident countries of Australia and the UK [Newnham et al. 2003a; Kubo and Corley 2002, 2004; Bollschweiler et al. 2001; Lord et al. 1998; Newnham et al. 2003b; Devesa et al. 1998; Registry 2000]. The age distribution of EAC peaks at 50 - 60 years and the male:female ratio is between 2:1 and 12:1 [Botterweck et al. 2000].

1.6.2 Etiology

ESCC is associated with many environmental factors including diet rich in preserved or pickled food, lack of fresh fruit and vegetables, vitamin and mineral deficiencies, and a thermal effect of hot food and beverages. Alcohol intake and smoking are also strong risk factors for ESCC [Farhadi et al. 2005; Bahmanyar and Ye 2006; Boeing et al. 2006]. Ethnic, obesity, esophageal sphincter-relaxing drugs, smoking and alcohol consumption have all been convicted as etiological factors in EAC [DeMeester and DeMeester 2000; DeMeester 2006; Lagergren et al. 2000; Lagergren and Jansson 2006; Lagergren et al. 1999a]. Cohort studies showed that gastroesophageal reflux and Barrett's disease represent causal factors for EAC [Solaymani-Dodaran et al. 2004; Lagergren et al. 1999b].

1.6.3 Prognosis

The prognosis of ESCC and EAC is poor and the overall tumor-specific lethality rate reaches up to 95 % [Lagarde et al. 2006]. Female appears to have better outcomes than male. The 5-year survival rate ranges from 5 % to 20 % for the patients undergoing operations with curative intent. Tumors in the upper esophagus associated with high operative risks. The immediate surgical results are consistently worse for ESCC than for EAC [Siewert and Ott 2007; Alexandrou et al. 2002; Abunasra et al. 2005]. This might be due to the fact that ESCC often existed in the mid or upper esophagus and is associated with other comorbidities such as age, chronic respiratory disease, liver disease and poor nutrition.

Chapter 2

Aim of Study

Hyaluronan plays an important role in modulating cell phenotypes such as cell motility, cell-cell and cell-matrix adhesion, cell proliferation and differentiation. Elevated hyaluronan levels in the cancer epithelium and peritumoral stroma are thought to promote tumor progression.

HAS isoforms, HAS1, HAS2 and HAS3v1, are shown to be transmembrane proteins and in charge of extracellular HA synthesis. HAS3v2 is a smaller splicing variant of HAS3 that has been described in cultured human keratinocytes but has not been studied with respect to function yet.

Therefore, the following questions were addressed in this Ph.D thesis:

- What is the subcellular localization of HAS3v2 in comparison to HAS3v1?
- Does HAS3v2 have enzymatic activity?
- Does HAS3v2 expression alter the cellular phenotype of cancer cells *in vitro* and *in vivo*?
- Is HAS3v2 expressed in human esophageal cancer patients?

Chapter 3

Material and Methods

3.1 Materials

4-Methylumbelliferone	Sigma-Aldrich, Munich
Acrylamide 40 %	BioRad, Munich
Ammonium persulfate (APS)	BioRad, Munich
DMEM cell culture medium	Gibco-Invitrogen, Karlsruhe
Hoechst 33324	Sigma-Aldrich, Munich
Image-iT LIVE Plasma Membrane marker	Invitrogen, Karlsruhe
ER Tracker red	Invitrogen, Karlsruhe
EndoFree Plamid Maxi Kit	Qiagen, Hilden
PageRule Prestained Protein Ladder	Fermentas, St.leon-Rot
Poly-L-Lysine	Sigma-Aldrich, Munich
Pronase	Sigma-Aldrich, Munich
Protaminsulfate	Sigma-Aldrich, Munich
RPMI 1640 cell culture medium	Sigma-Aldrich, Munich
Streptomyces Hyaluronidase	Sigma-Aldrich, Munich
Quantitect reverse transcription Kit	Qiagen, Hilden
CyQUANT NF Cell Proliferation Assay Kit	Invitrogen, Karlsruhe
Platimium SYBR Green qPCR supermix -UDG w/ROX	Invitrogen, Karlsruhe
Tri-Reagent	Sigma-Aldrich, Munich
Vectashield Antifade Mounting Medium	Vector Laboratories, CA, USA
Vitrogen 100	Collagen Corp, Palo Alto, CA.USA
Whatman-Paper	Schleichter und Schuell, Maidstone,England
PVDF-Membrane	Bio-Rad Laboratories, Hercules, CA, USA

Table 3.1: **Chemicals and Kits**

Electrophoresis chamber (Protein)	Mini-PROTEAN3 Electrophoresis cell, PowerPac 200 +300 Power Supply	BioRad, Munich
Fluorescent-Microscope incl. Camera and Software	Epifluorescent inverse microscope Axiovert 100	Zeiss, Oberkochen
Confocal Microscope	Zeiss LSM510	Zeiss, Oberkochen
Microscope	Leica Upright Microscope	Leica, Wetzlar
Protein-Transfer (Western-Blot	PerfectBlue Semi-Dry Elektroblotter	Prqlab, Erlangen
RNA, DNA quantification	Nanodrop-1000	Reqlab, Erlangen
Microplate reader (UV)	Multiskan Ascent	Thermo Fischer, Dreieich
Microplate reader (Fluorescence)	Fluoroskan Ascent	Thermo Fischer, Dreieich
PCR-Machine	Mastercycler Gradient	Eppendorf, Hamburg
Realtime-PCR-Machine	Applied Biosystems 7300 Real-Time PCR System	Applied Biosystems, Darmstadt
Centrifuge	Centrifuge 5415R	Eppendorf, Hamburg
Immunoblot imager	Odyssey Infrared Imaging System	Licor, Bad Homburg

Table 3.2: **Equipments**

1 × Running Buffer	250 mM Tris (Trishydromethylaminomethane) 1.9 mM Glycine 0.1 % SDS
1 × Protein Lysis Buffer	1 % SDS 1 mM PMSF (Phenylmethysulfonylfluoride) 10 mM Tris pH 7.4
2 × Loading Buffer	125 mM Tris pH 6.8 4 % SDS 10 % Glycerol
Stacking gel (5 %)	0.5 M Tris pH 6.8 0.625 ml 10 % SDS 50 μl dH_2O 3.895 ml 40 % Acrylamide 375 μl Temed 5 μl APS 10 %-0.1 g/ml 50 μl
Separating gel (10 %)	3 M Tris pH 8.7 0.975 ml 10 % SDS 75 μl dH_2O 4.545 ml 40 % Acrylamide 375 μl Temed 5 μl APS 10 %-0.1 g/ml 25 μl
Blocking Buffer	2 % (w/v) BSA in 1 × TBST
1 × Transfer-Buffer	1 × Running Buffer 20 % Methanol 0.01% SDS
10 × TBS	100 mM Tris / HCl 1.5 mM NaCl pH7.4
1 × TBST	1 × TBS 0.1 Tween 20

Table 3.3: **Recipe of Immunoblot**

	Human specific primers (5' - 3')	**Murine specific primers (5' - 3')**
HAS1 F	TACAACCAGAAGTTCCTGGG	CTATGCTACCAAGTATACCTCG
HAS1 R	CTGGAGGTGTACTTGGTAGC	TCTCGGAAGTAAGATTTGGAC
HAS2 F	GTGGATTATGTACAGGTTTGTGA	GAGATGGTGAAGGTCTTAGAG
HAS2 R	TCCAACCATGGGATCTTCTT	AAAGCCATCCAGTATCTCAC
HAS3v1 F	GAGATGTCCAGATCCTCAACAA	CTCAGTGGACTACATCCAGG
HAS3v1 R	CCCACTAATACACTGCACAC	GACATCTCCTCCAACACCTC
HYAL1 F	CTTCTATGACACGACAAACCA	GAAATGACAGATTATCTTCTGCCC
HYAL1 R	ATACTCCTTGATGGCCTGAC	TTGTCTGAGCTTAGCCAGAG
HYAL2 F	CTCATCTCTACCATTGGCGA	GCTTCAAGTATGGAGACCTG
HYAL2 R	GTGTCAGGTAATCTTTGAGGT	GGACACGTTGACTATGTAGG
CD44s F	CTGCTACCAGAGACCAAGAC	AGGATGACTCCTTCTTTATCCG
CD44s R	TCCATCTGATTCAGATCCATGAG	CTTGAGTGTCCAGCTAATTCG
RHAMM F	AACACTTTGATCCTTCAAAGGC	GAATATGAGAGCTCTAAGCCTG
RHAMM R	ATTCTTGACACTCCATAGGAGC	CCATCATACTCCTCATCTTTGTC
GAPDH F	CATTTCCTGGTATGACAACGA	GCTCATTTCCTGGTATGACAAT
GAPDH R	TCTCTTCCTCTTGTGCTCTTG	TCTCTTGCTCAGTGTCCTTG
HAS3v2 F	ATTCGGTGGACTACATCCAG	
HAS3v2 R	CTACTGCCATACCTTTCCCT	

Table 3.4: **Species specific primers for RT-qPCR**

3.2 *E. coli*

3.2.1 *E. coli* strains

The following strains of *E.c oli* were used for cloning and plasmid amplification. XL1-Blue: endA1 gyrA96(nal^R) thi-1 recA1 relA1 lac glnV44 F'[::Tn10 proAB$^+$ lacI^q Δ(lacZ)M15] hsdR17(r$_K{}^-$ m$_K{}^+$)

DH-5α: F$^-$ endA1 glnV44 thi-1 recA1 relA1 gyrA96 deoR nupG ϕ80d*lacZ*ΔM15 Δ(*lacZYA-argF*)U169, hsdR17(r$_K{}^-$ m$_K{}^+$), λ-

3.2.2 Generation of competent *E. coli* cells

E. coli were grown in 1 liter SOB medium at 37 $^\circ$C and harvested (4000 $\times$ g, 20 min, 4 $^\circ$C), when the OD 600 value of the culture reached 0.5 - 0.8. Cells were gently resuspended in 40 ml ice-cold TB buffer (10 mM Pipes, 55 mM $MnCl_2$, 15 mM $CaCl_2$, 250 mM KCl), incubated on ice for 20 min and again sedimented (4000 $\times$ g, 20 min, 4 $^\circ$C). Cells were gently resuspended in 20 ml ice-cold TB buffer and DMSO was added with gentle swirling to a final concentration of 7 %. After 10 min incubation on ice, cells were dispensed in 0.1 ml aliquots, chill-frozen in liquid nitrogen and stored at -80 $^\circ$C.

3.2.3 Transformation of *E. coli*

An aliquot of 0.1 ml competent cells was mixed with 2 μl ligation reaction mixture, incubated on ice for approximately 30 min, shocked at 42 $^\circ$C 30" and immediately transfered onto the ice. Then, 0.5 ml warm LB-medium (37 $^\circ$C)was

added to the cells and the mixture was incubated for 1 h at 37 $^{\circ}\mathrm{C}$ with vigorous shaking (250 rpm). Afterwards, transformed cells were transferred to LB-agar plates containing 50 μg/ml ampicillin.

3.2.4 Plasmid preparation

Colonies were picked and inoculated in 2.5 ml TB medium containing 50 μg/ml ampicillin and incubated overnight at 37 $^{\circ}\mathrm{C}$ with vigorous shaking (250 rpm). After approximately 14 hours, 2 ml of the culture were pelleted (6800 $\times$ g, 2 min, 4 $^{\circ}\mathrm{C}$). The cell pellet was mixed with 400 μl lysis solution (0.2 N NaOH, 1 % SDS), immediately neutralized with 300 μl 7.5 M NH_4OAC and kept for 10 min on ice, to precipitate genomic DNA and proteins, then sedimented at 14000 $\times$ g for 10 min at 4 $^{\circ}\mathrm{C}$. The plasmid DNA was precipitated from the supernatant with 500 μl 2-propanol and pelleted (14000 $\times$ g, 30 min, 4 $^{\circ}\mathrm{C}$). Finally, the DNA pellet was washed with 70 % EtOH, dried and resuspended in 50 μl TE (10 mM Tris-HCl pH 8.0, 1 mM EDTA) supplemented with 50 μg/ml RNaseA.

For Maxiprep, a single colony was picked and inoculated in a primary culture of 3 ml TB medium (containing selection reagent accordingly) and incubated for approx. 8 h at 37 $^{\circ}\mathrm{C}$ with vigorous shaking (250 rpm). Afterwards the initial culture was diluted 1:1000 into 250 ml selective TB medium and grown overnight. Bacterial cells were harvested by centrifugation (6000 $\times$ g, 15 min, 4$^{\circ}\mathrm{C}$) and the purification of plasmid DNA was performed with QIAGEN Endofree Plasmid Maxi Kit according to manufacturer's protocol. DNA concentration was determined spectrophotometricly by absorption at the wavelength of 260 nm.

3.3 Cell culture

PT1590 cells, skin fibroblasts and HEK cells were kindly provided by Dr. Stoecklein, Dr. Reifenberger and Dr. Mielke, respectively. PT1590 cells were grown in RPMI 1640 medium (Invitrogen, Karlsruhe) containing 10 % fetal bovine serum (Invitrogen, Karlsruhe) and 1 % penicillin/Streptomyces (Invitrogen, Karlsruhe). HEK cells and skin fibroblasts were grown in DMEM medium (Invitrogen, Karlsruhe) supplied with 10 % fetal bovine serum and 1 % penicillin/Streptomycin solution. Culture medium for stable transfected HEK cells was supplemented with puromycin (Invitrogen, Karlsruhe) at 0.4 μg/ml to maintain selection pressure. PT1590 and HEK cells were maintained as subconfluent monolayer cultures at 37 $^{\circ}\mathrm{C}$ under a humidified 5 % CO_2 atmosphere. For passaging, cell layers were washed once with PBS (Invitrogen, Karlsruhe), detached by a short trypsinization with Trypsin- EDTA solution (0.5 g/L of trypsin (1:250) and 0.2 g/L of EDTA·4Na) and reseeded with the density of 5000 cells/cm^2 for skin fibroblasts and 2000 cells/cm^2 for PT1590 and HEK cells, accordingly.

3.4 RNA isolation and cDNA reverse transcription

Total RNA from cultured cells and tissues was isolated using either the RNeasy mini kit (Qiagen, Hilden) or TriReagent (Sigma-Alderich, Muenchen). Before RNA isolation, the tumors from the xenograft model were homogenized by the Mixer Mill MM 200 (Retsch, Haan). The RNA concentration was determined by photometric measurement at 260 nm using Nanodrop-1000 (Peqlab, Erlangen). Aliquots of total RNA (1 μg) were applied for cDNA synthesis using Quantitect reverse transcription kit (Qiagen, Hilden). These experiments were performed

according to the manufactures' protocols.

3.5 Realtime RT quantitative PCR (qPCR)

Relative mRNA expression levels were quantified by qPCR. PCR was performed using an ABI 7300 real time system (Applied Biosystems, Darmstadt) with Platinum SYBR green qPCR SuperMix-UDG kit (Invitrogen, Karlsruhe). The reaction mixture for each gene contained 10 μl of Platinum SYBR green qPCR SuperMix-UDG, 5 μl cDNA and 2.5 μl of each primer (with final concentration of 10 pmol) in a final volume of 20 μl. Glyceraldehyde- 3-phosphate dehydrogenase (GAPDH) was chosen as the endogenous control using the same reaction mixture and conditions. All PCR primer sequences were designed by Primer3 software (http://frodo.wi.mit.edu/primer3/) (listed in section 3.1). The PCR amplification condition was as the following: 50 $^{\circ}\mathrm{C}$ for 2 min and 95 $^{\circ}\mathrm{C}$ for 2min, and this was followed by 40 cycles at 95 $^{\circ}\mathrm{C}$ for 30 s and then 60 $^{\circ}\mathrm{C}$ for 30 s. During the last steps, a temperature gradient between 95 $^{\circ}\mathrm{C}$ and 60 $^{\circ}\mathrm{C}$ was created for the analysis of the dissociation curves. This post-PCR dissociation curve was used to monitor the quality of PCR. No template controls, substituting water for cDNA, and a negative reverse transcription were used in each run. Target gene expression was calculated for each sample relative to the housekeeping gene, GAPDH, using the $2^{-\Delta\Delta C_t}$ method as described [Dai et al. 2007].

3.6 Quantification of HA from extra-, peri-and intracellular compartments

HA from the extracellular, pericellular and intracellular compartments of cultured cells were isolated and quantified as previously described [Wilkinson et al. 2006]. 24 hours after changing medium, culture supernatant was harvested and used for determination of extracellular HA. Next, cells were gently washed in PBS, trypsinized and centrifuged at 1000 $\times$ g for 5 min. The resulting supernatant was taken and HA determined in this fraction was defined as pericellular HA. Afterwards, the cell pellet was washed twice in PBS and centrifuged at 1000 $\times$ g for 5 min. Aliquots from the cell pellets were collected to isolate total protein. The protein concentration, which mimics the total cell number, was then quantified by Bradford protein assay (Bio-rad, München) and used to normalize the HA concentration. The HA from the cell pellet represented the intracellular HA fraction. The culture medium, the trypsin supernatant and the cell lysate were then digested by papain (5 mg/ml) in 0.1 M Tris-acetate, 5 mM EDTA, 5 mM L-cysteine hydrochloride at pH 7.3 for 24 hours at 60 $^{\circ}\mathrm{C}$. After digestion, papain was then inactivated by heating to 100 $^{\circ}\mathrm{C}$ for 20 min. The HA concentration was subsequently measured by a commercial HA ELISA test kit (Corgenix, Peterborough).

3.7 Cell proliferation

CyQUANT NF cell proliferation kit was used to measure the growth rate of PT1590 cells according to the manufacture's protocol. Briefly, PT1590 cells were seeded in a 96 well microplate at a density of 4000 cells per well. For

each condition, the cells were seeded as octuplicate. The CyQUANT NF dye reagent was diluted 1:500 in 1$\times$ HBSS buffer (Hank's buffered salt solution included in the kit). For the measurement, the culture medium was removed and 100 μl 1$\times$ dye reagent was dispensed to each microplate well. Instead of the dye reagent, 100 μl 1$\times$ HBSS buffer was used as the background count. The microplate was then incubated at 37 $^{\circ}\mathrm{C}$ for 30 min. Fluorescence intensity of each sample was measured using a fluorescence microplate reader (excitation at 485 nm and emission at 530 nm). The cells were first allowed to adhere for 4 hours. The control value was therefore taken after 4 hours adhesion. 24 hours after seeded, the cell density was again measured and the proliferation rate was calculated with normalization to the 4-hour initial value.

3.8 Cell adhesion

PT1590 cells were trypsinized and washed two times with PBS before assessing the adhesion. The cells were resuspended to 1 $\times$ 10^6 cells/ml with culture medium containing 10 % FCS. Subsequently, the cells were seeded in 96-well plates (100 μl per well). After 15 minutes of incubation at 37 $^{\circ}\mathrm{C}$, the unattached cells were washed away by PBS buffer. The attached cells were then fixed and stained by crystal violet solution containing 50 % methanol for 5 min at 22 $^{\circ}\mathrm{C}$ and washed 6 times with 100 μl ddH_2O. Finally, the cells were lysed by 100 μl 2 % SDS. A UV spectrometric microplate reader was used to determine the absorption at 540 nm.

3.9 Cell growth kinetics

After trypsinazation, cells were resuspended and seeded in 12-well plates at a density of 4000 cells per well. The cell number was determined by a Neubauer chamber at 1, 2, 3, 4, and 5 days after seeding. Before loading onto the Neubauer chamber, the cell suspension was mixed 1:1 with trypan blue to distinguish living and dead cells.

3.10 Intracellular HA staining & confocal imaging

Staining of intracellular hyaluronan was performed as previously described using a biotinylated hyaluronan-binding protein specific for hyaluronan [Evanko and Wight 1999]. Skin fibroblasts (2×10^5 per 6-well) were plated and grown on 22-mm^2 coverslips inserted into the wells for 24 hours in DMEM containing 10 % fetal bovine serum. Extracellular and pericellular hyaluronan was removed prior to fixation by incubating the cells with 2 U/ml *Streptomyces* hyaluronidase (Sigma-Aldrich, München) in culture medium at 37 $^\circ$C for 60 min. Cells were fixed in 3.7 % paraformaldehyde in PBS for 10 min at 22 $^\circ$C and then permeabilized with 0.5 % Triton X-100 for 10 min. Afterwards, cells were blocked with 1 % BSA in PBS for 1 hour at 22 $^\circ$C. The biotinylated HABP was used at a concentration of 2.5 μg/ml in PBS containing 1 % BSA for 1 hour at 22 $^\circ$C. The biotinylated HABP was further detected with Cy3-streptavidin. Nuclei were counterstained with Hoechst 33342 (Invitrogen, Karlsruhe) at 1 μg/ml in H_2O for 10 min at 22 $^\circ$C. Coverslips were mounted with Antifade Mounting Medium (Vector Laboratories, CA, USA). Controls for specificity of the intracellular hyaluronan staining included digestion of the cells with Streptomyces hyaluronidase after permeabi-

lization and without permeabilization before adding biotinylated HABP.

For microscopic analysis, a Zeiss inverted LSM 510 META confocal laser fluorescent microscope (Carl Zeiss, Jena) with 63 $\times$/1.4 NA oil-immersion objective was used. Hoechst 33342 was excited by diode laser at 351 nm. Argon laser was used to excite Cy3 at 543 nm wavelength. The emission signals were collected through proper filters. All the images, including the negative controls, were taken under the same condition.

3.11 Vector construction of stable transfection

The pMC-EYFP-P vector was used for YFP-HAS fusion protein construction. As shown in figure 3.1, the CMV promoter drives the expression of YFP fusion protein as well as the selection marker, namely puromycin resistant gene (pAC). Human HAS2, HAS3v1 and HAS3v2 coding sequences were isolated from total RNA of human smooth muscle cells by RT-PCR with primers indicated in table 3.5. The PCR products of HAS2 and HAS3v1 are about 1.7 kb and HAS3v2 about 0.9 kb respectively. The multicloning site is located at the c-terminal of the YFP coding sequence. N-terminal YFP-HAS fusion protein coding sequences were constructed using the MluI and EcoRI restriction sites. All the coding sequences were controlled by sequencing.

3.12 Construction of stably transfected cell lines

HEK cells were grown until they reach 80 % confluency in monolayer culture (25 cm^2). Then, HEK cells were splitted 1:4 24 hours before transfection. Cells

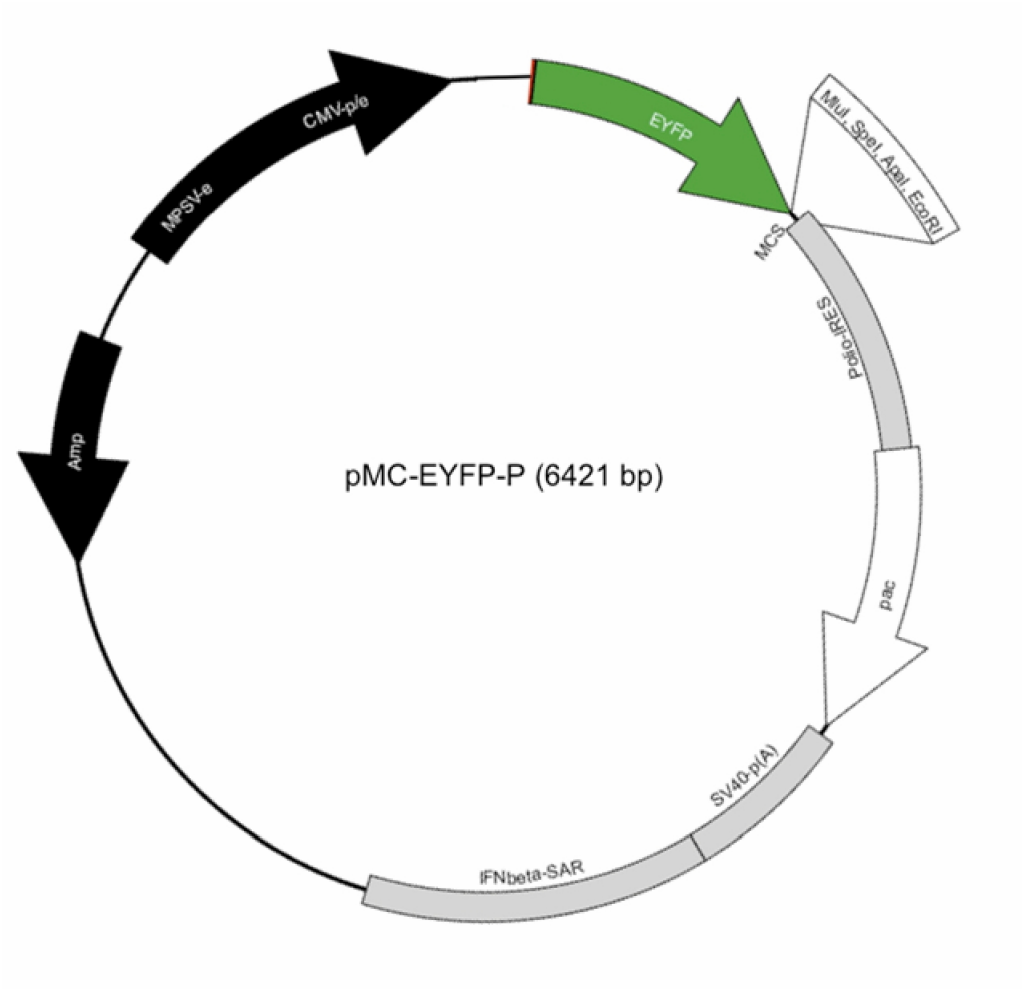

Figure 3.1: **Vector map of pMC-EYFP-P**

CMV promoter drives the expression of YFP fusion protein as well as the selection marker, namely puromycin resistant gene (pAC). The multicloning site is located at the c-terminal of the YFP coding sequence. Human HAS2, HAS3v1 and HAS3v2 coding sequences were isolated from total RNA of human smooth muscle cells by RT-PCR. N-terminal YFP-HAS fusion protein coding sequences were constructed using the MluI and EcoRI restriction sites.

	Primer sequences (5' - 3')
MluI-hHAS2-F	AAAACGCGTATGCATTGTGAGAGGTTTCT
EcoRI-hHAS2-R	AAAGAATTCTCATACATCAAGCACCATGT
MluI-hHAS3v1-F	AAAACGCGTATGCCGGTGCAGCTGACGACAG
EcoRI-hHAS3v1-R	AAAGAATTCTCACACCTCAGCAAAAGCCAAG
MluI-hHAS3v2-F	AAAACGCGTATGCCGGTGCAGCTGACGACAG
EcoRI-hHAS3v2-R	AAAGAATTCTCACTGCTCTCTAGAAACGTGG

Table 3.5: **Primers for YFP-HAS fusion protein construction**

were transfected with 1 μg DNA using Effectene Transfection Reagent (Qiagen, Hilden) according to the manufacturer's instructions. Transfection efficiency was monitored by fluorescence microscopy after 24 hours. The transfection efficiency appeared to be between 20 - 90 % depending on the construct used. 30 hours after transfection, cells were appropriately seeded into d-150 (150 mm in diameter) tissue culture dishes. Subsequently, stably transfected cell clones were selected by 0.4 μg/ml puromycin for 7 days. Stably expressing clones were then picked and reseeded in the 6-well in selection medium. For maintenance, the stable cell clones were cultured in selection medium.

3.13 Live-cell staining and imaging

The live-cell-imaging chamber (Ibidi, Martinsried) was coated with 200 μl poly-L-lysine (25 μg/ml) for 2 hours at 22 $^{\circ}\mathrm{C}$ under sterile condition. 24 hours before microscopy, the HEK cells were seeded in a live-cell-imaging chamber at a density of 5000 cells/cm^2. Before microscopy, the culture medium was exchanged by CO_2-independent medium (Invitrogen, Karlsruhe). An epifluorescent microscope and a 40 $\times$ oil immersion objective were used for imaging. The objective

holder was pre-warmed to 37 $^{\circ}\mathrm{C}$ before usage.

To study subcellular localization, cells were stained with either Image-iT LIVE plasma membrane labeling Kit (Invitrogen, Karlsruhe) or ER-Tracker Red (Invitrogen, Karsruhe) according to the manufacturer's protocol.

3.14 HAS enzymatic capture assay

Enzymatic activity of cellular HAS isoforms was determined in microsomal preparations. Briefly, cells were sonicated in microsome buffer (PBS containing 0.01 % SDS, 1 mM PMSF, 1mM EDTA, 20 mM DTT) for 12 min and were vortexed in between. The plasma membrane and nuclear fragments were then sedimented by centrifugation at 10,000 $\times$ g at 22 $^{\circ}\mathrm{C}$ for 20 min. Supernatants were collected for additional centrifugation at 100,000 $\times$ g for 1 hour at 4 $^{\circ}\mathrm{C}$. The pellet, which is enriched in microsomes, was resolved in 200 μl microsome G buffer (PBS containing 0.01 % SDS, 1 mM PMSF, 1 mM EDTA, 20 mM DTT with 30 % Glycerol) and stored at -20 $^{\circ}\mathrm{C}$ for overnight. Microsomes were mixed 1:1 with HAS buffer (PBS containing 2 mM $MgCl_2$, 1 mM UDP-Glucosamine, 1mM UDP-Glucuronic acid, 1 mM PMSF, 1 mM EDTA, 1 mM DTT) and incubated at 37 $^{\circ}\mathrm{C}$ for 24 hours. As control, half of the microsomal solution was treated with *Streptomyces* hyaluronidase for 2 hours at 37 $^{\circ}\mathrm{C}$ to remove the HA from the HA-HAS complex. Subsequently, 1 μg of biotinylated HABP was added to the microsomes with/without *Streptomyces* hyaluronidase treatment and incubated at 37 $^{\circ}\mathrm{C}$ for 1 hour. Strepavidin-agarose beads were added to each vial and incubated at 22 $^{\circ}\mathrm{C}$ for 1 hour. The agarose beads were pelleted by centrifugation and washed two times with PBS. Then, protein lysis buffer (receipt shown in section 3.15.1) was added to the agarose beads to elute proteins from the

beads. The protein lysate was collected by centrifugation and denatured for 5 min at 95 $^{\circ}\mathrm{C}$ prior to further analysis.

Microsomal preparations from YFP, YFP-HAS3v1 and YFP-HAS3v2 stably trasfected HEK cells were used for HAS enzymatic activity assay. Protein lysates were run on 10 % SDS-PAGE gels according to routine procedures. After blotting, the nutrocellulose membranes were blocked by blocking buffer (recipe in section 3.1) at 22 $^{\circ}\mathrm{C}$ for 1 hour. Then, the membranes were incubated with the YFP antibody (Clontech, France) dilluted 1:4000 in blocking buffer with gentle agitation overnight. Membranes were washes three times with 1 $\times$ TBST for 5 minutes each and further incubated with IRDye 800CW Goat Anti-Mouse IgG (Licor, Bad Homburg) with 1:5000 dilution in blocking buffer at 22 $^{\circ}\mathrm{C}$ for 1 hour. Finally, membranes were washed 6 times with 1 $\times$ TBST for 5 minutes each and images were taken and analyzed by Odyssie Imager (Licor, Bad Homburg).

3.15 Immunoblotting

Recipes of buffers and gels used for immunoblotting are listed in section 3.1

3.15.1 Protein isolation from cultured cell

Cell lysis was performed with lysis buffer (100 mM Tris-HCl, pH 6.8, 2 % Glycerol, 2 % SDS, 10 mM DTT, 0.7 M Urea, 10 mM EDTA, 1 mM PMSF, 0.02 % bromphenol blue). Cell lysates were homogenized by sonification for 15 min. Subsequently, samples were denatured at 95 $^{\circ}\mathrm{C}$ for 5 min. Protein sample were then stored at -20 $^{\circ}\mathrm{C}$.

3.15.2 SDS-Polyacrylamide Gel Electrophoresis (PAGE) & Coomassie staining

Protein lysates were run on 10 % SDS-PAGE gels according to routine procedures.

The SDS gel was stained by Pageblue protein stain solution (Fermentas, St. Leon-Roth) according to the manufacturer's protocol. Briefly, the gel was washed 3 times with 100 ml ddH_2O for 10 min each to wash SDS away. Then, the gel was soaked in the pageblue protein stain solution for 1 hour with gentle agitation. To remove the background staining, the gel was rinsed with ddH_2O for 5 min before imaging.

3.15.3 Blotting

Proteins were electrophoretically transferred from the gel to nitrocellulose membranes by the semi-dry method. Briefly, 3 Whatman papers were soaked in transfer buffer and then stacked on the cathode side of the gel. Then, the nitrocellulose membrane was shortly rinsed in the transfer buffer and carefully stacked on the anode side of the gel. Another 3 Whatman paper were stacked on top of the membrane after soaking in transfer buffer. Subsequently, the stack was placed between two graphite plates and the trans-membrane blotting was performed with constant volt 12 V for 1 hour.

Antibody	Company	Dilution Ratio
YFP (JL8)	Clontech	1:4000
β-Tubulin	Santa Cruz	1:10000
FAK	BD Bioscience	1:1000
phospho-FAK	Cell Signaling	1:1000
ERK	Cell Signaling	1:1000
phospho-ERK	Cell Signaling	1:1000
IRDye 800CW Goat Anti-Mouse IgG	Licor	1:5000
IRDye 680 Goat Anti-Rabbit IgG	Licor	1:5000

Table 3.6: **Antibody dilution ratios**

3.15.4 Immunodetection of protein

The nitrocellulose membrane was blocked in blocking buffer with gentle agitation for 1 hour at 22 $^{\circ}\mathrm{C}$. Afterwards, the first antibody was diluted in blocking buffer. The membrane was incubated in the first antibody solution on the shaker for either 1 hour at 22 $^{\circ}\mathrm{C}$ or overnight at 4 $^{\circ}\mathrm{C}$. Then, the membrane was washed three times in 1 $\times$ TBS containing 0.1 % Tween 20 for 5 min each. After washing, the membrane was soaked for 1 hour at 22 $^{\circ}\mathrm{C}$ with the secondary antibody. The secondary antibody was diluted with blocking buffer under corresponding ratio. The antibody dilution ratios are listed in table 3.6. The blot membrane was then immersed 5 times for je 3 min in 1 $\times$TBS containing 0.1 % Tween 20. Finally, the image was taken and analyzed by Odyssiey Imager (Licor, Bad Homburg).

3.16 Lentiviral transduction

3.16.1 Overexpression vector cloning

Lentiviral vectors can deliver large cDNAs to a variety of dividing and non-dividing cells, including terminally differentiated mammalian cells e.g. neurons, lymphocytes and macrophages. Due to the lack of toxicity and immune response, lentiviruses became a very attractive tool for gene delivery and possibly further use for human gene therapy. The safety of the lentiviral vectors has been improved with the generation of self-inactivating vectors and a minimal packaging system. For this study, a vector system constructed by Prof. Hanenberg was used [Dai et al. 2007]. The HIV envelope glycoprotein was replaced by VSV-G. To minimize the amount of HIV coding regions present in the packaging system, a second generation of the packaging system was develolped with extensive deletions of the viral genome. This 2^{nd} generation packaging system contains only the gag, pol, tat, and rev genes of HIV-1 and lacking all accessory genes, since accessory genes (vpr, vpu, vif and nef) are not required for efficient production of viral particles. The 2^{nd} generation lentivirus packaging system contains 3 plasmids. The pVSVG is the plasmid that encodes the envelope protein. pCD/NL-BH is the packaging plasmid and pCL1 was used as the transfer plasmid. The pCL1 is used as the mock vector, which is characterized by the EGFP expression (shown in figure 3.2). pCL1mcs was digested by restriction enzyme XhoI and EcoRI. The cDNA of human HAS3v2 was obtained by RT-PCR using total RNA from human smooth muscle cells with the following primers: XhoI-HAS3v2-F: AAACTCGAGATGCCGGTGCAGCTGACGACAG and EcoRI-HAS3v2-R: AAAGAATTCTCACTGCTCTCTAGAAACGTGG. Then, the human HAS3v2 cDNA was cloned into the multiple cloning site of pCL1mcs

to achieve the new plasmid named pCL1mcs-HAS3v2. The coding sequence of HAS3v2 in the pCL1mcs-HAS3v2 was confirmed by sequencing.

3.16.2 Lentivirus production

The day before transfection, HEK293T cells were seeded into d-100 (100 mm in diameter) cell culture dishes at a density of 2.5 - 3 $\times$ 10^6 cells per plate. DMEM medium supplied with 10 % heat-inactivated FCS (v/v) (PAN biotech, Aidenbach) and 1 $\times$ penicillin/Streptomycin (100 U/ml of penicillin, 100 μg/ml of Streptomycin) was used for virus production.

Transfection was carried out using polyethylenimine (PEI) (Sigma-Aldrich, München) method. 5 μg of transfer vector, either pCL1 mock or HAS3v2 over-expression vector pCL1mcs-HAS3v2, 5 μg of packaging plasmid (pCD/NL-BH) and 5 μg of envelope plasmid (pVSVG) were diluted with DMEM medium to a final volume of 2 ml in a sterile reaction tube. 45 μl of 1 mg/ml PEI was added to the vector mix, and then thoroughly vortexed. Afterwards, the mixture was incubated for 20 min at 22 $^{\circ}\mathrm{C}$ under sterile condition to allow the DNA-PEI complex form. The 293T culture medium was replaced with 4 ml DMEM with 10 % heat-inactivated FCS and 1 $\times$ Pen/Strep solution. Subsequently, the DNA-PEI complex was added drop-wise to the 293T. After gentle mixing, the 293T cells were incubated for 16 hours in the humidified incubator at 37 $^{\circ}\mathrm{C}$ and 5 % CO_2. Then, the transfection medium was changed to complete medium containing 10 mM sodium butyrate to induce the CMV promotor activity. 6 hours after induction, the culture medium was refreshed with 5 ml IMDM medium (Sigma-Aldrich, Muenchen) supplied with 10 % heat-inactivated FCS and 1 $\times$ Pen/Strep solution. The virus containing IMDM medium was harvested and filtered through a 0.45 μm sterile filter 24 hours after induction. Then, the medium was either

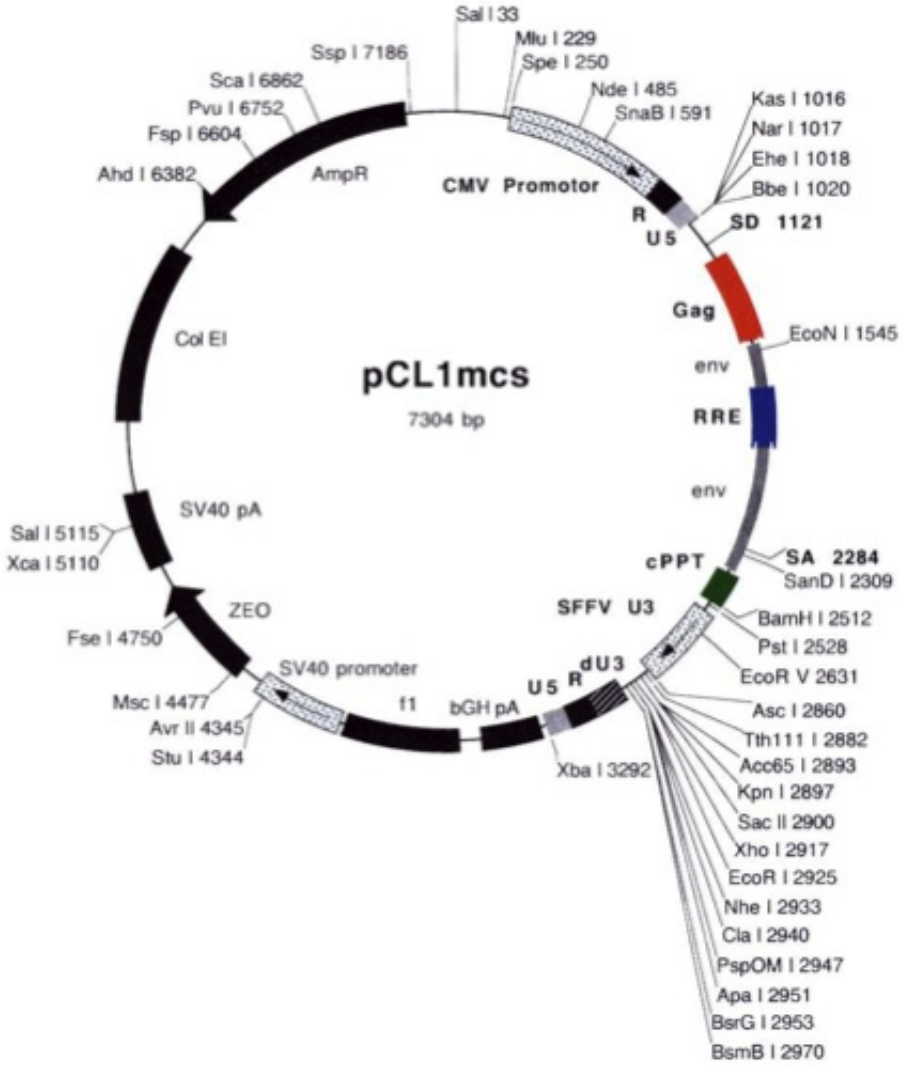

Figure 3.2: **Vector map of pCL1mcs**

The multicloning site is located after SFFV U3 fragment. Human HAS3v2 coding sequences was isolated from total RNA of human smooth muscle cells by RT-PCR and constructed using the XhoI and EcoRI restriction sites. CMV promoter drives the expression of either EGFP (mock control) or HAS3v2.

used for transduction directly or stored at -80 $^{\circ}\mathrm{C}$ after aliquots.

3.16.3 Lentivirus titration

The RETRO-TEK HIV-1 p24 Antigen ELISA (Zeptometrix , USA) is an enzyme linked immunoassay used to detect Human Immunodeficiency Virus Type 1 (HIV-1) p24 antigen. Microwells are coated with a monoclonal antibody specific for the p24 gag gene product of HIV-1. Viral antigen in the specimen specifically bound to the immobilized antibody during incubation. The captured antigen then detected with a high-titer human anti-HIV-1 antibody conjugated with biotin. Following a subsequent incubation with Streptavidin-Peroxidase, color develops as the bound enzyme reacts with the substrate. Resultant optical density is proportional to the amount of HIV-1 p24 antigen present in the specimen.

3.16.4 Lentiviral transduction

Both skin fibroblasts and PT1590 cells were grown 50 % - 70 % confluence before lentiviral transduction. DMEM medium was used for skin fibroblast while PT1590 cells were transduced in RPMI 1640 medium. Both medium were supplied with 10 % heat-inactivated FCS and 1 $\times$ Pen/Strep solution. For transduction, equal titers of virus were thawed on ice and diluted in the appropriated medium with 4 μg/ml protamine sulfate. Protamine sulfate is a small, positively charged molecule that binds to cell surfaces, neutralizes surface charge and thereby greatly enhances transduction by lentiviruses. The cell culture medium was changed 24 hours and 96 hours after transduction.

3.17 Xenograft of EAC cells in nude mice

3.17.1 Tumor inoculation

10 weeks-old NMRI nu/nu mice were used for subcutaneous tumor formation after xenografting of PT1590 cells. Five days after lentiviral transduction, cell injections were performed with 100 μl cell suspension containing 1 $\times$ 10^6 cells. Cells were harvested, counted and washed two times using PBS. Then, the pellets were resuspended in PBS. After cleaning the skin with alcohol, tumor cell suspensions were injected s.c. using an 1 ml insulin syringe into both flanks, and the mice were monitored for 35 days after xenografting. The animal experiments were approved by the local animal facility and the Landesamt fr Natur, Umwelt und Verbraucherschutz, NRW.

3.17.2 Growth curve

Starting at 14 days after injection, tumor diameters were measured with digital calipers every 3 or 4 days. The tumor volume in mm^3 was calculated by the formula: $Volume = (Length \times width \times height) \times \pi/2$. The tumor growth was monitored by determining of the cumulative tumor volume until harvesting. The wet weight of tumors were measured at harvesting.

3.17.3 Immunohistochemistry

The mice were sacrificed by asphyxiation with CO_2 and the tumors were dissected. Part of the tumors were embedded in OCT Tissue Tek (Sakura Finetek, Netherlands), frozen at -40 $^\circ$C isopentane and stored at -80 $^\circ$C. Cryostat CM

3050 from Leica Instruments was used to cut 2 μm thick cryosections. Sections were loaded on Superfrost slides (Fisher Scientific, USA) and stored at -20 $^{\circ}\mathrm{C}$.

For immunohistrochemistry, the cryo-sections were blocked with 10 % fetal calf serum and 1 % bovine serum albumin for 1 hour at room temperature. For hyaluronan staining, the slides were subsequently incubated with biotinylated HAbP (2 μg/ml; Seikagaku, Tokyo, Japan) at 4 $^{\circ}\mathrm{C}$ overnight. After three washes with phosphate-buffered saline (PBS), the sections were incubated with avidin-biotin peroxidase (Sigma, St. Louis, MO), and the color was developed with 3,3'-diaminobenzidine (DAB; Sigma). Nuclei were stained with hemalaun solution (Merck, Darmstadt, Germany). As a negative control, sections were incubated with *Streptomyces* hyaluronidase (ICN, Costa Mesa, CA) at a concentration of 2 U/ml (1 hour, 37 $^{\circ}\mathrm{C}$) before HA staining. Proliferation marker, Ki67, was stained using rabbit anti- human/mouse ki67 antibody (1:25; Novus Biologicals, Littleton, CO) and sheep anti-rabbit IgG (peroxidase-conjugate, 1:50; Sigma-Aldrich, Steinheim, Germany). DAB detection was as as described for HA staining

The images were taken at 100 $\times$ magnification with a Leica Upright Microscope (Leica, Wetzlar).

3.18 Statistical analysis

Quantitative results are presented as mean values $\pm$ standard error of the mean (SEM). Data sets were compared either by unpaired T-test or one way ANOWA using the software PRISM Graphad 5.0. *p value* $<$ *0.05* was regarded as statistically significant.

Chapter 4

Results

4.1 *In silico* enzymatic activity analysis of HAS3v2

4.1.1 Human HAS3 splicing variants: HAS3v1 & HAS3v2.

There are three mammalian hyaluronan synthase isoforms, namely HAS1, HAS2 and HAS3. The structures of these three genes are evolutionary conserved in mammalian species. Human HAS3 has two splicing variants: HAS3v1 and HAS3v2. As shown in figure 4.1 A, both splicing variants share the first two coding exons. The coding sequence on the last exon of HAS3v1 is different and longer than the one of HAS3v2. However, HAS3v2 spans over a longer part on the genome. The predicted protein topologies of both splicing variants are shown in figure 4.1 B. The prediction is based on hydropathy plots [Weigel et al. 1997]. Accordingly, HAS3v1 is predicted to have seven transmembrane domains, while HAS3v2 has only two. The intracellular loop between the 2^{nd} and the 3^{rd} transmembrane domain (66-383AA) of HAS3v1 is predicted to be the catalytic domain, through which hyaluronan is synthesized. The putative catalytic domain is based on the *in silico* evolutionary homologous analysis. HAS3v2 contains part of the catalytic domain (66-246AA) followed by a 35AA long c-terminal tail that is unique for HAS3v2..

4.1.2 Glycosyl transferase 2 domain.

Whether HAS3v2 contains a putative catalytic center was tested *in silico* by pfam (http://pfam.sanger.ac.uk/). Pfam is a database of protein families that includes their annotations and multiple sequence alignments generated using hidden Markov models. As shown in figure 4.2 A, the active glycosyl transferase

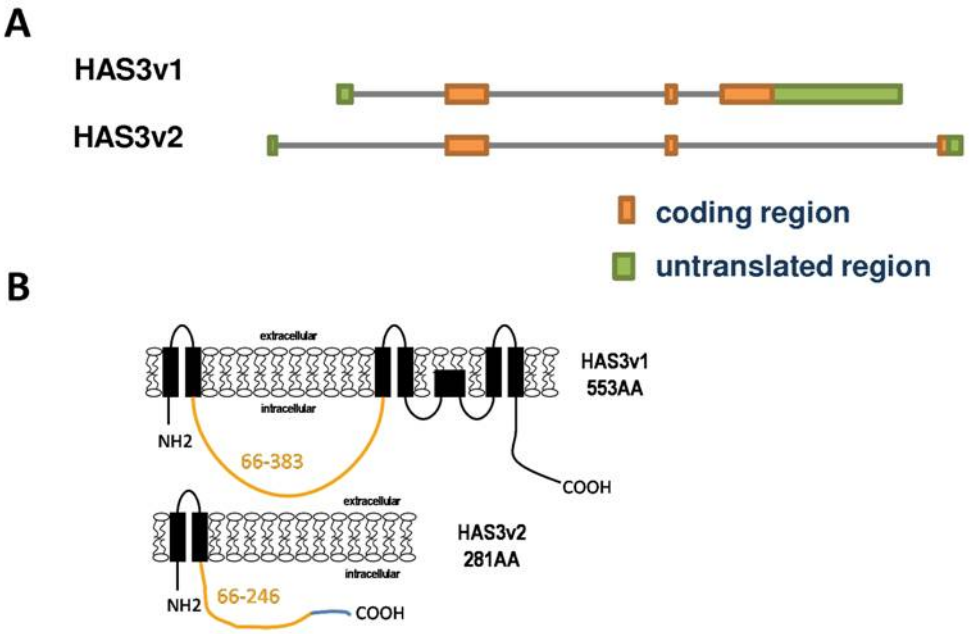

Figure 4.1: **Genomic and topological structure of human HAS3 isoforms**
(**A**): genomic structure of human HAS3 splicing variants; (**B**): predicted topological protein structure of HAS3 splicing variants. The orange intracellular part of HAS3v1 and HAS3v2 are identical in AA sequence. The blue part on the c-terminal of HAS3v2 indicates its unique AA composition.

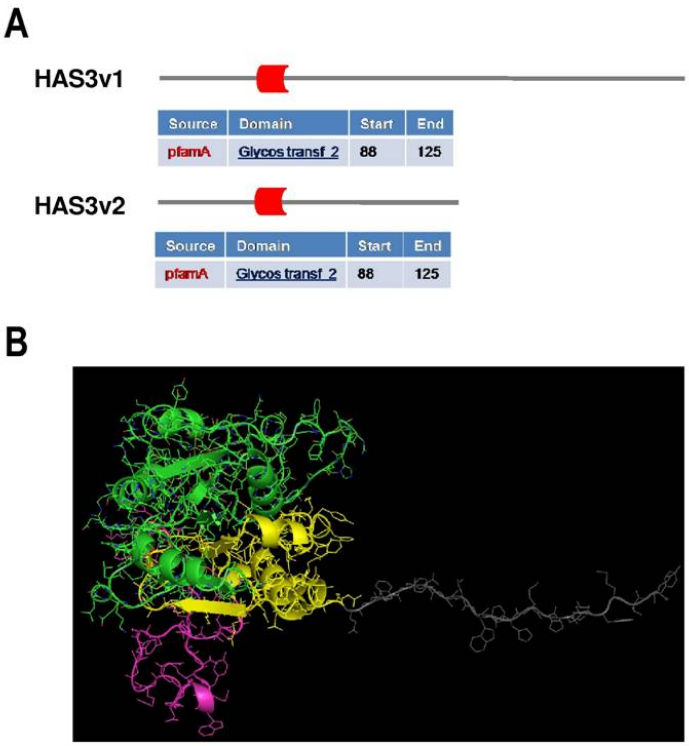

Figure 4.2: ***In silico* prediction of glycosyl transferase activity of HAS3v2**
(**A**): functional domain prediction using pfam. Glycosyl transferase 2 domain (red block) is detected from HAS3v1 and HAS3v2 (grey line indicates the AA sequence).; (**B**): 3D protein structure prediction of the active center of HAS3v1 and HAS3v2. The green overlay indicates the identical structure between HAS3v1 and HAS3v2. The yellow part is unique for HAS3v1 and pink part for HAS3v2 respectively.

2 domain was predicted for the amino acid sequence between AA 88 to AA 124 of both HAS3v1 and HAS3v2. This domain is localized within the predicted catalytic centers of HAS3v1 and HAS3v2. The glycosyl transferase 2 domain is the only enzymatic domain found in HAS3v1. Further, HAS3v1 is known to be an active hyaluronan synthase.

In addition, 3D protein structures of both the catalytic loop of HAS3v1 and the c-terminal intracellular tail of HAS3v2 were simulated using the software hhpred (http://toolkit.tuebingen.mpg.de/hhpred/). These two protein structures

were overlapped to analyze the structural similarity. As shown in figure 4.2 B, the overlap between the catalytic centers from HAS3v1 and HAS3v2 is indicated by the green color. Of note, the glycosyl transferase 2 domain is localized on this green overlap as well. The pink part is unique for HAS3v2 while the yellow part only exists in HAS3v1. Therefore, HAS3v2 might also function as active hyaluronan synthase, despite its truncated structure and the lack of 5 transmembrane domains compared to HAS3v1.

4.2 Subcellular localization of human HAS3v2

4.2.1 Localization of HAS3v2 as analyzed by YFP-HAS fusion protein.

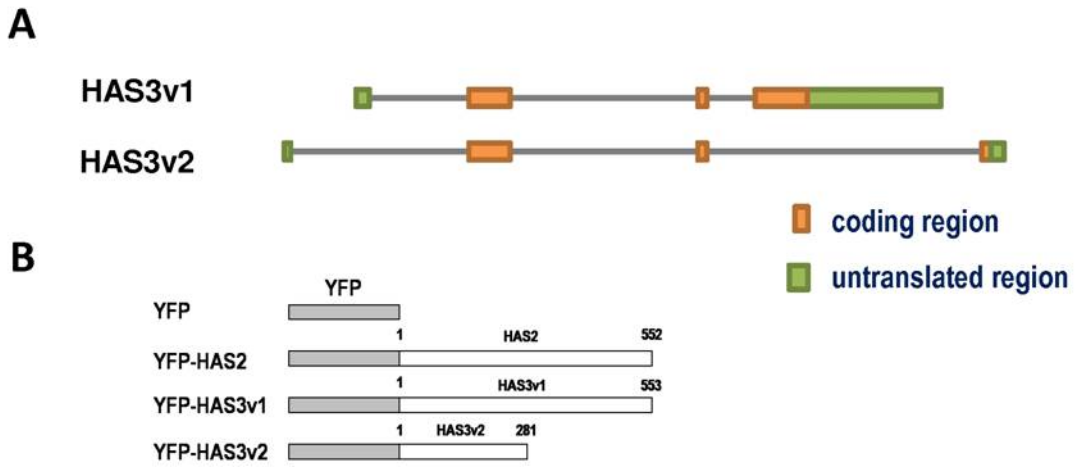

Figure 4.3: **Schematic structure of YFP-HAS fusion protein**

(**A**): Genomic structure of human HAS3; (**B**): Scheme of YFP-HAS fusion protein

To address the subcellular localization of HAS3v2, YFP fusion proteins were constructed. Figure 4.3 B shows the scheme of the plasmids. The CMV promoter was used to drive the expression of YFP-HAS fusion proteins. RT-PCR

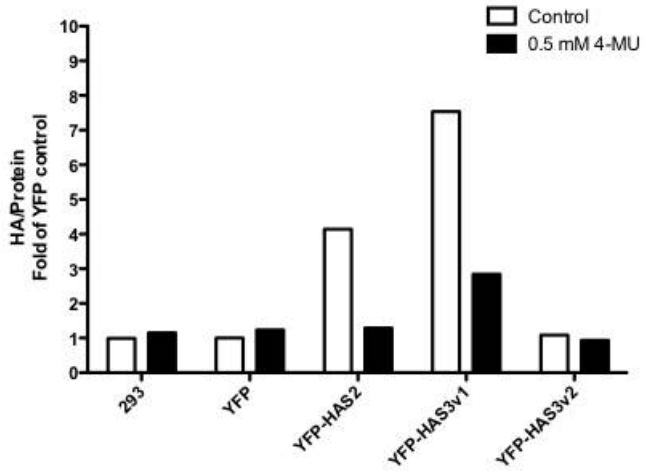

Figure 4.4: **HA quantification of extracellular secretion after YFP-HAS transfections**
After transfection of HEK 293 cells, HA concentration was determined from cell culture supernatant and normalized to cellular protein. In addition, 4-MU was used to inhibit HA synthesis. Data are normalized to YFP Control. white bar: without 4-MU; black bar: with 0.5 mM 4-MU; representative result out of triplicate experiment

was performed to obtain the full-length coding sequences of human HAS2, HAS3v1 and HAS3v2 from total RNA of human smooth muscle cells. Afterwards, these sequences were cloned to fuse onto the 3' end of YFP coding sequence. The YFP-HAS chimera were over-expressed by transfecting the target cell hosts. The mock YFP expression vector served as control.

4.2.2 Transfection of YFP-HAS2 and YFP-HAS3 causes increased HA in culture medium.

HEK 293 cells were selected as the host, in which YFP, YFP-HAS2, YFP-HAS3v1 and YFP-HAS3v2 stablely overexpressed. The stable cell clones were selected by puromycin beginning 24 hours after transfection. Colonies were picked after 7 days of selection. The culture medium from these stable cell

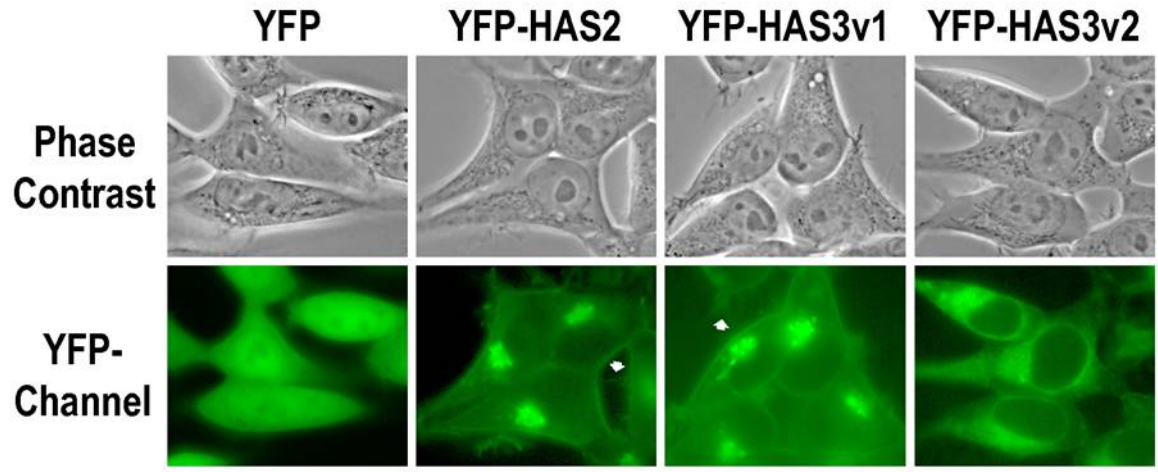

Figure 4.5: **Subcellular localization of YFP-HAS fusion proteins**
HEK 293 cells were transfected with YFP-HAS expression vectors and selected by promycin. After isolation of stable clones, the expression of YFP fusion proteins were monitored by fluorescence microscopy. Upper panel: phase contrast; lower panel: YFP channel. White arrows indicate the microvilli structure on plasma membrane. Magnification: 400 $\times$

lines were collected for measuring HA secretion within 24 hours after medium change. As is shown in figure 4.4, overexpression of YFP-HAS2 and YFP-HAS3v1 induced extracellular HA up to 7 fold within 24 hours compared to YFP mock control. The overproduction of HA could be attenuated by a specific inhibitor of hyaluronan synthases, namely 4-methylumbelliferone (4-MU). This indicates that the YFP-HAS fusion proteins are active. However, overexpressing YFP-HAS3v2 in HEK cell did not lead to increased HA secretion of HA in the cell culture medium.

4.2.3 The subcellular localization of HAS3v2 is different from HAS3v1 and HAS2.

The sub-cellular expression patterns of the YFP-HAS fusion proteins were examined by fluorescent microscopy. As shown in figure 4.5, the YFP mock con-

struct shows ubiquitous YFP signal throughout the cell, as well as in the nucleus. The expression patterns of YFP-HAS2 and YFP-HAS3v1 are similar. Importantly, these two YFP fusion proteins are expressed at the circumstance of the cell indicating the plasma membrane localization. In addition, increased microvilli structures can also be observed (indicated by white arrow in figure 4.5). YFP-HAS2 and YFP-HAS3v1 were also detected in cytosol. However, the fluorescent signal of YFP-HAS3v2 was localized in the cytosol characterized by a network-like structure. Furthermore, there was no clear signal surrounding the cell, suggesting that the YFP-HAS3v2 may not expressed in the plasma membrane.

4.2.4 Subcellularly, HAS3v2 does reside the ER and Golgi.

A plasma membrane marker was introduced to evaluate whether HAS3v2 is localized in the plasma membrane. As shown in figure 4.6 A, in case of YFP-HAS3v1 and YFP-HAS2 the YFP signal surrounding the cell overlapped with the cy3 signal from the plasma membrane marker. However, there was no overlap between the YFP signal from YFP-HAS3v2 and the plasma membrane marker. This illustrates that, unlike HAS2 and HAS3v1, HAS3v2 is not present in the plasma membrane. The YFP mock control shows ubiquitous signal inside the cell.

Endoplasmic reticulum (ER) has an interconnected-network structure in the cell, which is similar to the YFP-HAS3v2 expression pattern. HAS3v2 also has two predicted hydrophobic transmembrane domains. Therefore, it is suspected that HAS3v2 might be present in the ER. Cy3-ER marker was utilized for the co-localization experiment. In figure 4.6 B, the YFP mock control showed overlap with the ER-Golgi marker, which was expected due to the ubiquitous localization

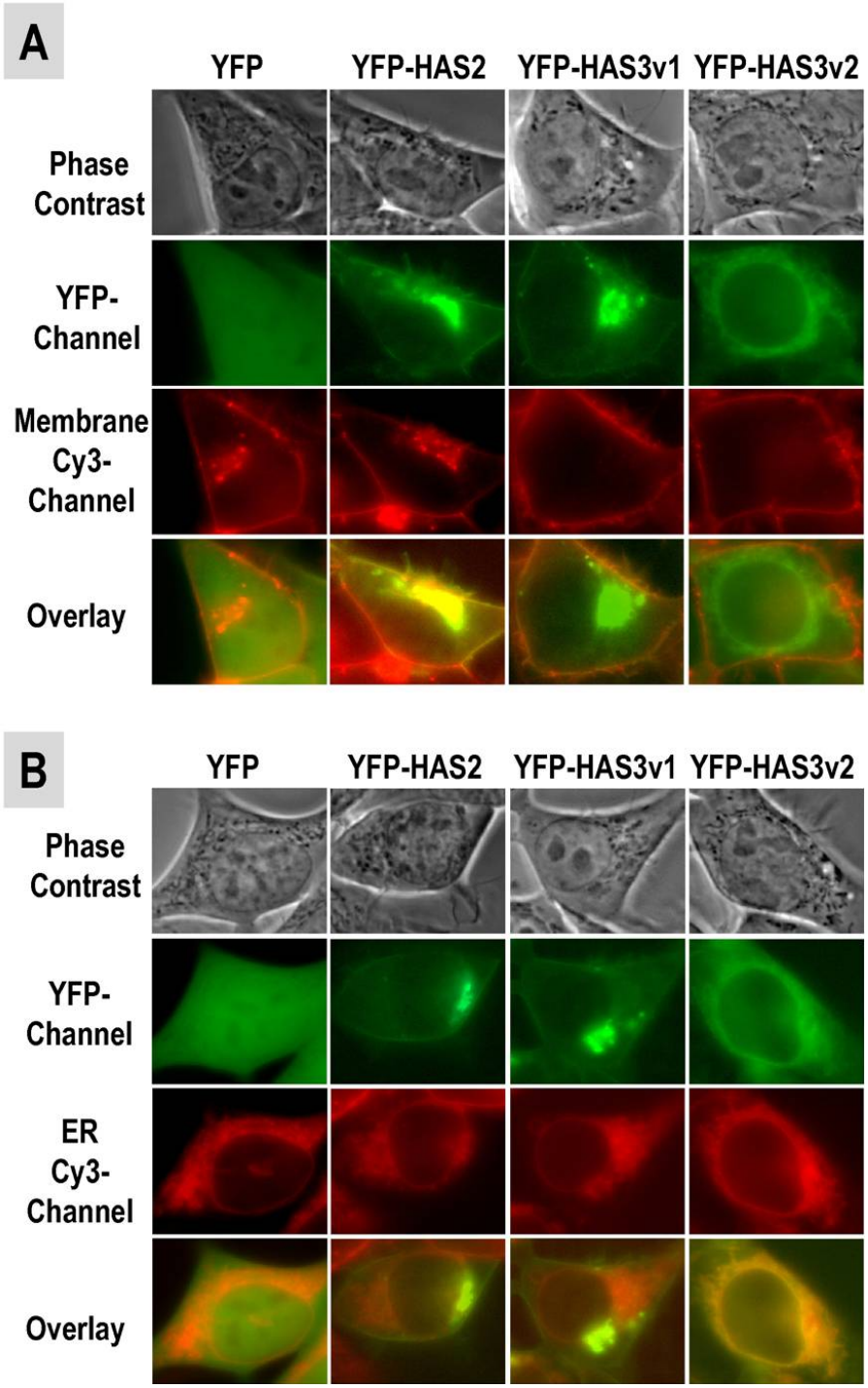

Figure 4.6: **Co-localization analysis using plasma membrane and ER marker**

(**A**): Cy3 conjugated plasma membrane marker; (**B**): Cy3 conjugated ER marker. Magnification: 400 $\times$

inside the cell. Also, partial overlap of the ER marker and the accumulated intracellular YFP signal from YFP-HAS2 and YFP-HAS3v1 was observed. The phase contrast pictures revealed that the condensed intracellular YFP signal of both YFP-HAS2 and YFP-HAS3v1 can be tracked to the golgi apparatus. This might be explained by the fact that both HAS2 and HAS3v1 are processed in the golgi and further transported to the plasma membrane. Importantly, the subcellular interconnected-network-like expression pattern of HAS3v2 showed a complete overlap with the ER marker, which suggested that HAS3v2 is indeed localized in the ER.

4.3 Biological function of HAS3v2

4.3.1 Overexpression of HAS3v2 causes a increase of intracellular hyaluronan.

Due to the ER localization of HAS3v2, HA-ELISA was performed in order to quantify the extracellular, pericellular as well as the intracellular hyaluronan of YFP-HAS3v2 compared to YFP transfected cells. For the extracellular and pericellular hyaluronan, there were no significant differences between YFP-HAS3v2 and YFP mock. Yet, there was significantly more intracellular hyaluronan from YFP-HAS3v2 compared to YFP mock (figure 4.7 A).

Subsequently, the HAS3v2 was overexpressed in human skin fibroblast using the lentiviral vector. Five days after transduction, the samples were collected for quantifying hyaluronan in the three different cellular compartments. As shown in figure 4.7 B, significant induction of intracellular hyaluronan occured in response to the overexpression of HAS3v2 compared to pCL1 mock.

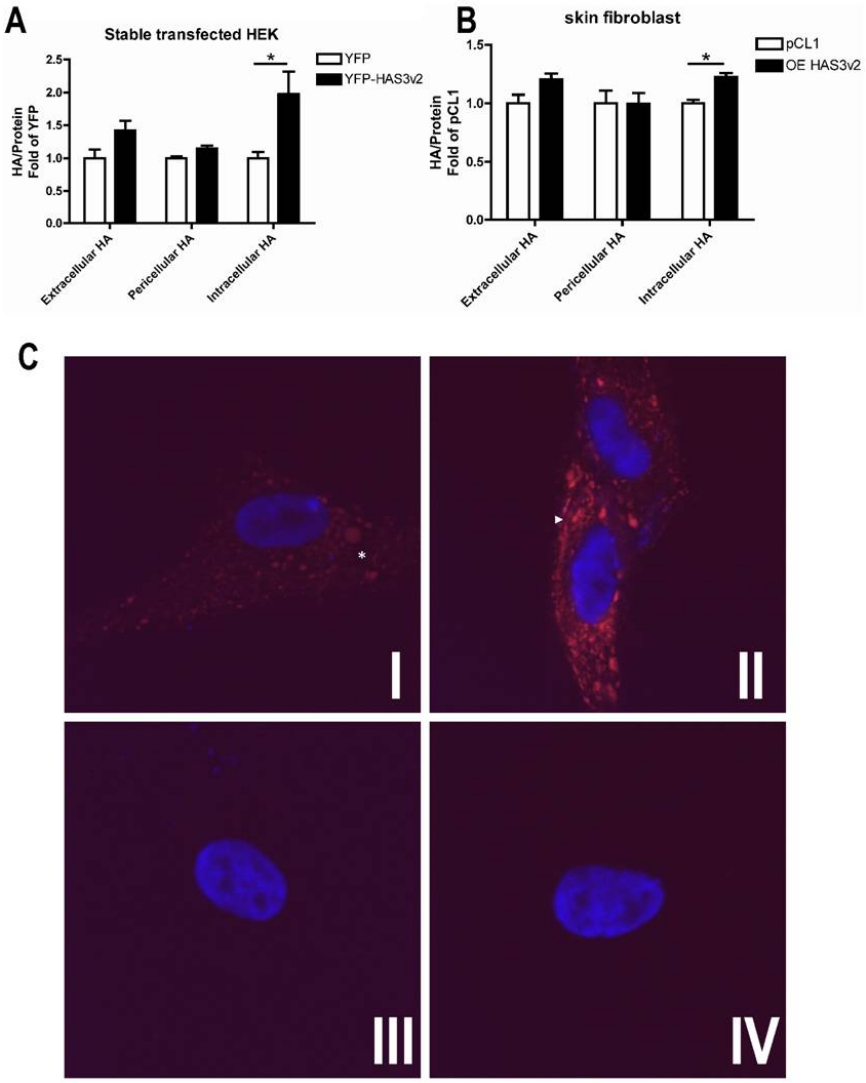

Figure 4.7: **HAS3v2 increases intracellular HA.**

Extra-, peri- and intracellular HA from stablely transfected HEK cells (**A**) and lentiviral transducted skin fibroblasts (**B**) were quantified by HA ELISA. Immunocytochemical analysis of intracellular HA from lentivirally transduced skin fibroblasts (**C**): pCL1 mock, permeabilized (**I**); overexpression of HAS3v2, permeabilized (**II**); overexpression of HAS3v2, non-permeabilized (**III**); overexpression of HAS3v2, *streptomyces* hyaluronidase digestion after permeabilization (**IV**). The HAS3v2 overexpression leads to a new localization pattern of intracellular HA (white triangle) compared to pCL1 mock (white star).

No statistically significant differences of extracellular and pericellular hyaluronan were observed between pCL1 mock and the overexpression of HAS3v2.

Beside the HA quantification by ELISA, intracellular hyaluronan was stained using the biotinylated HABP (HA binding protein). Skin fibroblasts were transducted either by pCL1 mock or HAS3v2 lentivirus prior to intracellular HA staining. Skin fibroblasts were fixed on the glass cover slides five days after transduction with either pCL1 mock (I) or HAS3v2 overexpression (II) lentiviruses. Then, the cells were digested by hyaluronidase before permabilizing the cell membrane. This procedure removes the extra- and pericellular hyaluronan. Afterwards, the cells were stained by biotin-HABP and cy3-streptavidin. Hoechst 33342 is used to indicate the cell nuclei. Images were taken by using confocal laser microscopy. As shown in figure 4.7 C, overexpression of HAS3v2 (II) in human skin fibroblast led to enhanced intracellular HA compared to pCL1 (I) mock control. To prove the specificity of intracellular staining, two negative controls were included. The HAS3v2 overexpressing skin fibroblasts were stained either without permeabilization of the cell membrane (III) or after *streptomyces* hyaluronidase digestion of permeabilized cells (IV). Both negative controls showed no positive staining, which confirms the specificity of the stainings in (I) and (II).

4.3.2 HAS3v2 might be an active intracellular hyaluronan synthase.

Intracellular HA may arise from both endocytosis and *de novo* synthesis [Evanko and Wight 1999]. Further, intracellular HA also accumulates on the outer membrane of ER. Therefore, HAS3v2 might be a promising candidate for an intra-

cellular hyaluronan synthase. The modified HAS enzymatic capture assay was used to investigate whether HAS3v2 can mediate HA synthesis [Kyossev and Weigel 2007]. As illustrated in figure 4.8 A, hyaluronan synthases form a complex with HA after synthesis. Biotinylated HABP was used to bind the HA of the HA-HAS complex so that the whole complex (bHABP-HA-HAS) can be co-immunoprecipitated by streptavidin conjungated agarose. As negative control, *Streptomyces* hyaluronidase was used to digest the HA from the complex before incubating with biotinylated HABP. After digesting the HA by hyaluronidase, hyaluronan synthases can not bind to the agarose anymore. As a result, no co-immunoprecititated HAS can be detected.

Microsomes are the raw membrane fraction of the cells, which contains mainly ER and golgi apparatus. Microsomes, which were isolated from YFP, YFP-HAS3v1 and YFP-HAS3v2 transfected HEK 293 cells were incubated with UDP-glucoronic acid and UDP-acetyglucosamine overnight. Subsequently, the modified HAS enzymatic capture assay was performed as described above. The proteins linked to the agarose were washed out by protein lysis buffer for western blot. YFP antibody was used to detect the YFP epitope of the fusion proteins. The result is shown in figure 4.8 B. YFP is not immunoprecipitated indicating the specificity of the experiment. However, both YFP-HAS3v1 and YFP-HAS3v2 were co-precipitated. The YFP-HAS3v1 fusion protein has a predicted molecular weight of 90 kDa, which has in line with the signal of the immunoblot shown in figure 4.8 B. The double bands formed in case of YFP-HAS3v1 might be due to posttranslational modifications. This also suggests that c-terminal truncation of HAS3v1 does not affect its enzymatic activity. The molecular weight of YFP-HAS3v2 fusion protein is 58 kDa, which was also detected on the YFP westernblot after the enzymatic capture assay. The co-precipitations were prevented by digesting the HA-HAS complex with hyaluronidase as a negative

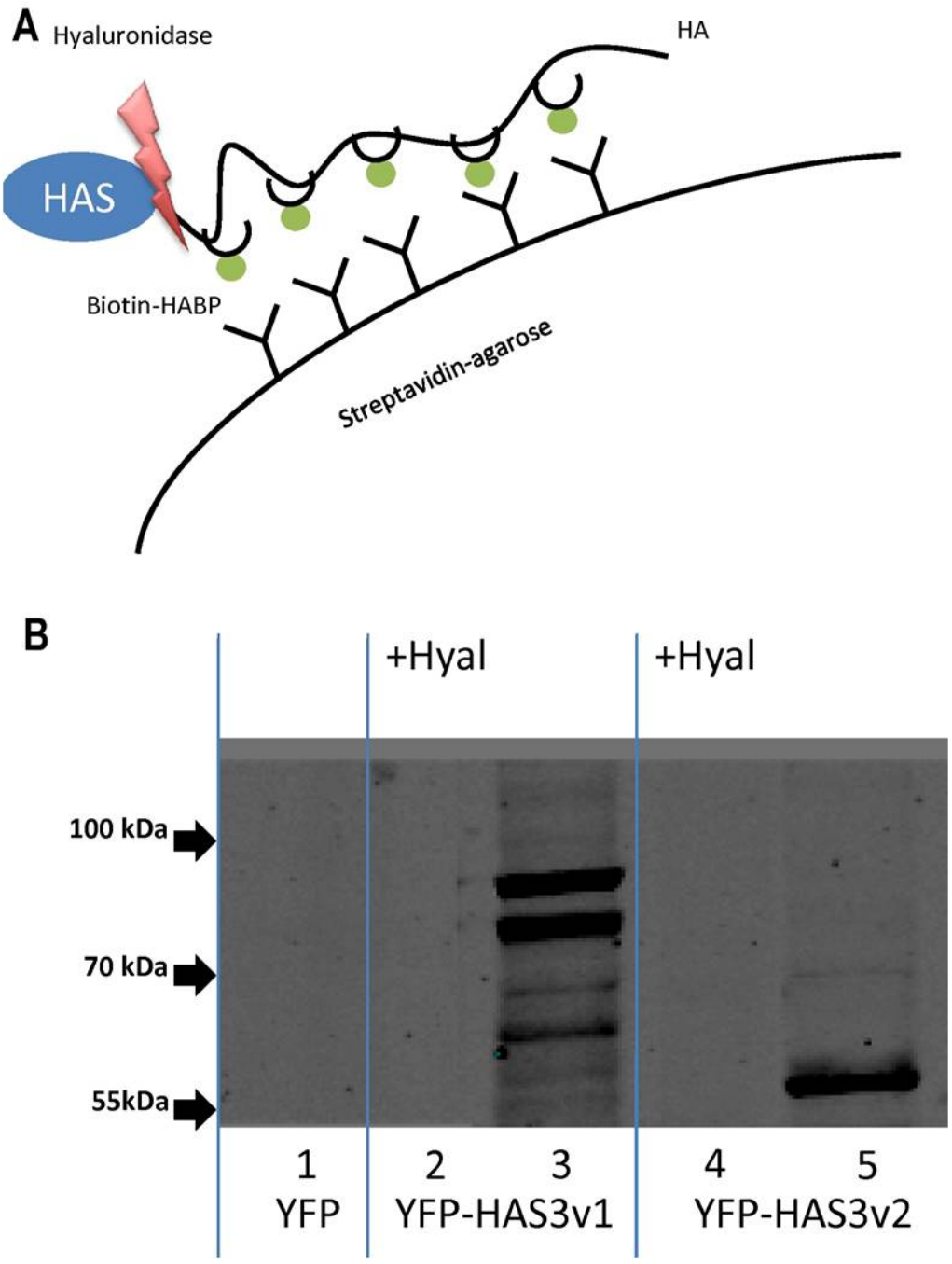

Figure 4.8: **HA-HAS3v2 complex is detected by modified HAS enzymatic capture assay** (**A**): Scheme of modified HAS enzymatic capture assay. Further details are given in section 3.14; (**B**): Immunoblot analysis of the YFP epitope with the protein samples from modified enzymatic capture assay. Microsomes from YFP (1), YFP-HAS3v1 (2, 3) and YFP-HAS3v2 (4, 5) stably transfected HEK 293 cells were used for the assay. Hyaluronidase digestion (lane 2, 4) was performed prior to addition of biotinylated HABP.

control. This indicates that HAS3v2 might be an active hyaluronan synthase.

4.4 HAS3v2 in esophagus adenocarcinoma

4.4.1 Upregulation of HAS3v2 in esophageal adenocarcinoma (EAC)

Biopsies were collected from patients who suffered from either esophageal squamous cell carcinoma (ESCC) or esophageal adenocarcinoma (EAC). After the surgical intervention, samples were stored immediately in liquid nitrogen. Total RNA was isolated and the relative expression levels of hyaluronan synthase isoforms were quantified by realtime RT qPCR. All the data were then normalized to the average of the mucosa group. As shown in figure 4.9, HAS3v1 is upregulated in ESCC compared to mucosa and other HAS isoforms remain constant. In contrast, only HAS3v2 was significantly upregulated in the ADC group compared to mucosa.

4.4.2 In EAC, the expression level of HAS3v2 is positively correlated with the TNM tumor staging.

HAS3v2 is upregulated in EAC compared to mucosa. Therefore, it appeared important to examine whether the induction of HAS3v2 was correlated with tumor progression. Tumor stage and grading were classified by routine histopathologic assessment according to the UICC (Union Internationale Contre le Cancer) Classification for Malignant Tumors. Then, the relative expression levels of HAS3v2 from each tumor sample was plotted against the respective its TNM

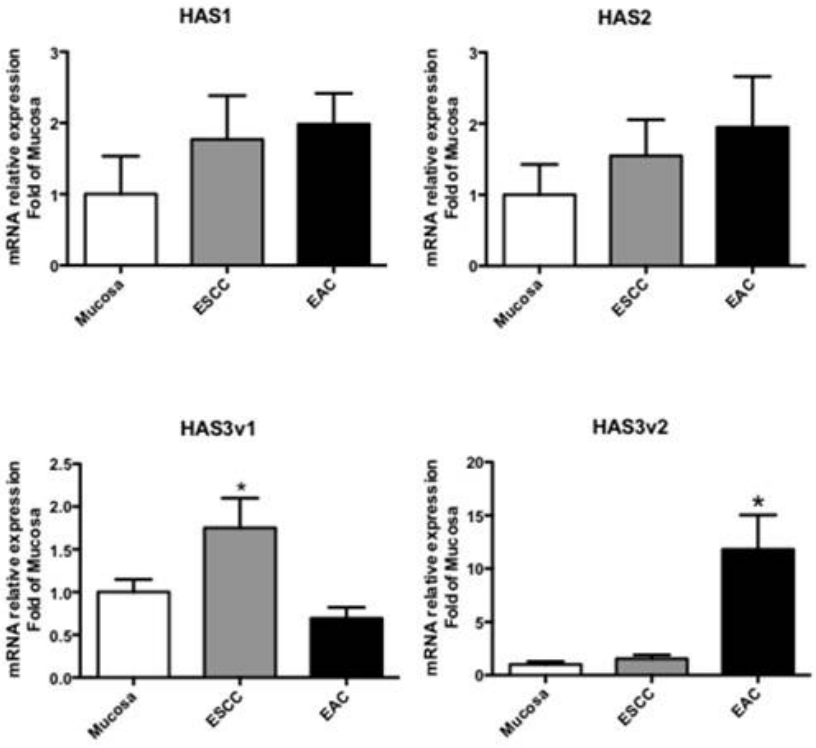

Figure 4.9: **Expression level of HAS isoforms in human ESCC and EAC compared to mucosa**

mRNA expression was determined by RT-qPCR from tumor material removed during surgery. As control, healthy mucosal tissue from the circumstance of the excised tumors was used. One-way ANOWA method was used for statistic analysis. n=13 for mucosa control, 12 for ESCC and 40 for EAC, respectively.

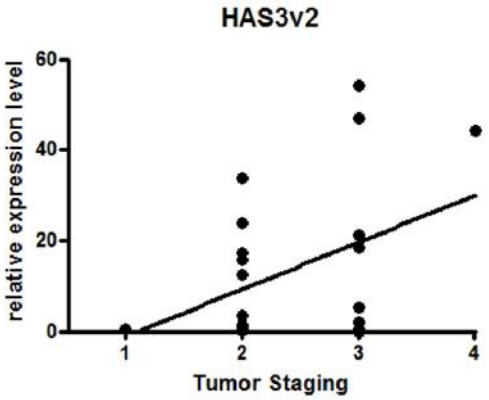

Figure 4.10: **HAS3v2 expression level is positively correlated with EAC TNM tumor staging**

mRNA expression was determined by RT-qPCR from tumor material removed during surgery. As control, healthy mucosal tissue from the circumstance of the excised tumors was used. Correlation coefficient method was used for statistic analysis. n=5 for T1, 16 for T2, 17 for T3 and 2 for T4, respectively.

tumor staging. As is shown in figure 4.10, HAS3v2 expression correlates with increasing tumor staging. Correlation coefficient method was used for statistic analysis.

4.5 Functinal analysis of HAS3v2 in EAC cells *in vitro*

4.5.1 Overexpression of HAS3v2 in EAC cells leads to a pro-proliferative phenotype *in vitro*.

HAS3v2 was strongly upregulated in EAC. Therefore, the functional analysis of HAS3v2 was performed in EAC cell line, i.e. PT1590. PT1590 cells were transduced with either pCL1 mock or HAS3v2 overexpression lentivirus. The

proliferation assay was performed 5 days after transduction. As shown in figure 4.11 A, overexpression of HAS3v2 led to enhanced proliferation compared to pCL1 mock transduced cells. Furthermore, growth curves were determined by cell counting. Five days after transduction, the cells were re-plated at a density of 1000 cells/cm^2 in 12-well plates and were counted daily by using the Neubauer chamber for 5 days after plating. As shown in figure 4.11 B, cells overexpressing HAS3v2 grew significantly faster than pCL1 mock transduced cells, which led to an increasing difference in cell number.

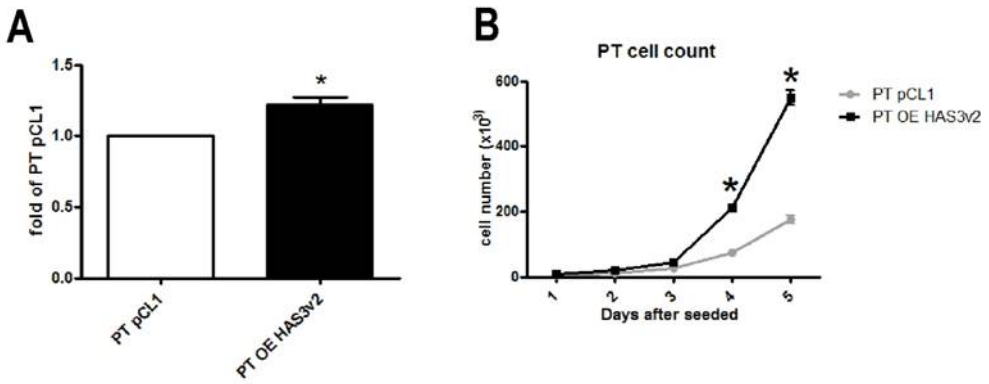

Figure 4.11: **HAS3v2 overexpression leads to a pro-proliferative phenotype.**
(**A**): Cell proliferation was measured by CyQUANT NF proliferation assay kit, (n=4); (**B**): Growth kinetics were determined by cell counting, (n=4). * $p < 0.05$

4.5.2 ERK1/2 is phosphorylated in response to overexpression of HAS3v2.

As described in the previous section, HAS3v2 caused increased proliferation *in vitro*. One hypothesis was that HAS3v2 causes intracellular HA accumulation which in turn might induce intracellular signalling via RHAMM and activation of MAP-kinase pathway. Therefore, we investigated the phosphorylation level of ERK1/2, one of the MAP kinases, that directly interacts with RHAMM. Figure

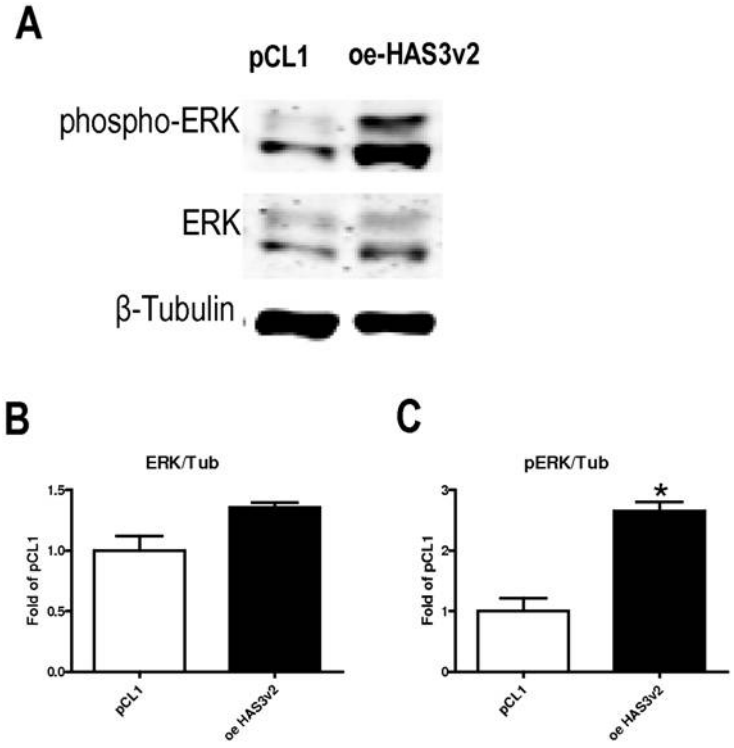

Figure 4.12: **HAS3v2 enhances phosphorylation of ERK1/2.**

PT1590 human EAC cells were lentivirally transduced with either pCL1 mock or HAS3v2 overexpression, grown in 10 % FCS. The culture medium was changed to FCS-free medium 4 days after transduction to eliminate the exogenous stimuli. Proteins were harvested for immunoblot 24 hours after FCS-free treatment. (**A**): Representative immunoblot of phosphorylated ERK and total ERK; intensity quantification of ERK (**B**) and phospho-ERK (**C**) immunoblots using fluorescent secondary antibodies and the Licor Odyssie imager. β-tubulin was taken as loading control (n=3). * $p < 0.05$

4.12 A shows that overexpression of HAS3v2 increased the phosphorylation of ERK1/2 dramatically. The increase in phosphorylation is more than 2 fold (shown in figure 4.12 C).

4.5.3 HAS3v2 enhances cell adhesion by inducing both expression and phosphorylation of focal adhesion kinase (FAK).

Furthermore, the cell adhesion was determined after overexpressing HAS3v2 in PT1590. Five days after transduction, cells were plated in the 96 well plates and were washed after 30 minutes. Cells attached to the plate were then stained with crystal violet. The absorption was measured by UV spectrometry at 540 nm. As shown in figure 4.13 A, overexpession of HAS3v2 causes increased cell adhesion ability. This might be due to the enhanced phosphorylation of focal adhesion kinase (FAK) as evidenced by western blotting (figure 4.13 B, D).

4.6 Functional analysis of HAS3v2 in xenograft model *in vivo*

4.6.1 Overexpression of HAS3v2 promotes tumor growth *in vivo*.

In order to study the physiological and pathological function, we overexpressed HAS3v2 in PT1590 cell with the lentiviral vector as described for the *in vitro* analysis. The mock vector, which led to the overexpression of EGFP, was used

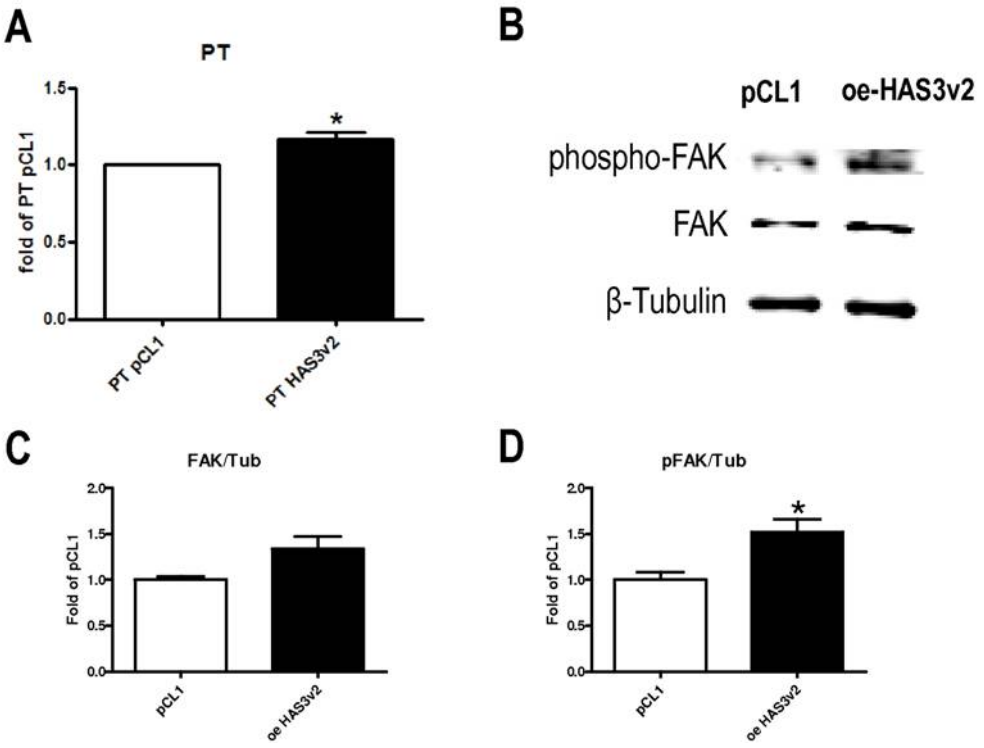

Figure 4.13: **HAS3v2 enhances cell adhesion by inducing both expression and phosphorylation of focal adhesion kinase (FAK).**

PT1590 human EAC cells were lentivirally transduced with either pCL1 mock or HAS3v2 overexpression, grown in 10 % FCS. The culture medium was changed to FCS-free medium 4 days after transduction to eliminate the exogenous stimuli. Proteins were harvested for immunoblot 24 hours after FCS-free treatment. (**A**): Cell adhesion assay, (n=4); (**B**): Representative immunoblot of phosphorylated FAK and total FAK; intensity quantification of FAK (**C**) and phospho-FAK (**D**) immunoblots using fluorescent secondary antibodies and the Licor Odyssie imager. β-tubulin was taken as loading control (n=3). * $p < 0.05$

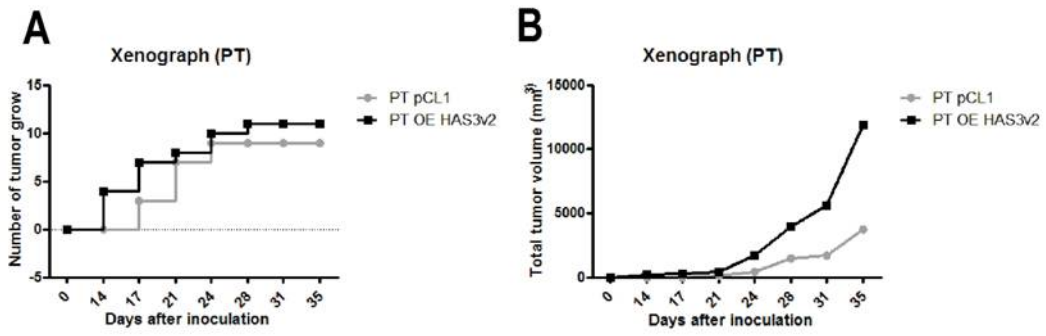

Figure 4.14: **Xenograft model of EAC**

PT1590 human EAC cells were lentivirally transduced with either pCL1 mock or HAS3v2 overexpression, grown in 10 % FCS. For xenografting, 1×10^6 cells were subcutaneously and bilaterally into the flanks of NMRI nu/nu mice at the age of 10 weeks. (**A**)Timecourse of tumor numbers; (**B**): Cumulative tumor volume as determined by digital caliper; n=9 for pCL1 mock and n=11 for HAS3v2 overexpression.

as control. NMRI nu/nu mice were used for subcutaneous tumor formation. 1×10^6 PT1590 cells were injected into both flanks, and the mice were monitored for 35 days after xenografting. During the experimental period, tumor volumes were measured every 3 or 4 days. As illustrated in figure 4.14 B, the HAS3v2 overexpression group shows larger cumulative tumor volume compared to the mock group. Furthermore, tumors from the HAS3v2 overexpression group became visible earlier than the mock group. However, the number of tumors growing from both groups were similar 35 days after inoculation (figure 4.14 A).

After 35 days, the experiment was ended and tumor volume and tumor wet weight were determined. The results are shown in figure 4.15. The average tumor volume of group overexpressing HAS3v2 is significantly larger than of the mock group. Also, overexpressing HAS3v2 increases the tumor wet weight. Representative image from each group is shown in figure 4.15 C. These results suggest that the progression of HAS3v2 overexpressing tumors is faster than of the mock transduced tumors.

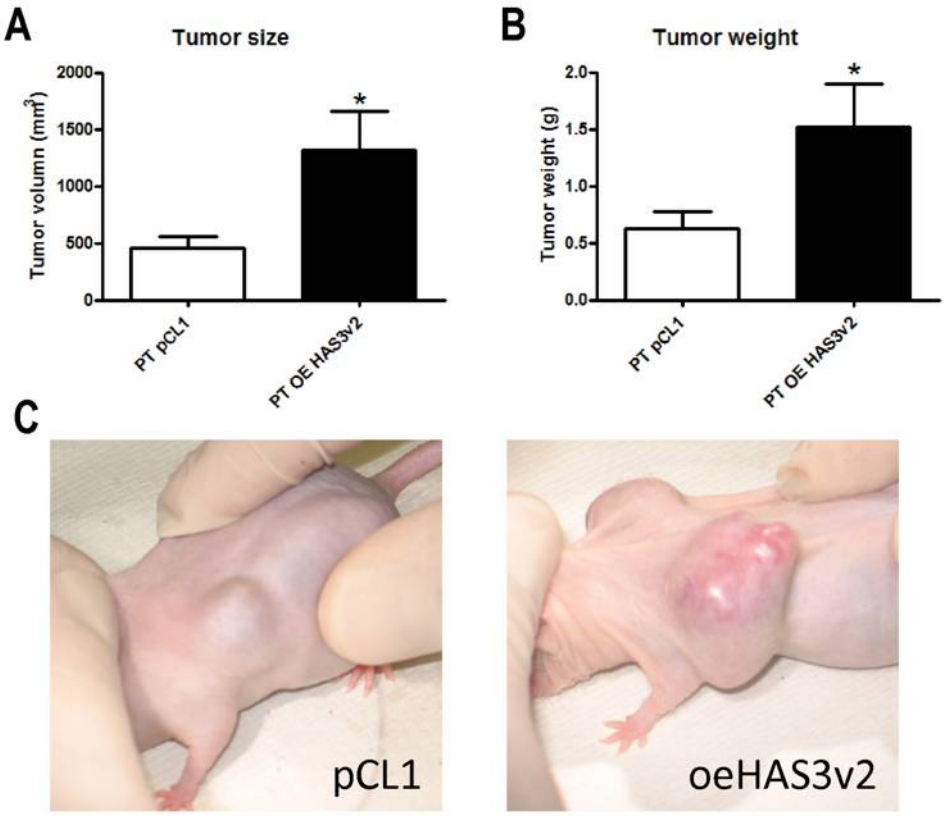

Figure 4.15: **HAS3v2 increases tumor volume and tumor wet weight in the xenograft model.**

PT1590 EAC cells were lentivirally transduced and xenografted into NMRI nu/nu mice. After 35 days, mock control (pCL1) and HAS3v2 overexpressing (oeHAS3v2) tumors were removed and tumor progression was compapred. (**A**)Tumor volume was determined by digital caliper. (n=9-11); (**B**): Tumor wet weight (n=9-11); (**C**): Representative tumor image from each group. * $p < 0.05$

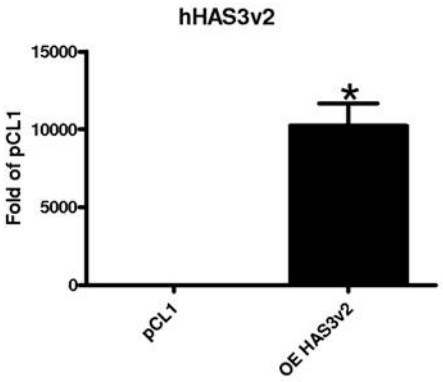

Figure 4.16: **Relative quantification of HAS3v2 mRNA from xenograft**
Total RNA was isolated from xenograft tumors derived from mock and HAS3v2 overexpression transduced PT1590 cells. After 35 days, NMRI nu/nu mice were sacrificed to remove tumors and gene expression was determined by RT-qPCR. (n=9-11). * $p < 0.05$

4.6.2 Overexpression of HAS3v2 in tumor cells leads to induction of HAS3 in stromal cells.

RNA from the xenograft tumor was isolated for realtime qPCR analysis. The tumor contains both human cancer cells and mouse stromal cells. Therefore, species specific primer pairs were designed to quantify the gene regulation of tumor and stroma separately. As shown in figure 4.16, HAS3v2 mRNA remains highly induced in tumor of the overexpression group at 35 days after innoculation. The expression level of HA related genes, namely HAS1, HAS2, HAS3v1, Hyal1, Hyal2, and HA receptors CD44s and RHAMM, were also quantified. For the quantification, species specific primers were used that allowed to distinguish between murine/stroma gene expression and human/tumor gene expression. In the tumors, the indicated genes were not significant regulated in response to HAS3v2 overexpression. However, murine HAS3v1 in the stroma of HAS3v2 overexpressing tumors was stimulated up to about 6 fold compared to the pCL1 mock group (figure 4.18, 4.17).

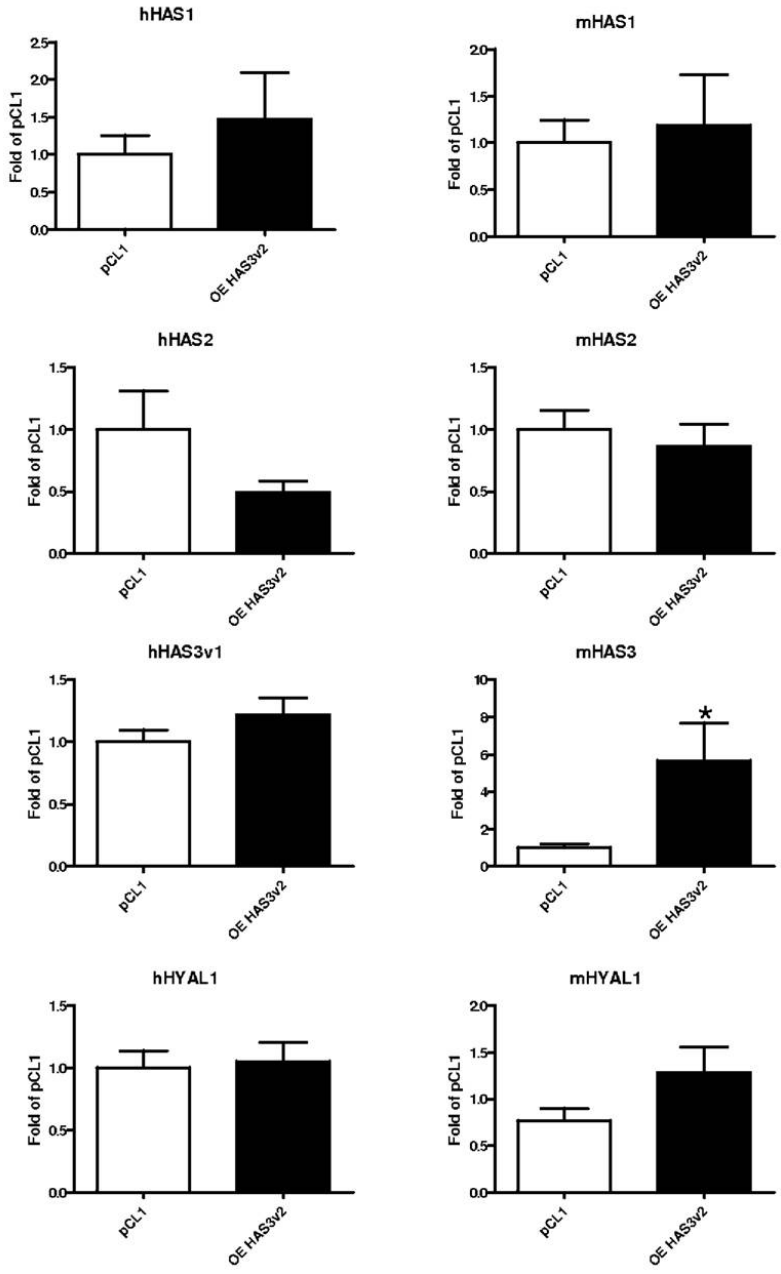

Figure 4.17: **Species specific expression profile of HA-associated genes in the xenograft, part A**

Total RNA was isolated from xenograft tumors derived from mock and HAS3v2 overexpression transduced PT1590 cells. After 35 days, NMRI nu/nu mice were sacrificed to remove tumors and gene expression was determined by RT-qPCR. Left column: human/tumor gene expression; right column: murine/stroma gene expression(n=9-11). * $p < 0.05$

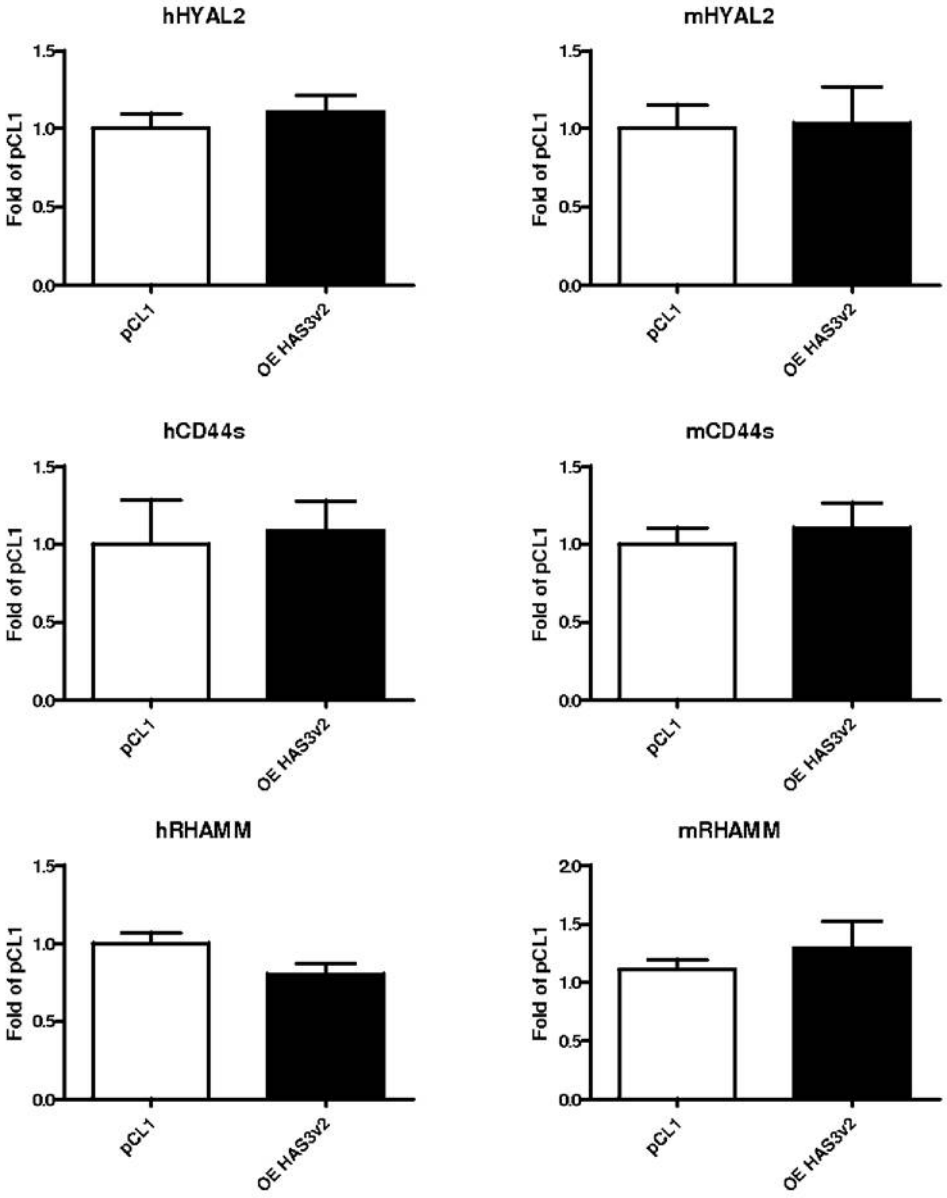

Figure 4.18: **Species specific expression profile of HA-associated genes in the xenograft, part B**

Total RNA was isolated from xenograft tumors derived from mock and HAS3v2 overexpression transduced PT1590 cells. After 35 days, NMRI nu/nu mice were sacrificed to remove tumors and gene expression was determined by RT-qPCR. Left column: human/tumor gene expression; right column: murine/stroma gene expression(n=9-11). * $p < 0.05$

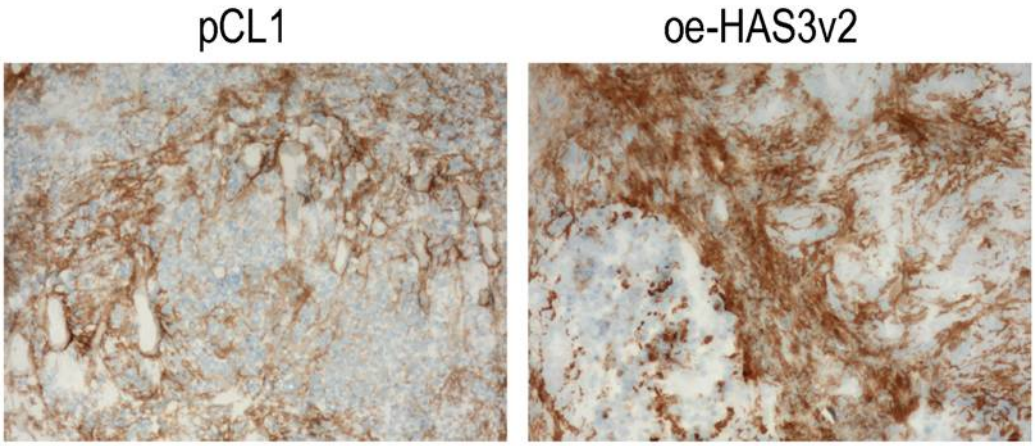

Figure 4.19: **Affinity histochemical analysis of HA in xenograft tumors**
PT1590 EAC cells were lentivirally transduced and xenografted into NMRI nu/nu mice. After 35 days, mock control (pCL1) and HAS3v2 overexpressing (oeHAS3v2) tumors were removed and analyzed with respect to HA accumulation by affinity histochemistry using biotinylated HABP. (n=9-11). Representative image from each group were selected. Magnification: 100 $\times$.

4.6.3 HA content in stroma is elevated in the HAS3v2 overexpression group.

Xenograft tumors were also analyzed by immunohistochemistry. Biotinylated HABP was used to detect hyaluronan in immunohistochemical analysis. As shown in figure 4.19, more HA was detected in the stroma of HAS3v2 overexpressing tumors compared to the mock control tumor. Tumorial associated hyaluronan showed no obvious difference between the HAS3v2 and the mock group. The accumulation of HA in stroma could be the consequence of HAS3v1 upregulation in murine stroma cells as shown in figure figure 4.18 and 4.17.

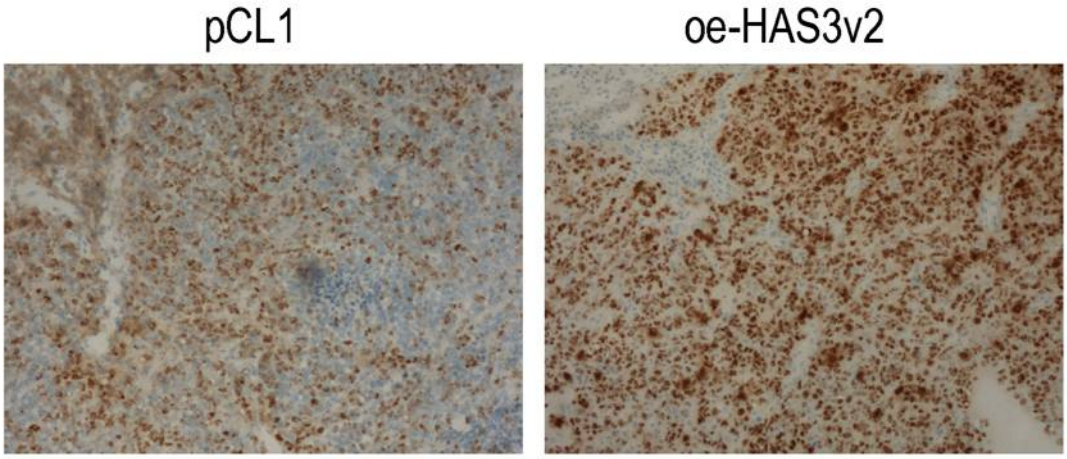

Figure 4.20: **Immunohistochemical analysis of proliferation in xenograft tumor**
PT1590 EAC cells were lentivirally transduced and xenografted into NMRI nu/nu mice. After 35 days, mock control (pCL1) and HAS3v2 overexpressing (oeHAS3v2) tumors were removed and analyzed with respect to proliferation rate by immunohistochemistry. Ki67 was stained as a proliferation marker. Cells, which are positive for the staining, indicate that they are in G1, S, G2 or M phase of the cell cycle. (n=9-11). Representative image from each group were selected. Magnification: 100 $\times$.

4.6.4 HAS3v2 induces proliferation *in vivo*.

In vivo proliferation rate was determined by immunohistochemical staining of the proliferation marker, Ki 67. Figure 4.20 shows that there were more Ki 67 cells after HAS3v2 overexpression compared to the mock group suggesting that HAS3v2 is also pro-proliferative *in vivo*.

4.7 Epidermal growth factor receptor (EGFR) signal cascades regulates the expression of HAS3v2.

4.7.1 EGF induces HAS3v2 mRNA expression in EAC cells.

EGF signaling plays an important role in the progression of different types of cancers including esophageal cancer. Therefore, we investigated whether the EGF signaling pathway may influence the expression of HAS3v2. PT1590 cells were starved in serum-free medium 24 hours before stimulation. Then, PT1590 cells were stimulated by epidermal growth factor with and without Cetuximab, a blocking antibody of the EGF receptor. Total RNA was harvested 4 hours and 24 hours after induction. As shown in figure 4.21, there was no significant regulation of HAS3v2 by EGF at 4 hours. However, 24 hours after EGF stimulation, strong upregulation of HAS3v2 was observed. This upregulation was completely blocked by Cetuximab. This result suggests that the EGFR signal cascade is able to regulate the HAS3v2.

4.7.2 The expression levels of EGFR and HAS3v2 are positively correlated in EAC.

EGFR is a member of ErbB family, which consists of four structurally related receptor tyrosine kinases. Overexpression or overactivity of EGFR has been shown to be associated with a number of cancers, including lung cancer and esophageal cancer. qPCR was performed to measure the EGFR mRNA expression level of the EAC samples introduced in section 4.4.2. For quantification, the data were normalized to the expression level of mucosa. Figure 4.22

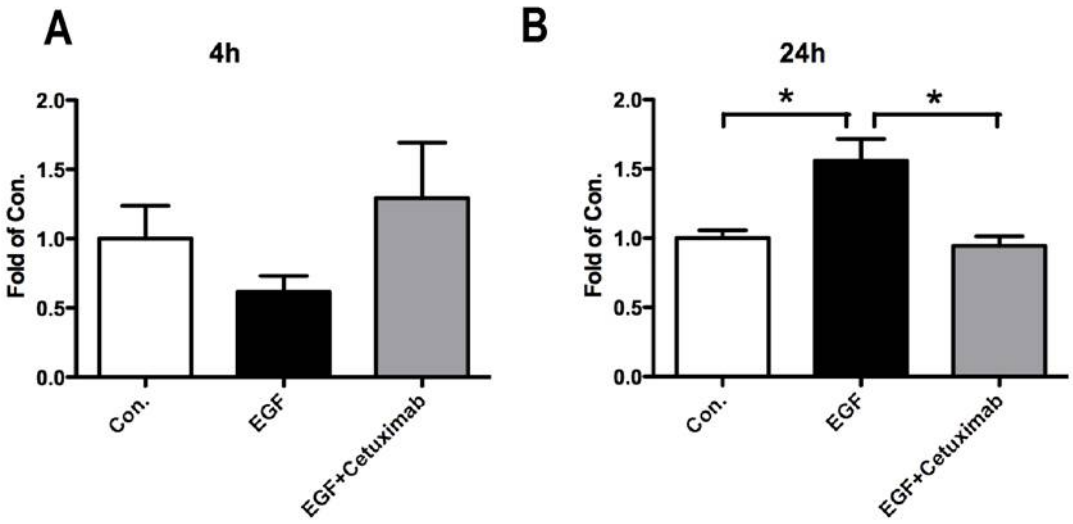

Figure 4.21: **EGF stimulates HAS3v2 expression *in vitro*.**

PT1590 EAC cells were serum starved for 24 hours and stimulated with EGF (10 ng/ml) or EGF (10 ng/ml) plus Cetuximab (10 ng/ml) for 4 and 24 hours. HAS3v2 expression was determined by RT-qPCR. HAS3v2 mRNA expression was quantified for 4 hours after (**A**) stimulation and 24 hours after stimulation (**A**). Relative expression data was normalized to control. (n=6). $p < 0.05$

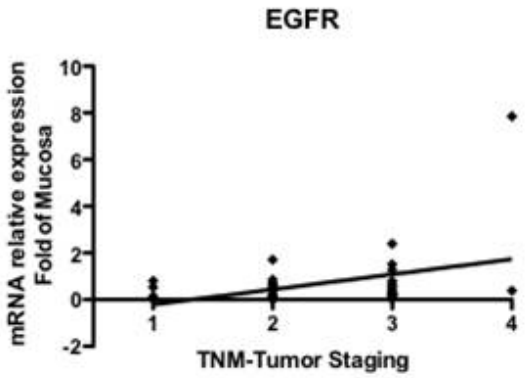

Figure 4.22: **mRNA expression level of EGFR in relationship to TNM staging in human EAC.**

mRNA expression was determined by RT-qPCR from tumor material removed during surgery. As control, healthy mucosal tissue from the circumstance of the excised tumors was used. Correlation coefficient method was used for statistic analysis. n=5 for T1, 16 for T2, 17 for T3 and 2 for T4, respectively.

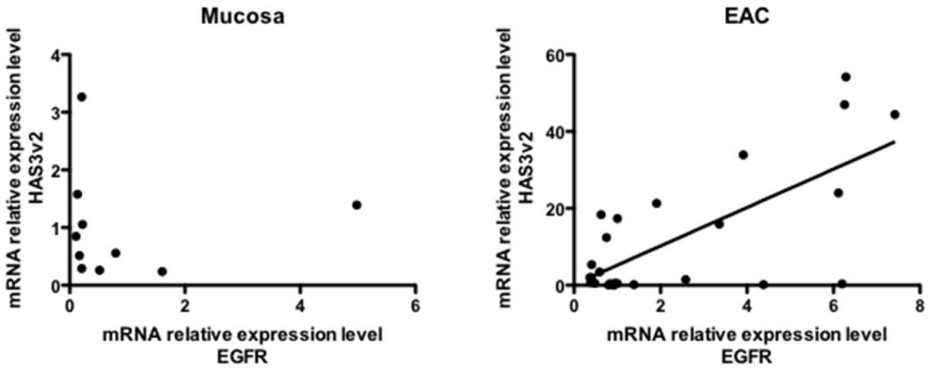

Figure 4.23: **mRNA expression levels of EGFR and HAS3v2 are correlated in human EAC.** mRNA expression was determined by RT-qPCR from tumor material removed during surgery. As control, healthy mucosal tissue from the circumstance of the excised tumors was used. Correlation coefficient method was used for statistic analysis. n=5 for T1, 16 for T2, 17 for T3 and 2 for T4, respectively. The correlation between EGFR and HAS3v2 is analyzed in both mucosa group (**A**)and EAC group (**B**)

showed that the mRNA expression level of EGFR was related to the tumor staging. In addition, it was analyzed whether HAS3v2 and EGFR expression were correlated in both mucosa and EAC specimens. For the EAC group, a positive correlation between the expression level of HAS3v2 and EGFR was observed (figure 4.23 A). However, HAS3v2 shows no correlation with the EGFR in the mucosa group (figure 4.23 B). Taking together, the results suggested the EGF signaling pathway might be involved in the upregulation of HAS3v2 during EAC progression in patients.

Chapter 5

Discussion

5.1 HAS3v2 might be an intracellular HA synthase.

5.1.1 Intracellular HA originates from both endocytosis and *de novo* synthesis.

Hyaluronan is a high molecular weight glycosaminoglycan generally regarded as an extracellular matrix molecule. The function of hyaluronan is to promote cell locomotion and proliferation, and it plays a role in wound healing and developmental processes such as cell differentiation and migration. In addition to its role in the extracellular matrix, hyaluronan has also been identified in the cytoplasm and nuclei of cells from different tissues both *in vivo* and *in vitro* [Margolis et al. 1976; Londoño and Bendayan 1988; Kan 1990; Ripellino et al. 1988; Eggli and Graber 1995; Evanko and Wight 1999; Furukawa and Terayama 1977, 1979; Ripellino et al. 1989; Hascall et al. 2004; Evanko et al. 2004]. Furthermore, a number of hyaluronan binding proteins exist intracellularly that may be important in regulation of the cell cycle or in gene transcription [Hofmann et al. 1998; Grammatikakis et al. 1995; Deb and Datta 1996; Zhang et al. 1998]. For example, a vertebrate homologue of the cell cycle control protein CDC37 was cloned and found to bind hyaluronan [Grammatikakis et al. 1995], and an intracellular form of the hyaluronan receptor, RHAMM, was shown to regulate ERK kinase activity [Zhang et al. 1998].

The source of intracellular hyaluronan is not yet clear. Evanko and Wight showed that hyaluronan could be taken up by endocytosis from the extracellular space [Evanko and Wight 1999]. However, exogenous fluoresceinated hyaluronan was confined to the endosomes and did not co-localize with the endogenous hyaluronan network in the cytoplasm, suggesting that some of the

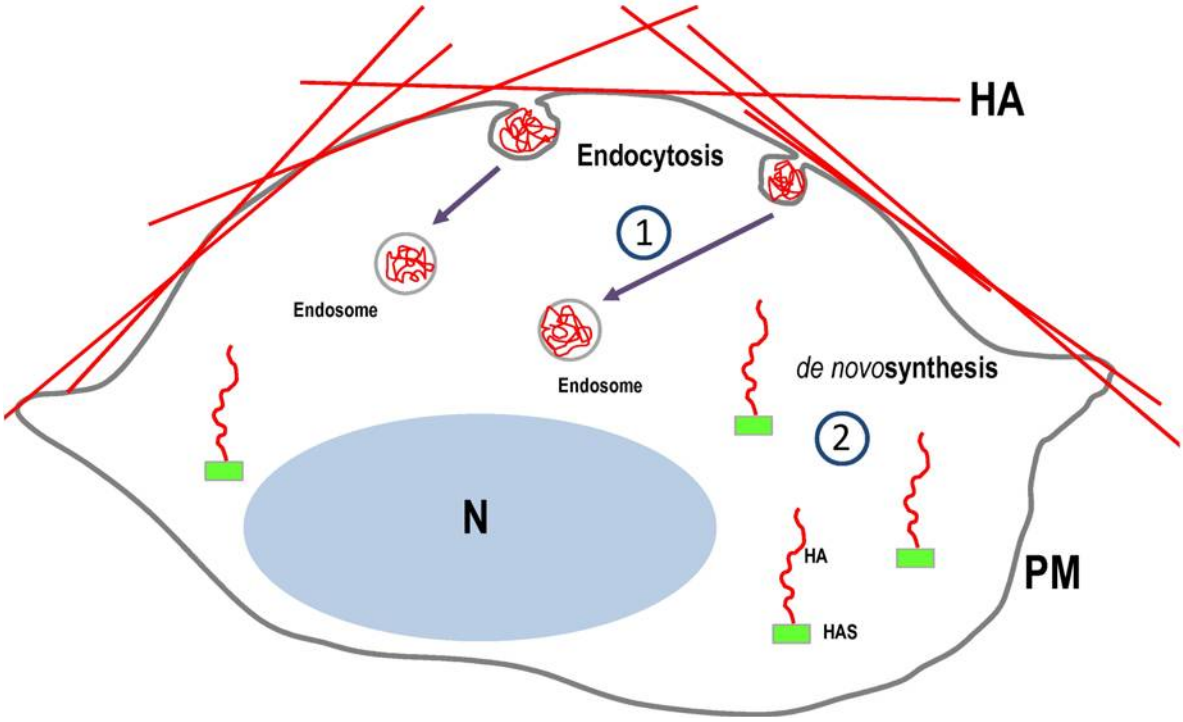

Figure 5.1: **Scheme of possible sources of intracellular hyaluronan**
Intracellular HA originated from endocytosis (1) and possiblely also from intracellular *de novo* synthesis (2). However, the site organelle where intracellular *de novo* synthesis of HA occurs is not known. N, nucleus; PM, plasma membrane.

cytoplasmic hyaluronan must be derived from intracellular sources and not from internalization of extracellular hyaluronan (figure 5.1). No evidence indicates that HAS1, HAS2, and HAS3v1 can synthesize hyaluronan inside the cell, which might be due to their plasma membrane localization. This rises the suggestion that there is another active hyaluronan synthase localized inside the cell [Evanko and Wight 1999].

5.1.2 Evidence for the activity of HAS3v2

There are three hyaluronan synthase isoforms in human, namely HAS1, HAS2, and HAS3 [Spicer et al. 1997b]. It is shown that all three HAS isoforms are localized on the plasma membrane and synthesize extracellular hyaluronan [Weigel et al. 1997]. Human hyaluronan synthases are transmembrane proteins that contain seven putative transmembrane domains [Weigel et al. 1997]. The intracellular loop between the 2^{nd} and the 3^{rd} transmembrane domain is predicted to be the catalytic center [Yoshida et al. 2000]. A cysteine residue in the intracellular loop is reported to be highly conserved from bacterial to mammalian HAS and the modification of this cysteine can partially inhibit enzyme activity [Weigel et al. 1997]. This suggests that the cysteine residue is critical for HAS enzymatic activity.

Human HAS3 has two splicing variants, namely HAS3v1 and HAS3v2 [Sayo et al. 2002; Monslow et al. 2003]. HAS3v2 is the shorter splicing variant of HAS3 and consists of only 281 amino acids (553 AA for HAS3v1). HAS3v2 shows only 2 transmembrane domains in *in silico* analysis. Instead of intracellular loop, HAS3v2 contains an intracellular c-terminal end of 215 AA in length, which also contains the highly conserved cysteine residue (shown as black circle in figure 1.2). This raises the possibility that HAS3v2 might also be an active hyaluronan synthase despite of its truncated size. In order to identify the activity center in HAS3v2, protein functional analysis was performed *in silico* using Pfam database [Finn et al. 2008]. The only functional domain, glycosyl transferase 2 domain, is shared by both HAS3 splicing variants. This protein domain is presented in all the active hyaluronan synthases found so far [Weigel and DeAngelis 2007]. The glycosyl transferase 2 domain reaches from AA 88 to AA124 in both HAS3v1 and HAS3v2. This indicates the potential role of

HAS3v2 in HA synthesis. In addition, we performed a 3D protein structure simulation for the intracellular loop of HAS3v1 and the intracellular c-terminal end of HAS3v2, where the glycosyl transferase 2 domain is localized. The similarity of 3D protein structure of HAS3 splicing variants was analyzed based on an overlay algorithm [Soding 2005; Soding et al. 2005]. As shown in figure 4.2, the green part indicates highly similar regions in protein conformation between HAS3v1 and HAS3v2. Of note, the glycosyl transferase 2 domain is also localized in this overlay.

Furthermore, *in silico* analysis revealed that HAS3v2 contains an evolutionary conserved cysteine which is proofed to be critical for the HAS enzymatic activity. HAS3v2 also shares the glycosyl transferase 2 domain with other active hyaluronan synthases. Furthermore, predicted 3D protein structures of the putative active center from HAS3v1 and HAS3v2 are similiar. All these results suggest that HAS3v2 could be an active hyaluronan synthase. Therefore, functional studies of HAS3v2 were performed.

HAS3v2 is predicted to have only 2 transmembrane domains. However, there are 7 transmembrane domains presented on the other HAS isoforms, i.e. HAS1, HAS2 and HAS3v1 [Weigel et al. 1997]. Thus, it was not clear whether HAS3v2 does also localize to the plasma membrane.

As reported, the N-terminal GFP-HAS2 and GFP-HAS3v1 fusion proteins are active with respect to HA synthesis [Rilla et al. 2005; Kultti et al. 2006]. The first 261 AA sequence on the N-terminal of HAS3v2 protein is identical to HAS3v1. Therefore, N-terminal YFP-HAS fusion proteins were constructed to investigate the subcellular localization of HAS3v2 (shown in figure 4.3). The results indicated that HAS3v2 was not localized in the plasma membrane but on the ER inside the cell. By protein translation, the predicted intracellular parts of

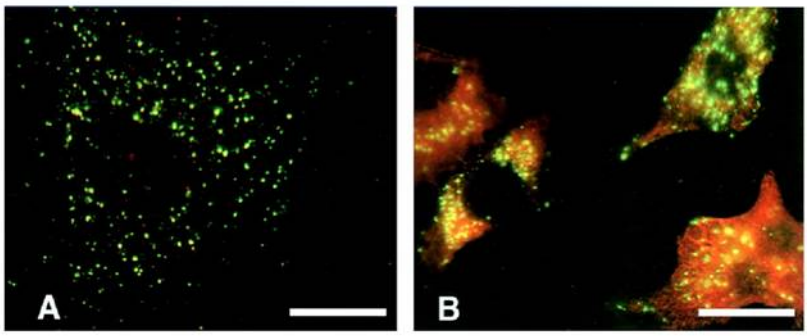

Figure 5.2: **Intracellular HA originates from both endocytosis and *de novo* synthesis.** Fluoresceinated hyaluronan (Green) is uptaken by endocytosis (**A**), and the cells were further stained for intracellular HA (Red) (**B**). Bars = 25 μm. Images were taken from [Evanko and Wight 1999]

the protein reside in the outer membrane part of ER. Therefore, the c-terminal tail of HAS3v2 might extend of the outer ER membrane. If HAS3v2 was active, it could synthesize HA on the ER membrane. This might provide an explanation why intracellular HA was accumulated on the outer ER membrane but not in the ER lumen [Evanko and Wight 1999]. Further, Evanko and Wight showed that endocytosis of the exogenous hyaluronan is not the only source of intracellular HA (figure 5.2). Hyaluronan remains attached to HA synthases during synthesis [Kyossev and Weigel 2007]. Thereby, HA would remain localized on the outer ER membrane during its synthesis by HAS3v2 and this could, at least partially, compliment the intracellular HA localization pattern besides endocytosis of exogenous hyaluronan.

HAS3v2 was overexpressed in both HEK cells and skin fibroblasts. Then, intracellular HA was quantified using HA ELISA. HAS3v2 caused increased intracellular HA level in both cell lines. In addition, intracellular HA images were taken by confocal microscope. The vesicular staining pattern in the cytosol might due to the endocytosis of exogenous HA [Evanko and Wight 1999]. In addition, a network-like intracellular HA signal (shown in figure 4.7, white arrow

indicated compared to white star in mock group) was detected. This pattern could not be explained by the endocytosis but might be due to the intracellular *de novo* synthesis on the surface of ER by HAS3v2.

Hyaluronan is attached to the HAS during the synthesis [Kyossev and Weigel 2007]. Enzymatic capture assay experiments showed that a HA-HAS3v2 complex exists in microsome preparations after supplementation with activated UDP-sugers. However, the experiment was performed using microsomes isolated from transfected HEK cells. Microsomes consisted of raw membranes, mainly derived from ER and golgi apparatus. However, minor proportions of plasma membrane could have been included. Therefore, hyaluronan could have also been synthesized by HAS1, HAS2 and HAS3v1 originating from the plasma membrane. One possible alternative explanation for the fact that HA-HAS3v2 complexes were detected is that the HAS3v2 binds to hyaluronan that was synthesized by HAS1-3 from plasma membrane contamination. However, that would require that HAS3v2 is at least a HA binding protein.

Currently, there are two known HA binding domain, namely LINK and GLA domain [Day and Prestwich 2002]. Pfam and SMART (http://smart.embl-heidelberg.de/) databases contain large collections of protein families [Finn et al. 2008; Schultz et al. 1998; Ponting et al. 1999; Letunic et al. 2009]. Neither LINK nor GLA domains were detected on HAS3v2 by analyzing through both pfam and SMART databases. Further, overexpression of HAS3v2 led to increased intracellular HA levels. Furthermore, if HAS3v2 was a HA binding protein, the only possible explanation for increased intracellular HA is that HAS3v2 binds to hyaluronan and protect it from hyaluronidase digestion. However, hyaluronidase digestions completely eliminated hyaluronan on both permeabilized HAS3v2 overexpressing skin fibroblasts and microsomes isolated from HAS3v2 transfected HEK cell.

Thus, no protecting effect could be observed. Therefore, the enzymatic capture assay strongly suggested the activity of HAS3v2 as hyaluronan synthase.

5.2 HAS3v2 is a potential tumor marker for EAC.

Esophageal cancer is the 6^{th} most frequent cancer worldwide [Parkin et al. 1999]. Squamous cell carcinoma (ESCC) and adenocarcinoma (EAC) are the two main subtypes of esophageal cancer [Blot 1995]. The prognosis for both subtypes is rather poor with a 5-year relative survival rate between 11% and 15% [Lagarde et al. 2006]. Hyaluronan is known to be important for tumor progression in various cancer types [Auvinen et al. 2000; Ropponen et al. 1998; Lipponen et al. 2001; Anttila et al. 2000; Setälä et al. 1999]. HA synthesis is correlated with the mRNA level of HAS isoforms. Therefore, we first analyzed the regulation of HAS isoforms during tumor progression of both ESCC and EAC.

HAS3v2 was highly upregulated in EAC, but not in ESCC, compared to the mucosa group. However, the expression levels of other HAS isoforms remained constant in EAC. Importantly, the HAS3v2 expression level was also correlated to the tumor staging. This indicates that HAS3v2 is a potential tumor marker for esophageal adenocarcinoma. In addition, HAS3v2 induced intracellular hyaluronan accumulation, that often correlates with cell proliferation [Evanko and Wight 1999]. Elevated cytosolic HA was detected in different cancer types [Corte et al. 2006; Vizoso et al. 2004; Ruibal et al. 2003]. Further, intracellular HA binding protein RHAMM was reported to play important roles in tumor progression [Giannopoulos and Schmitt 2006; Hus et al. 2008; Rein et al. 2003; Tolg et al. 2003; Yamano et al. 2008; Zlobec et al. 2008]. These

facts encouraged us to study the pathological function of HAS3v2 in esophageal adenocarcinoma.

5.3 HAS3v2 is a candidate for an oncogene.

5.3.1 RHAMM pathway promotes tumor progression.

Both CD44 and RHAMM are hyaluronan receptors and play important roles in regulating cell behaviors including tumor progression [Turley et al. 2002]. CD44 is a transmembrane protein, while RHAMM is located on the plasma membrane as well as in the cytosolic compartment [Turley 1980]. The basal expression level of RHAMM is low in normal tissue [Turley et al. 2002; Evanko et al. 2007; Slevin et al. 2007]. However, it is reported to be highly expressed in several advanced cancers [Giannopoulos and Schmitt 2006; Hus et al. 2008; Rein et al. 2003; Tolg et al. 2003; Yamano et al. 2008; Zlobec et al. 2008; Pujana et al. 2007]. According to the observations, one might speculate that excessive cytosolic RHAMM might be activated by intracellular HA and in turn induce tumor progression. Therefore, HAS3v2 regulated cell phenotype might be mediated through the RHAMM signaling pathway.

5.3.2 HAS3v2 might induce the RHAMM signaling pathway to regulate cell behavior.

Overexpression of HAS3v2 increases the proliferation rate both *in vitro* and in xenograft experiments in nude mice. One reason is that the ERK1/2 kinase phosphorylation was induced by overexpression of HAS3v2. ERK1/2 phospho-

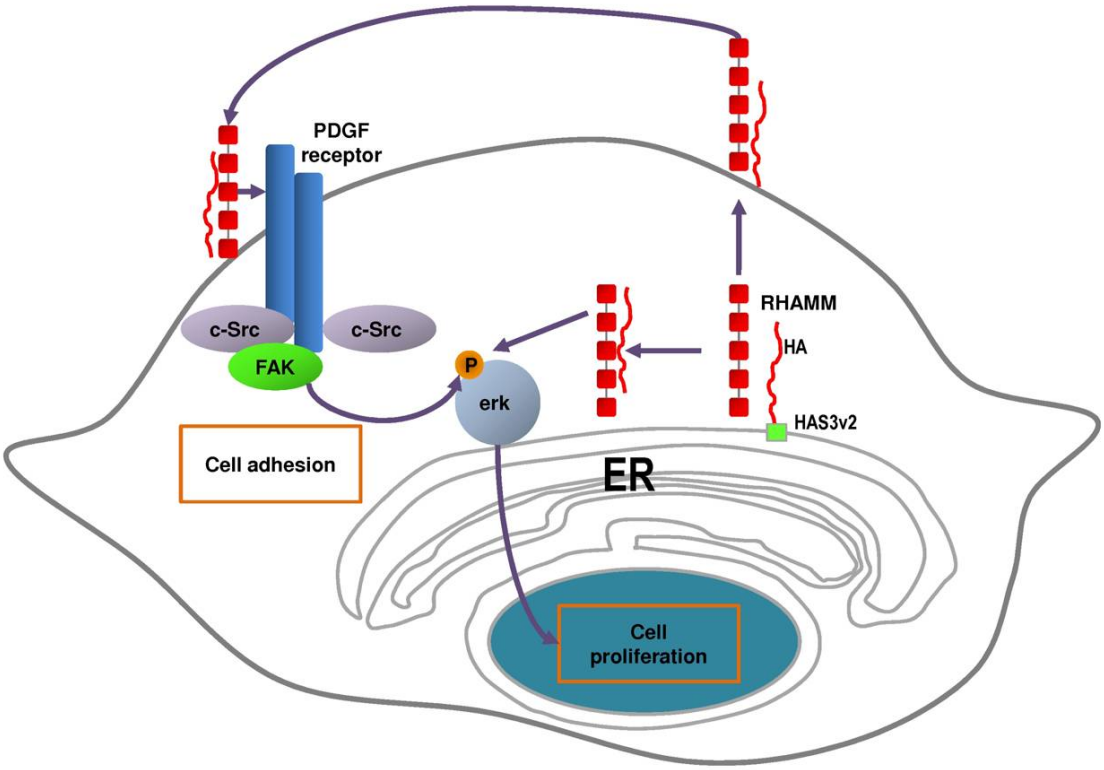

Figure 5.3: **HAS3v2 might regulate cancer cell phenotype though RHAMM.**
HAS3v2 overexpression leads to intracellular HA accumulation. The intracellular HA might bind to RHAMM to induce phosphorylation of the ERK kinase. Phosphorylated ERK can induce cell proliferation by activating the ERK signaling cascades. After binding to intracellular HA, RHAMM can also translocate to the plasma membrane and interact with PDGF receptor in an autocrine manner. Consequently, activated PDGF receptor can phosphorylate focal adhesion kinase (FAK). This leads to improved cell adhesion. Phosphorylated FAK can also contribute to the ERK phosphorylation to promote cell proliferation.

rylation can be enhanced through the RHAMM signal cascade and thereby induce the cell proliferation [Turley et al. 2002]. This leads to the hypothesis that HAS3v2 can increase the intracellular HA and that intracellular HA can trigger the RHAMM signaling pathway (shown in figure 5.3). After activation, ERK1/2 kinase activates further signal cascades either by phosphorylation of downstream targets like ELK1 or by translocating to the nucleus to initiate downstream protein expression and thereby promote cell cycle progression.

Protein export is considered to be dependent upon access to the classical secretory pathway through the ER/Golgi route [Hathout 2007; Simpson et al. 2007]. Protein secretion through this route requires an N-terminal signal peptide, that is responsible for most of the constitutive export of proteins [Hathout 2007; Simpson et al. 2007]. However, the primary structure of RHAMM lacks this signal peptide for classical secretion [Maxwell et al. 2008]. Emerging evidence reveals that some cytoplasmic proteins, e.g. RHAMM, can be exported via an alternative mechanism that does not require the known structural secretion cues (shown in figure 5.4) [Chivasa et al. 2006, 2005; Tjalsma et al. 2006]. Therefore, RHAMM may be activated by interacting with intracellular hyaluronan and the activated HA-RHAMM complex is subsequently exported to the ECM through the non-conventional protein export routes. Specifically, one RHAMM splicing variant (splice variant xy) has been shown to interact with the PDGF receptor and to trigger the PDGF pathway. However it has not been demonstrated directly whether HA binding to RHAMM is necessary for this transactivation of the PDGF receptor [Zhang et al. 1998]. Activated PDGF signaling pathway can stimulate FAK phosphorylation [Turley et al. 2002]. Therefore, intracellular activation of RHAMM, translocation of RHAMM to the extracellular compartment and activation of a growth factor receptor that crosstalks to focal adhesion complexes and FAK may be responsible for the result presented here that HAS3v2

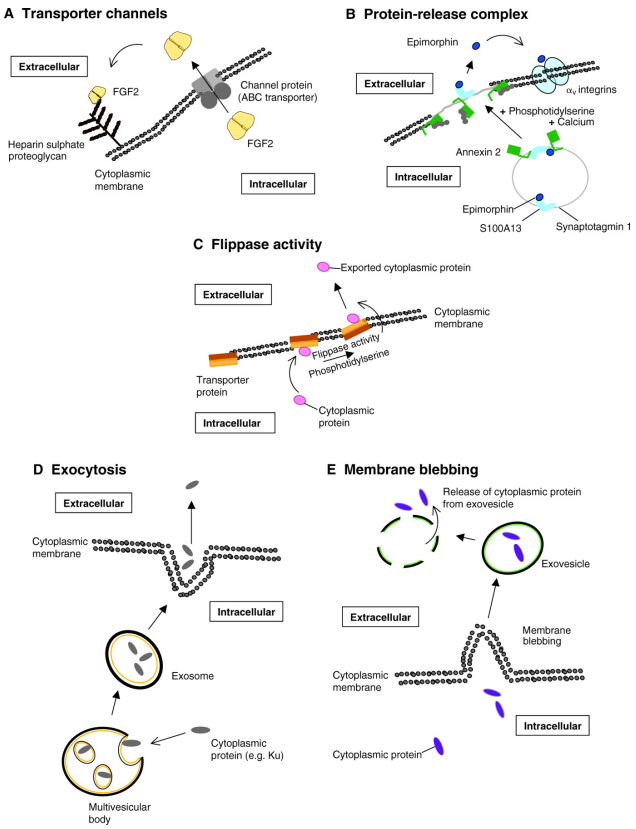

Figure 5.4: **Routes for non-conventional protein export**

(**A**) Transporter channels. Cytoplasmic proteins can be exported through transporter-protein channels and then captured by cell-surface counter receptors. As an example, FGF2 is shown being exported through the ABC transporter and then captured by a heparin sulphate proteoglycan [Nickel 2005; Prudovsky et al. 2008 Apr 1]. (**B**) Protein-release complex. Other cytoplasmic proteins, such as epimorphin, associate with a protein-release complex that is composed of S100A13 and synaptotagmin 1 that then binds to annexin 2. The epimorphin protein-release complex is localized to, and flipped through, the cytoplasmic membrane in response to Ca^{2+} and phosphatidylserine. Released epimorphin then binds to α_v-integrin, resulting in activation of morphogenic signaling cascades [Radisky et al. 2003]. (**C**) Flippase activity. An alternate route of export results from cytoplasmic proteins binding to transporter proteins that have intrinsic flippase activity when stimulated by phosphatidylserine [Daleke 2003]. (**D**,**E**) Exocytosis and membrane blebbing. Additional mechanisms of non-conventional export include exocytosis (**D**) and membrane blebbing (**E**). Cytoplasmic and/or nuclear proteins such as Ku are released by exocytosis of exosomes [Paupert et al. 2007], but cytoplasmic proteins can also be exported in vesicles formed by membrane blebbing [Huot et al. 1998]. Figure was taken from [Maxwell et al. 2008]

overexpression causes elevated FAK phosphorylation and cell adhesion in vitro. Phosphorylated FAK can further stimulate ERK phosphorylation and thereby lead to an amplified ERK signaling response and proliferation. Taken together, as a working hypothesis it is proposed that RHAMM is activated by intracellular HA and then exported to the ECM to trigger the PDGF pathway through direct interaction with PDGF receptor. Figure 5.3 shows the hypothetical scheme of HAS3v2 mediated RHAMM signaling pathway. In future experiments, it should be addressed if the effects of HAS3v2 overexpression are indeed dependent on RHAMM and/or a growth factor receptor.

5.3.3 Stroma cells can also be influenced by HAS3v2 upregulation in cancer cells.

Immunohistochemical analysis revealed increased hyaluronan in the stroma but not around cancer cells after xenografting HAS3v2 overexpressing EAC cells. The expression level of HAS3v1 in stroma was upregulated by HAS3v2 overexpression in cancer cells as determined by mouse specific analysis of HAS3v1 mRNA expression. The upregulation of stromal HAS3v1 explained the increase of stromal hyaluronan. One possible explanation for the induction of stromal hyaluronan in this model is that the overexpression of HAS3v2 activated via RHAMM the malignant phenotype of the xenografted EAC cells (shown in figure 5.5). These activated EAC in turn released factors such as growth factors or cytokines that stimulated the stromal cells to express HAS3v1. In efficient pathway how HAS3v1 is induced is the activation of NF-κB, which was confirmed by promoter analysis [Monslow et al. 2003].

Quantitative PCR results indicated that the mRNA levels of HAS1, HAS2 and

HAS3v1 in cancer cells are high enough to perform HA synthesis. However, by affinity histochemistry the cancer cells were nearly all HA negative except the outer layer of the cancer colonies that were in contact with stromal cells. The HA poor phenotype could be explained by the hypothesis that the cancer cells inside the tumor are lacking of the substrates for HA synthesis, namely UDP-glucoronic acid and UDP-glucosamine. This may also explain why there was no intracellular HA accumulation despite of strong overexpression of HAS3v2. Alternatively, the tumor cells degrade hyaluronan and generate small hyaluronan fragments that can not be stained by HABP.

Taking together, HAS3v2 induced tumor proliferation and cause changes in the stroma environment that might also contribute to tumor progression.

5.3.4 Other intracellular hyaladherins might be involved in HAS3v2 mediated signal transduction.

IHABP4 is a HA binding protein localized in the cytosol and nucleus [Huang et al. 2000]. Upregulation of IHABP4 is observed in several cancer types [Kobarg et al. 1997]. IHABP4 interacts with RACK1 and regulates the cell survival by inducing the protein kinase C pathway [Nery et al. 2004]. In addition, human CDC37 was also identified to be an intracellular HA binding protein, whose homologue in *Saccharomyces cerevisiae* functions as a cell division cycle control protein [Grammatikakis et al. 1995]. Furthermore, HABP1 is detected as an intracellular hyaladherin as well, although it is found also on the plasma membrane and thereby promote cell adhesion[Gupta et al. 1991; Gupta and Datta 1991; Muta et al. 1997; Dedio et al. 1998; Simos and Georgatos 1994]. HABP1 is highly expressed in various cancer types including esophageal adenocarci-

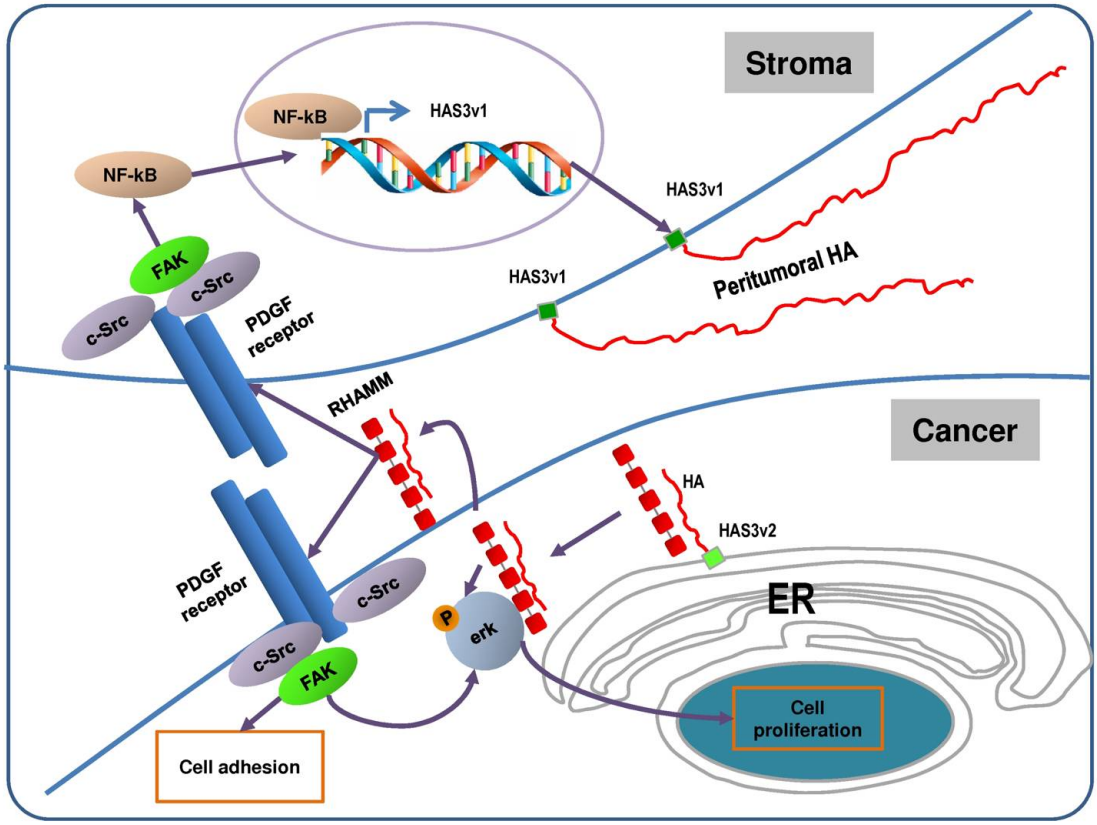

Figure 5.5: **HAS3v2 regulates both cancer and stromal cell phenotype though RHAMM** Overexpression of HAS3v2 in cancer cells induces cell proliferation and adhesion possiblely through RHAMM signaling cascade. RHAMM can be activated by binding to intracellular HA and translocated to the plasma membrane. There, activated RHAMM might also interact with the PDGF receptor of stromal cells in a paracrine manner. This can induce the FAK phophorylation in stromal cells. The transcriptional factor, NF-κB is a downstream target of the FAK signaling pathway. Promoter analysis revealed NF-κB binding sites in the putative promoter region of HAS3v1. After activation, NF-κB can translocate into the cell nucleus and promote HAS3v1 expression. Consequently, the upregulation of HAS3v1 in stromal cells leads to increased HA in stromal part of the tumor.

noma [Rubinstein et al. 2004]. Taking together, intracellular HA accumulation by HAS3v2 overexpression may lead to interaction between hyaluronan and those intracellular hyaladherins. Further experiments will be needed to prove whether intracellular hyaladherins are involved in the observed biological effects of HAS3v2.

5.3.5 Natural antisense RNA effect of HAS3v2

DERPC (Decreased Expression in Renal and Prostate Cancer) is a novel tumor repressor gene. Human DERPC is localized on the chromosome 16q22.1 close to human HAS3. The expression level of DERPC is observed to be downregulated in prostate and renal cancer [Sun et al. 2002], but shows no regulation during breast cancer progression [Green et al. 2009]. Overexpression of DERPC leads to inhibited proliferation of prostate cancer cells *in vitro* [Sun et al. 2002]. As shown in figure 5.6, mRNA of DERPC is complementary to the mRNA of HAS3v2. Complementary RNA can cause RNA degradation due to the mechanism of RNA interference (RNAi) [Werner et al. 2009]. This means upregulation of HAS3v2 mRNA can lead to the downregulation of DERPC. Consequently, cell proliferation rate might be enhanced due to the downregulation of the proliferation repressor, DERPC.

5.4 Therapeutic implications for HAS3v2 in cancer

There are various alterations that affect EGF receptor (EGFR) in human cancers [Henson and Gibson 2006]. EGFR is often mutated in the intracellular domain rendering the tyrosine kinase constitutively active. Furthermore, some tumors

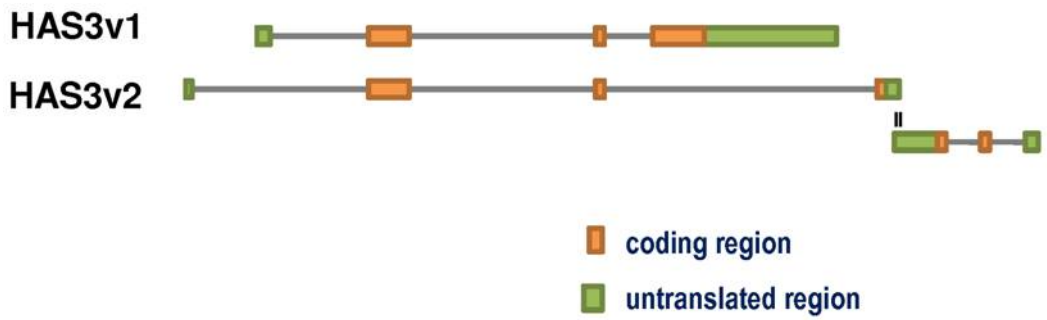

Figure 5.6: **HAS3v2 mRNA contains an antisense sequence against DERPC**
The mRNA complementary region between HAS3v2 and DERPC is indicated as ||. DERPC consists of three splicing variants and all of them contain the complementary sequence against HAS3v2.

increase the production of EGF-related growth factors leading to the persistent activation of ErbB receptors, which play important roles in tumor progression [Zhang et al. 2007].

Activation of the EGF receptor results in autophosphorylation of key tyrosine residues (figure 5.7) [Yarden 2001; Jorissen et al. 2003]. These tyrosine phosphorylation sites allow proteins to bind through their Src homology 2 (SH2) domains and lead to the activation of downstream signalling cascades including the RAS/extracellular signal regulated kinase (ERK) pathway, the phosphatidylinositol 3-kinase (PI3) pathway and the Janus kinase/Signal transducer and activator of transcription (JAK/STAT) pathway [Kisseleva et al. 2002]. These pathways act in a coordinated manner to regulate cell behavior, e.g. cell survival.

EGF signaling pathway has become a therapeutic target for cancer treatment [Zhang et al. 2007]. Cetuximab is a monoclonal antibody that prevents EGFR signaling by binding to the ligand binding and receptor dimerisation domains and is approved for treatment of colorectal and head-neck cancer [Van Cutsem et al. 2009; Egloff and Grandis 2009]. Further understanding of EGF signaling will undoubtedly improve the understanding of oncogenesis and possibly provide

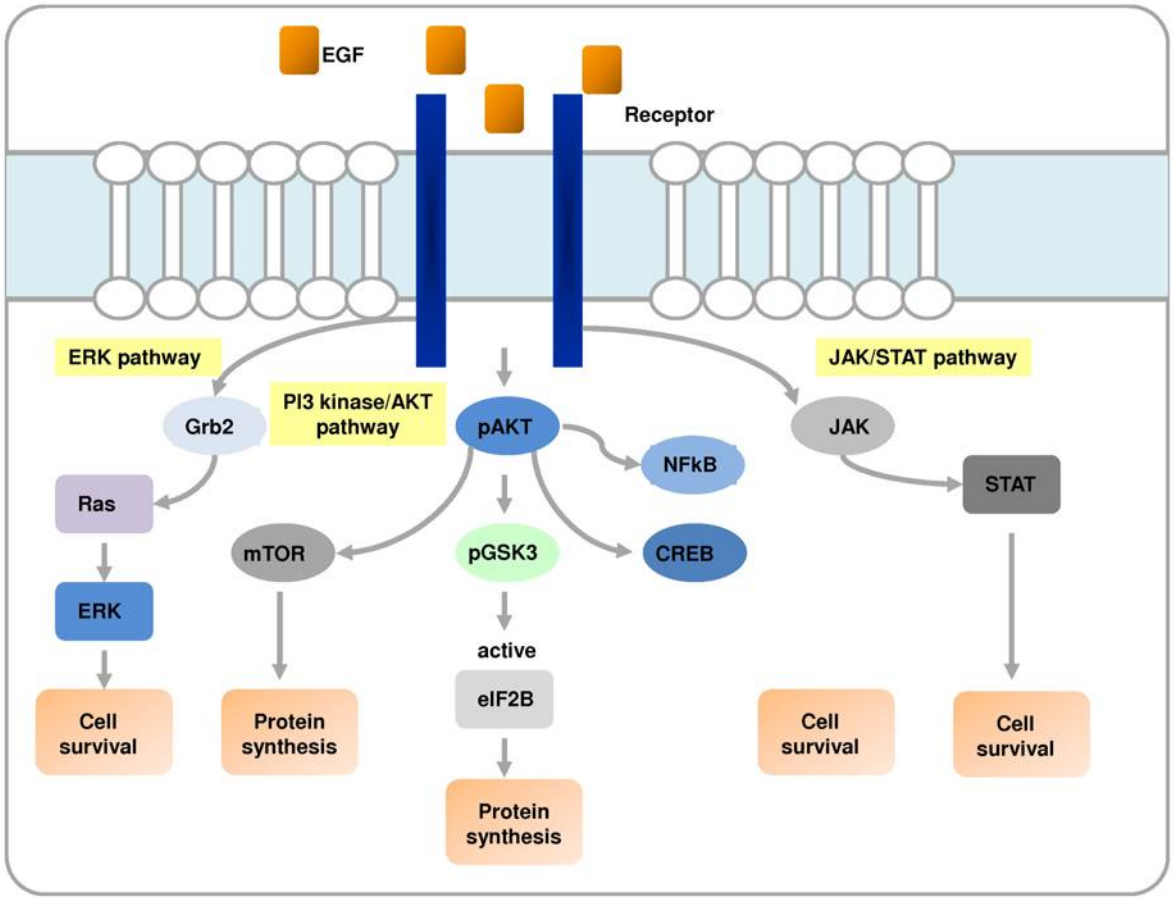

Figure 5.7: **Scheme of EGFR signaling pathway**

Activation of the EGF receptor results in autophosphorylation of key tyrosine residues within the EGFR. These tyrosine phosphorylation allow adaptor proteins to bind through their Src homology 2 (SH2) domains and leads to the activation of downstream signalling cascades including the RAS/extracellular signal regulated kinase (ERK) pathway, the phosphatidylinositol 3-kinase (PI3) pathway and the Janus kinase/Signal transducer and activator of transcription (JAK/STAT) pathway. These pathways act in a coordinated manner to promote cell survival.

novel targets for therapeutic intervention.

EGF was identified here to stimulate the expression of HAS3v2 *in vitro*. Importantly, the expression of HAS3v2 and EGFR in EAC patients are correlated. This suggested that HAS3v2 could be regulated by EGFR signaling both *in vitro* and *in vivo*. If HAS3v2 was a functional downstream target of EGFR in tumor, it could contribute to increased cancer cell proliferation and adhesion in response to EGF. Therefore, reduction of HAS3v2 expression might be one aspect of the anti-cancer effect of EGF-inhibitory pharmacology. However, it might also be considered that HAS3v2 could play a role for the occurrence of tumors resistant to anti-EGF therapy and HAS3v2 could be targeted specifically.

5.5 Open questions and perspective

The data presented in this thesis give rise to many further questions that will be addressed in future experiments.

1. HAS3v2 is shown to be located on the ER. However, no known ER retention signal was found on the AA sequence of HAS3v2 by *in silico* analysis. Therefore, the mechanism of ER targeting of HAS3v2 nees to be identified.

2. Recombinant HAS3v2 could be purified from hyaluronan deficient organisms, such as *E. coli*. HAS enzymatic capture assay with purified HAS3v2 protein could further proof that HAS3v2 is indeed an active hyaluronan synthase.

3. Promoter analysis of HAS3v2 could discover regulatory mechanisms in addition to EGFR signaling pathway.

4. Specific antibody is required to detect HAS3v2 in protein expression.

5. It is impossible to knock down the HAS3v2 specifically by RNAi due to the transcriptome structure. A neutralization antibody to HAS3v2 might be a promising option to advance the experimental data on HAS3v2 function and to test the potential therapeutic value.

Chapter 6

Summary

Hyaluronan is a large glycosaminoglycan mainly presented in the extracellular matrix as well as in the intracellular compartment. Hyaluronan is synthesized by three hyaluronan synthase isoforms, namely HAS1, HAS2 and HAS3. HAS3v2 is a smaller splicing variant of HAS3 with 281 AA in length. Here, biological and pathological functions of HAS3v2 were investigated for the first time.

HAS3v2 localizes on membrane of the endoplasmic reticulum as shown by stable overpression of YFP-HAS3v2 fusion protein. Overexpression of HAS3v2 leads to increased intracellular hyaluronan. A HA-HAS3v2 complex was also detected in microsomes of YFP-HAS3v2 overexpressing cells using the HAS enzymatic capture assay. This indicated HAS3v2 is an intracellular hyaluronan synthase or at least HA binding protein.

Esophageal cancer is one of the 10 most frequent tumor types worldwide, which is distinguished into two major subtypes: squamous cell carcinoma (ESCC) and adenocarcinoma (EAC). HAS3v2 is upregulated only in human EAC and also correlated with TNM staging. This suggested that HAS3v2 is a potential tumor marker for EAC. Lentiviral overexpression of HAS3v2 promotes cell proliferation rate both *in vitro* and after xenografting of HAS3v2 overexpressing EAC cells in nude mice . This phenotype was, at least partially, caused by enhanced ERK1/2 kinase phosphorylation. HAS3v2 also stimulated the phosphorylation of focal adhesion kinase (FAK) and improve EAC cell adhesion. Both phosphorylations could be the consequence of activated RHAMM signaling. Overexpression of HAS3v2 in cancer cells also stimulated HAS3v1 mRNA expression in stromal cells of EAC xenograft, which led to increased stromal HA levels. The stromal HA has been reported to provide microenvironment in favor for progression and metastasis.

The expression of HAS3v2 in EAC was regulated by EGF pathway and the blocking antibody of EGFR, Cetuximab, diminished the EGF-induced HAS3v2 upregulation. Furthermore, the mRNA expression of HAS3v2 and EGFR are positively correlated in EAC patients.

Taken together, HAS3v2 promotes malignant tumor cell phenotype and could be a diagnostic oncogene and a potential therapeutic target for EAC.

Bibliography

K Meyer and JW Palmer. The polysaccharide of the vitreous humor. *Journal of Biological Chemistry*, 1934.

J R Fraser, T C Laurent, and U B Laurent. Hyaluronan: its nature, distribution, functions and turnover. *Journal of internal medicine*, 242:27–33, July 1997. ISSN 0954-6820.

JH Fessler and LI Fessler. Electron microscopic visualization of the polysaccharide hyaluronic acid. *Proceedings of the National Academy of Sciences*, 1966.

N Itano and K Kimata. Molecular cloning of human hyaluronan synthase. *Biochemical and biophysical research communications*, 222:816–20, May 1996a. ISSN 0006-291X.

A M Shyjan, P Heldin, E C Butcher, T Yoshino, and M J Briskin. Functional cloning of the cdna for a human hyaluronan synthase. *The Journal of biological chemistry*, 271:23395–9, September 1996. ISSN 0021-9258.

A P Spicer, M L Augustine, and J A McDonald. Molecular cloning and characterization of a putative mouse hyaluronan synthase. *The Journal of biological chemistry*, 271:23400–6, September 1996. ISSN 0021-9258.

A P Spicer, J S Olson, and J A McDonald. Molecular cloning and characterization of a cdna encoding the third putative mammalian hyaluronan synthase.

The Journal of biological chemistry, 272:8957–61, April 1997a. ISSN 0021-9258.

Tetsuya Sayo, Yoshinori Sugiyama, Yoshito Takahashi, Naoko Ozawa, Shingo Sakai, Osamu Ishikawa, Masaaki Tamura, and Shintaro Inoue. Hyaluronan synthase 3 regulates hyaluronan synthesis in cultured human keratinocytes. *The Journal of investigative dermatology*, 118:43–8, January 2002. ISSN 0022-202X.

Jamie Monslow, John D Williams, Nadine Norton, Carol A Guy, Iain K Price, Sharon L Coleman, Nigel M Williams, Paul R Buckland, Andrew P Spicer, Nicholas Topley, Malcolm Davies, and Timothy Bowen. The human hyaluronan synthase genes: genomic structures, proximal promoters and polymorphic microsatellite markers. *Int J Biochem Cell Biol*, 35(8):1272–1283, 2003. ISSN 1357-2725 (Print).

A P Spicer, M F Seldin, A S Olsen, N Brown, D E Wells, N A Doggett, N Itano, K Kimata, J Inazawa, and J A McDonald. Chromosomal localization of the human and mouse hyaluronan synthase genes. *Genomics*, 41:493–7, May 1997b. ISSN 0888-7543.

A P Spicer and J A McDonald. Characterization and molecular evolution of a vertebrate hyaluronan synthase gene family. *The Journal of biological chemistry*, 273:1923–32, January 1998. ISSN 0021-9258.

P L DeAngelis. Hyaluronan synthases: fascinating glycosyltransferases from vertebrates, bacterial pathogens, and algal viruses. *Cellular and molecular life sciences : CMLS*, 56:670–82, November 1999. ISSN 1420-682X.

Todd D Camenisch, Joyce A Schroeder, Judy Bradley, Scott E Klewer, and John A McDonald. Heart-valve mesenchyme formation is dependent on hyaluronan-augmented activation of erbb2-erbb3 receptors. *Nature medicine*, 8:850–5, August 2002. ISSN 1078-8956.

P H Weigel, V C Hascall, and M Tammi. Hyaluronan synthases. *The Journal of biological chemistry*, 272:13997–4000, May 1997. ISSN 0021-9258.

T Asplund, J Brinck, M Suzuki, M J Briskin, and P Heldin. Characterization of hyaluronan synthase from a human glioma cell line. *Biochimica et biophysica acta*, 1380:377–88, May 1998. ISSN 0006-3002.

N Itano and K Kimata. Expression cloning and molecular characterization of has protein, a eukaryotic hyaluronan synthase. *The Journal of biological chemistry*, 271:9875–8, April 1996b. ISSN 0021-9258.

M Yoshida, N Itano, Y Yamada, and K Kimata. In vitro synthesis of hyaluronan by a single protein derived from mouse has1 gene and characterization of amino acid residues essential for the activity. *The Journal of biological chemistry*, 275:497–506, January 2000. ISSN 0021-9258.

P L DeAngelis and P H Weigel. Immunochemical confirmation of the primary structure of streptococcal hyaluronan synthase and synthesis of high molecular weight product by the recombinant enzyme. *Biochemistry*, 33: 9033–9, August 1994. ISSN 0006-2960.

P L DeAngelis and A M Achyuthan. Yeast-derived recombinant dg42 protein of xenopus can synthesize hyaluronan in vitro. *The Journal of biological chemistry*, 271:23657–60, September 1996. ISSN 0021-9258.

Tobias Schulz, Udo Schumacher, and Peter Prehm. Hyaluronan export by the abc transporter mrp5 and its modulation by intracellular cgmp. *The Journal of biological chemistry*, 282:20999–1004, July 2007. ISSN 0021-9258.

Peter Prehm and Udo Schumacher. Inhibition of hyaluronan export from human fibroblasts by inhibitors of multidrug resistance transporters. *Biochemical pharmacology*, 68:1401–10, October 2004. ISSN 0006-2952.

N Itano, T Sawai, M Yoshida, P Lenas, Y Yamada, M Imagawa, T Shinomura, M Hamaguchi, Y Yoshida, Y Ohnuki, S Miyauchi, A P Spicer, J A McDonald, and K Kimata. Three isoforms of mammalian hyaluronan synthases have distinct enzymatic properties. *The Journal of biological chemistry*, 274: 25085–92, August 1999a. ISSN 0021-9258.

J Brinck and P Heldin. Expression of recombinant hyaluronan synthase (has) isoforms in cho cells reduces cell migration and cell surface cd44. *Experimental cell research*, 252:342–51, November 1999. ISSN 0014-4827.

G I Frost, A B Csóka, T Wong, R Stern, and T B Csóka. Purification, cloning, and expression of human plasma hyaluronidase. *Biochemical and biophysical research communications*, 236:10–5, July 1997. ISSN 0006-291X.

B Strobl, C Wechselberger, D R Beier, and G Lepperdinger. Structural organization and chromosomal localization of hyal2, a gene encoding a lysosomal hyaluronidase. *Genomics*, 53:214–9, October 1998. ISSN 0888-7543.

G Lepperdinger, J Müllegger, and G Kreil. Hyal2–less active, but more versatile? *Matrix biology : journal of the International Society for Matrix Biology*, 20: 509–14, December 2001. ISSN 0945-053X.

S K Rai, F M Duh, V Vigdorovich, A Danilkovitch-Miagkova, M I Lerman, and A D Miller. Candidate tumor suppressor hyal2 is a glycosylphosphatidylinositol (gpi)-anchored cell-surface receptor for jaagsiekte sheep retrovirus, the envelope protein of which mediates oncogenic transformation. *Proceedings of the National Academy of Sciences of the United States of America*, 98: 4443–8, April 2001. ISSN 0027-8424.

G Kreil. Hyaluronidases–a group of neglected enzymes. *Protein science : a publication of the Protein Society*, 4:1666–9, September 1995. ISSN 0961-8368.

R K Batra, J C Olsen, D K Hoganson, B Caterson, and R C Boucher. Retroviral gene transfer is inhibited by chondroitin sulfate proteoglycans/glycosaminoglycans in malignant pleural effusions. *The Journal of biological chemistry*, 272:11736–43, May 1997. ISSN 0021-9258.

R Zaidel-Bar, M Cohen, L Addadi, and B Geiger. Hierarchical assembly of cell-matrix adhesion complexes. *Biochemical Society transactions*, 32:416–20, June 2004. ISSN 0300-5127.

Kirsi Rilla, Hanna Siiskonen, Andrew P Spicer, Juha M T Hyttinen, Markku I Tammi, and Raija H Tammi. Plasma membrane residence of hyaluronan synthase is coupled to its enzymatic activity. *The Journal of biological chemistry*, 280:31890–7, September 2005. ISSN 0021-9258.

Anne Kultti, Kirsi Rilla, Riikka Tiihonen, Andrew P Spicer, Raija H Tammi, and Markku I Tammi. Hyaluronan synthesis induces microvillus-like cell surface protrusions. *The Journal of biological chemistry*, 281:15821–8, June 2006. ISSN 0021-9258.

Anthony J Day and Glenn D Prestwich. Hyaluronan-binding proteins: tying up the giant. *The Journal of biological chemistry*, 277:4585–8, February 2002. ISSN 0021-9258.

R K Margolis, C P Crockett, W L Kiang, and R U Margolis. Glycosaminoglycans and glycoproteins associated with rat brain nuclei. *Biochimica et biophysica acta*, 451:465–9, December 1976. ISSN 0006-3002.

I Londoño and M Bendayan. High-resolution cytochemistry of neuraminic and hexuronic acid-containing macromolecules applying the enzyme-gold approach. *The journal of histochemistry and cytochemistry : official journal of the Histochemistry Society*, 36:1005–14, August 1988. ISSN 0022-1554.

F W Kan. High-resolution localization of hyaluronic acid in the golden hamster oocyte-cumulus complex by use of a hyaluronidase-gold complex. *The Anatomical record*, 228:370–82, December 1990. ISSN 0003-276X.

JA Ripellino, M. Bailo, RU Margolis, and RK Margolis. Light and electron microscopic studies on the localization of hyaluronic acid in developing rat cerebellum. *Journal of Cell Biology*, 106:845–855, 1988.

PS Eggli and W. Graber. Association of hyaluronan with rat vascular endothelial and smooth muscle cells. *Journal of Histochemistry and Cytochemistry*, 43:689–697, 1995.

Aimin Wang and Vincent C Hascall. Hyperglycemia, intracellular hyaluronan synthesis, cyclin d3 and autophagy. *Autophagy*, 5:864–5, August 2009. ISSN 1554-8635.

S P Evanko and T N Wight. Intracellular localization of hyaluronan in proliferating cells. *The journal of histochemistry and cytochemistry : official journal of the Histochemistry Society*, 47:1331–42, October 1999. ISSN 0022-1554.

V Assmann, J F Marshall, C Fieber, M Hofmann, and I R Hart. The human hyaluronan receptor rhamm is expressed as an intracellular protein in breast cancer cells. *Journal of cell science*, 111 (Pt 1:1685–94, June 1998. ISSN 0021-9533.

M Hofmann, C Fieber, V Assmann, M Göttlicher, J Sleeman, R Plug, N Howells, O Von Stein, H Ponta, and P Herrlich. Identification of ihabp, a 95 kda intracellular hyaluronate binding protein. *Journal of cell science*, 111 (Pt 1: 1673–84, June 1998. ISSN 0021-9533.

L. Huang, N. Grammatikakis, M. Yoneda, S.D. Banerjee, and B.P. Toole. Molecular characterization of a novel intracellular hyaluronan-binding protein. *Journal of Biological Chemistry*, 275:29829–29839, 2000.

Eva A Turley, Paul W Noble, and Lilly Y W Bourguignon. Signaling properties of hyaluronan receptors. *The Journal of biological chemistry*, 277:4589–92, February 2002. ISSN 0021-9258.

J Kobarg, S Schnittger, C Fonatsch, H Lemke, M A Bowen, F Buck, and H P Hansen. Characterization, mapping and partial cdna sequence of the 57-kd intracellular ki-1 antigen. *Experimental and clinical immunogenetics*, 14: 273–80, January 1997. ISSN 0254-9670.

Flávia C Nery, Dario O Passos, Vera S Garcia, and Jörg Kobarg. Ki-1/57 interacts with rack1 and is a substrate for the phosphorylation by phorbol 12-myristate 13-acetate-activated protein kinase c. *The Journal of biological chemistry*, 279:11444–55, March 2004. ISSN 0021-9258.

N Grammatikakis, A Grammatikakis, M Yoneda, Q Yu, S D Banerjee, and B P Toole. A novel glycosaminoglycan-binding protein is the vertebrate homologue of the cell cycle control protein, cdc37. *The Journal of biological chemistry*, 270:16198–205, July 1995. ISSN 0021-9258.

S Gupta, R B Batchu, and K Datta. Purification, partial characterization of rat kidney hyaluronic acid binding protein and its localization on the cell surface. *European journal of cell biology*, 56:58–67, October 1991. ISSN 0171-9335.

S Gupta and K Datta. Possible role of hyaluronectin on cell adhesion in rat histiocytoma. *Experimental cell research*, 195:386–94, August 1991. ISSN 0014-4827.

T Muta, D Kang, S Kitajima, T Fujiwara, and N Hamasaki. p32 protein, a splicing factor 2-associated protein, is localized in mitochondrial matrix and is functionally important in maintaining oxidative phosphorylation. *The Journal of biological chemistry*, 272:24363–70, September 1997. ISSN 0021-9258.

J Dedio, W Jahnen-Dechent, M Bachmann, and W Müller-Esterl. The multiligand-binding protein gc1qr, putative c1q receptor, is a mitochondrial protein. *Journal of immunology (Baltimore, Md. : 1950)*, 160:3534–42, April 1998. ISSN 0022-1767.

G Simos and S D Georgatos. The lamin b receptor-associated protein p34 shares sequence homology and antigenic determinants with the splicing factor 2-associated protein p32. *FEBS letters*, 346:225–8, June 1994. ISSN 0014-5793.

M Majumdar, J Meenakshi, S K Goswami, and K Datta. Hyaluronan binding protein 1 (habp1)/c1qbp/p32 is an endogenous substrate for map kinase and is translocated to the nucleus upon mitogenic stimulation. *Biochemical and biophysical research communications*, 291:829–37, March 2002. ISSN 0006-291X.

Anupama Kamal and K Datta. Upregulation of hyaluronan binding protein 1 (habp1/p32/gc1qr) is associated with cisplatin induced apoptosis. *Apoptosis : an international journal on programmed cell death*, 11:861–74, May 2006. ISSN 1360-8185.

W X Guo, B Ghebrehiwet, B Weksler, K Schweitzer, and E I Peerschke. Upregulation of endothelial cell binding proteins/receptors for complement component c1q by inflammatory cytokines. *The Journal of laboratory and clinical medicine*, 133:541–50, June 1999. ISSN 0022-2143.

J Meenakshi, K Anupama, S K Goswami, and K Datta. Constitutive expression of hyaluronan binding protein 1 (habp1/p32/gc1qr) in normal fibroblast cells perturbs its growth characteristics and induces apoptosis. *Biochemical and biophysical research communications*, 300:686–93, January 2003. ISSN 0006-291X.

Aniruddha Sengupta, Rakesh K Tyagi, and Kasturi Datta. Truncated variants of hyaluronan-binding protein 1 bind hyaluronan and induce identical morphological aberrations in cos-1 cells. *The Biochemical journal*, 380:837–44, June 2004. ISSN 1470-8728.

Anindya Roy Chowdhury, Ilora Ghosh, and Kasturi Datta. Excessive reactive oxygen species induces apoptosis in fibroblasts: role of mitochondrially accumulated hyaluronic acid binding protein 1 (habp1/p32/gc1qr). *Experimental cell research*, 314:651–67, February 2008. ISSN 0014-4827.

Daniel B Rubinstein, Alexei Stortchevoi, Michael Boosalis, Raheela Ashfaq, Berhane Ghebrehiwet, Ellinor I B Peerschke, Fabien Calvo, and Thierry Guillaume. Receptor for the globular heads of c1q (gc1q-r, p33, hyaluronan-binding protein) is preferentially expressed by adenocarcinoma cells. *International journal of cancer. Journal international du cancer*, 110:741–50, July 2004. ISSN 0020-7136.

J E Scott, C Cummings, A Brass, and Y Chen. Secondary and tertiary structures of hyaluronan in aqueous solution, investigated by rotary shadowing-electron microscopy and computer simulation. hyaluronan is a very efficient network-forming polymer. *The Biochemical journal*, 274 (Pt 3:699–705, March 1991. ISSN 0264-6021.

C B Henry and B R Duling. Permeation of the luminal capillary glycocalyx is determined by hyaluronan. *The American journal of physiology*, 277:H508–14, August 1999. ISSN 0002-9513.

Bryan P Toole. Hyaluronan: from extracellular glue to pericellular cue. *Nature reviews. Cancer*, 4:528–39, July 2004. ISSN 1474-175X.

B P Toole. Hyaluronan and its binding proteins, the hyaladherins. *Current opinion in cell biology*, 2:839–44, October 1990. ISSN 0955-0674.

B P Toole. Hyaluronan in morphogenesis. *Seminars in cell & developmental biology*, 12:79–87, April 2001. ISSN 1084-9521.

P H Weigel, S J Frost, C T McGary, and R D LeBoeuf. The role of hyaluronic acid in inflammation and wound healing. *International journal of tissue reactions*, 10:355–65, January 1988. ISSN 0250-0868.

M T Longaker, E S Chiu, N S Adzick, M Stern, M R Harrison, and R Stern. Studies in fetal wound healing. v. a prolonged presence of hyaluronic acid characterizes fetal wound fluid. *Annals of surgery*, 213:292–6, April 1991. ISSN 0003-4932.

Paul W Noble. Hyaluronan and its catabolic products in tissue injury and repair. *Matrix biology : journal of the International Society for Matrix Biology*, 21: 25–9, January 2002. ISSN 0945-053X.

Carol A De la Motte, Vincent C Hascall, Judith Drazba, Sudip K Bandyopadhyay, and Scott A Strong. Mononuclear leukocytes bind to specific hyaluronan structures on colon mucosal smooth muscle cells treated with polyinosinic acid:polycytidylic acid: inter-alpha-trypsin inhibitor is crucial to structure and function. *The American journal of pathology*, 163:121–33, July 2003. ISSN 0002-9440.

Alana K Majors, Richard C Austin, Carol A De la Motte, Reed E Pyeritz, Vincent C Hascall, Sean P Kessler, Ganes Sen, and Scott A Strong. Endoplasmic reticulum stress induces hyaluronan deposition and leukocyte adhesion. *The Journal of biological chemistry*, 278:47223–31, November 2003. ISSN 0021-9258.

E A Turley. The control of adrenocortical cytodifferentiation by extracellular matrix. *Differentiation; research in biological diversity*, 17:93–103, January 1980. ISSN 0301-4681.

V Assmann, D Jenkinson, J F Marshall, and I R Hart. The intracellular hyaluronan receptor rhamm/ihabp interacts with microtubules and actin filaments. *Journal of cell science*, 112 (Pt 2:3943–54, November 1999. ISSN 0021-9533.

M Crainie, A R Belch, M J Mant, and L M Pilarski. Overexpression of the receptor for hyaluronan-mediated motility (rhamm) characterizes the malignant clone in multiple myeloma: identification of three distinct rhamm variants. *Blood*, 93:1684–96, March 1999. ISSN 0006-4971.

J Entwistle, C L Hall, and E A Turley. Ha receptors: regulators of signalling to the cytoskeleton. *Journal of cellular biochemistry*, 61:569–77, June 1996. ISSN 0730-2312.

B D Lynn, E A Turley, and J I Nagy. Subcellular distribution, calmodulin interaction, and mitochondrial association of the hyaluronan-binding protein rhamm in rat brain. *Journal of neuroscience research*, 65:6–16, July 2001. ISSN 0360-4012.

Christopher A Maxwell, Jonathan J Keats, Mary Crainie, Xuejun Sun, Tim Yen, Ellen Shibuya, Michael Hendzel, Gordon Chan, and Linda M Pilarski. Rhamm is a centrosomal protein that interacts with dynein and maintains spindle pole stability. *Molecular biology of the cell*, 14:2262–76, June 2003. ISSN 1059-1524.

C L Hall, B Yang, X Yang, S Zhang, M Turley, S Samuel, L A Lange, C Wang, G D Curpen, R C Savani, A H Greenberg, and E A Turley. Overexpression of the hyaluronan receptor rhamm is transforming and is also required for h-ras transformation. *Cell*, 82:19–26, July 1995. ISSN 0092-8674.

S Mohapatra, X Yang, J A Wright, E A Turley, and A H Greenberg. Soluble hyaluronan receptor rhamm induces mitotic arrest by suppressing cdc2 and

cyclin b1 expression. *The Journal of experimental medicine*, 183:1663–8, April 1996. ISSN 0022-1007.

Sindy Sohr and Kurt Engeland. Rhamm is differentially expressed in the cell cycle and downregulated by the tumor suppressor p53. *Cell cycle (Georgetown, Tex.)*, 7:3448–60, November 2008. ISSN 1551-4005.

M Brecht, U Mayer, E Schlosser, and P Prehm. Increased hyaluronate synthesis is required for fibroblast detachment and mitosis. *The Biochemical journal*, 239:445–50, October 1986. ISSN 0264-6021.

Stephen P Evanko, Markku I Tammi, Raija H Tammi, and Thomas N Wight. Hyaluronan-dependent pericellular matrix. *Advanced drug delivery reviews*, 59:1351–65, November 2007. ISSN 0169-409X.

Mark Slevin, Jurek Krupinski, John Gaffney, Sabine Matou, David West, Horace Delisser, Rashmin C Savani, and Shant Kumar. Hyaluronan-mediated angiogenesis in vascular disease: uncovering rhamm and cd44 receptor signaling pathways. *Matrix biology : journal of the International Society for Matrix Biology*, 26:58–68, January 2007. ISSN 0945-053X.

Shlomo Nedvetzki, Erez Gonen, Nathalie Assayag, Reuven Reich, Richard O Williams, Robin L Thurmond, Jing-Feng Huang, Birgit A Neudecker, Fu-Sheng Wang, Fu-Shang Wang, Eva A Turley, and David Naor. Rhamm, a receptor for hyaluronan-mediated motility, compensates for cd44 in inflamed cd44-knockout mice: a different interpretation of redundancy. *Proceedings of the National Academy of Sciences of the United States of America*, 101:18081–6, December 2004. ISSN 0027-8424.

Cornelia Tolg, Sara R Hamilton, Kerry-Ann Nakrieko, Fatemeh Kooshesh, Paul Walton, James B McCarthy, Mina J Bissell, and Eva A Turley. Rhamm-/- fibroblasts are defective in cd44-mediated erk1,2 motogenic signaling,

leading to defective skin wound repair. *The Journal of cell biology*, 175: 1017–28, December 2006. ISSN 0021-9525.

Krzysztof Giannopoulos and Michael Schmitt. Targets and strategies for t-cell based vaccines in patients with b-cell chronic lymphocytic leukemia. *Leukemia & lymphoma*, 47:2028–36, October 2006. ISSN 1042-8194.

I Hus, M Schmitt, J Tabarkiewicz, S Radej, K Wojas, A Bojarska-Junak, A Schmitt, K Giannopoulos, A Dmoszyńska, and J Roliński. Vaccination of b-cll patients with autologous dendritic cells can change the frequency of leukemia antigen-specific cd8+ t cells as well as cd4+cd25+foxp3+ regulatory t cells toward an antileukemia response. *Leukemia : official journal of the Leukemia Society of America, Leukemia Research Fund, U.K*, 22: 1007–17, May 2008. ISSN 1476-5551.

D T Rein, K Roehrig, T Schöndorf, A Lazar, M Fleisch, D Niederacher, H G Bender, and P Dall. Expression of the hyaluronan receptor rhamm in endometrial carcinomas suggests a role in tumour progression and metastasis. *Journal of cancer research and clinical oncology*, 129:161–4, March 2003. ISSN 0171-5216.

Cornelia Tolg, Raymoond Poon, Riccardo Fodde, Eva Ann Turley, and Benjamin Aaron Alman. Genetic deletion of receptor for hyaluronan-mediated motility (rhamm) attenuates the formation of aggressive fibromatosis (desmoid tumor). *Oncogene*, 22:6873–82, October 2003. ISSN 0950-9232.

Yukio Yamano, Katsuhiro Uzawa, Keiji Shinozuka, Kazuaki Fushimi, Takashi Ishigami, Hitomi Nomura, Katsunori Ogawara, Masashi Shiiba, Hidetaka Yokoe, and Hideki Tanzawa. Hyaluronan-mediated motility: a target in oral squamous cell carcinoma. *International journal of oncology*, 32:1001–9, May 2008. ISSN 1019-6439.

I Zlobec, L Terracciano, L Tornillo, U Günthert, T Vuong, J R Jass, and A Lugli. Role of rhamm within the hierarchy of well-established prognostic factors in colorectal cancer. *Gut*, 57:1413–9, October 2008. ISSN 1468-3288.

Miguel Angel Pujana, Jing-Dong J Han, Lea M Starita, Kristen N Stevens, Muneesh Tewari, Jin Sook Ahn, Gad Rennert, Víctor Moreno, Tomas Kirchhoff, Bert Gold, Volker Assmann, Wael M Elshamy, Jean-François Rual, Douglas Levine, Laura S Rozek, Rebecca S Gelman, Kristin C Gunsalus, Roger A Greenberg, Bijan Sobhian, Nicolas Bertin, Kavitha Venkatesan, Nono Ayivi-Guedehoussou, Xavier Solé, Pilar Hernández, Conxi Lázaro, Katherine L Nathanson, Barbara L Weber, Michael E Cusick, David E Hill, Kenneth Offit, David M Livingston, Stephen B Gruber, Jeffrey D Parvin, and Marc Vidal. Network modeling links breast cancer susceptibility and centrosome dysfunction. *Nature genetics*, 39:1338–49, November 2007. ISSN 1546-1718.

V Assmann, C E Gillett, R Poulsom, K Ryder, I R Hart, and A M Hanby. The pattern of expression of the microtubule-binding protein rhamm/ihabp in mammary carcinoma suggests a role in the invasive behaviour of tumour cells. *The Journal of pathology*, 195:191–6, September 2001. ISSN 0022-3417.

C Wang, A D Thor, D H Moore, Y Zhao, R Kerschmann, R Stern, P H Watson, and E A Turley. The overexpression of rhamm, a hyaluronan-binding protein that regulates ras signaling, correlates with overexpression of mitogen-activated protein kinase and is a significant parameter in breast cancer progression. *Clinical cancer research : an official journal of the American Association for Cancer Research*, 4:567–76, March 1998. ISSN 1078-0432.

G R Screaton, M V Bell, D G Jackson, F B Cornelis, U Gerth, and J I Bell. Genomic structure of dna encoding the lymphocyte homing receptor cd44

reveals at least 12 alternatively spliced exons. *Proceedings of the National Academy of Sciences of the United States of America*, 89:12160–4, December 1992. ISSN 0027-8424.

I Stamenkovic, A Aruffo, M Amiot, and B Seed. The hematopoietic and epithelial forms of cd44 are distinct polypeptides with different adhesion potentials for hyaluronate-bearing cells. *The EMBO journal*, 10:343–8, February 1991. ISSN 0261-4189.

U Günthert, M Hofmann, W Rudy, S Reber, M Zöller, I Haussmann, S Matzku, A Wenzel, H Ponta, and P Herrlich. A new variant of glycoprotein cd44 confers metastatic potential to rat carcinoma cells. *Cell*, 65:13–24, April 1991. ISSN 0092-8674.

L A Goldstein and E C Butcher. Identification of mrna that encodes an alternative form of h-cam(cd44) in lymphoid and nonlymphoid tissues. *Immunogenetics*, 32:389–97, January 1990. ISSN 0093-7711.

W Lou, D Krill, R Dhir, M J Becich, J T Dong, H F Frierson, W B Isaacs, J T Isaacs, and A C Gao. Methylation of the cd44 metastasis suppressor gene in human prostate cancer. *Cancer research*, 59:2329–31, May 1999. ISSN 0008-5472.

N S Verkaik, J Trapman, J C Romijn, T H Van der Kwast, and G J Van Steenbrugge. Down-regulation of cd44 expression in human prostatic carcinoma cell lines is correlated with dna hypermethylation. *International journal of cancer. Journal international du cancer*, 80:439–43, January 1999. ISSN 0020-7136.

Pu Yan, Annick Mühlethaler, Katia Balmas Bourloud, Maja Nenadov Beck, and Nicole Gross. Hypermethylation-mediated regulation of cd44 gene expression in human neuroblastoma. *Genes, chromosomes & cancer*, 36:129–38, February 2003. ISSN 1045-2257.

G Borland, J A Ross, and K Guy. Forms and functions of cd44. *Immunology*, 93:139–48, February 1998. ISSN 0019-2805.

B Greenfield, W C Wang, H Marquardt, M Piepkorn, E A Wolff, A Aruffo, and K L Bennett. Characterization of the heparan sulfate and chondroitin sulfate assembly sites in cd44. *The Journal of biological chemistry*, 274:2511–7, January 1999. ISSN 0021-9258.

L Zhang, G David, and J D Esko. Repetitive ser-gly sequences enhance heparan sulfate assembly in proteoglycans. *The Journal of biological chemistry*, 270:27127–35, November 1995. ISSN 0021-9258.

James W Legg, Charlotte A Lewis, Maddy Parsons, Tony Ng, and Clare M Isacke. A novel pkc-regulated mechanism controls cd44 ezrin association and directional cell motility. *Nature cell biology*, 4:399–407, June 2002. ISSN 1465-7392.

S J Neame and C M Isacke. Phosphorylation of cd44 in vivo requires both ser323 and ser325, but does not regulate membrane localization or cytoskeletal interaction in epithelial cells. *The EMBO journal*, 11:4733–8, December 1992. ISSN 0261-4189.

Joanna Cichy and Ellen Puré. The liberation of cd44. *The Journal of cell biology*, 161:839–43, June 2003. ISSN 0021-9525.

J Lesley, R Hyman, and P W Kincade. Cd44 and its interaction with extracellular matrix. *Advances in immunology*, 54:271–335, January 1993. ISSN 0065-2776.

L Y Bourguignon, V B Lokeshwar, J He, X Chen, and G J Bourguignon. A cd44-like endothelial cell transmembrane glycoprotein (gp116) interacts with extracellular matrix and ankyrin. *Molecular and cellular biology*, 12:4464–71, October 1992. ISSN 0270-7306.

L Y Bourguignon, D Zhu, and H Zhu. Cd44 isoform-cytoskeleton interaction in oncogenic signaling and tumor progression. *Frontiers in bioscience : a journal and virtual library*, 3:d637–49, July 1998. ISSN 1093-4715.

V B Lokeshwar, N Iida, and L Y Bourguignon. The cell adhesion molecule, gp116, is a new cd44 variant (ex14/v10) involved in hyaluronic acid binding and endothelial cell proliferation. *The Journal of biological chemistry*, 271: 23853–64, September 1996. ISSN 0021-9258.

Hideaki Nakazawa, Shuichi Yoshihara, Daisuke Kudo, Hajime Morohashi, Ikuko Kakizaki, Atsushi Kon, Keiichi Takagaki, and Mutsuo Sasaki. 4-methylumbelliferone, a hyaluronan synthase suppressor, enhances the anticancer activity of gemcitabine in human pancreatic cancer cells. *Cancer chemotherapy and pharmacology*, 57:165–70, January 2006. ISSN 0344-5704.

Zsuzsanna Pályi-Krekk, Márk Barok, Jorma Isola, Markku Tammi, János Szöllosi, and Peter Nagy. Hyaluronan-induced masking of erbb2 and cd44-enhanced trastuzumab internalisation in trastuzumab resistant breast cancer. *European journal of cancer (Oxford, England : 1990)*, 43:2423–33, November 2007. ISSN 0959-8049.

J P Pienimaki, K Rilla, C Fulop, R K Sironen, S Karvinen, S Pasonen, M J Lammi, R Tammi, V C Hascall, and M I Tammi. Epidermal growth factor activates hyaluronan synthase 2 in epidermal keratinocytes and increases pericellular and intracellular hyaluronan. *The Journal of biological chemistry*, 276:20428–35, June 2001. ISSN 0021-9258.

Susanna Karvinen, Sanna Pasonen-Seppänen, Juha M T Hyttinen, Juha-Pekka Pienimäki, Kari Törrönen, Tiina A Jokela, Markku I Tammi, and Raija Tammi. Keratinocyte growth factor stimulates migration and hyaluronan

synthesis in the epidermis by activation of keratinocyte hyaluronan synthases 2 and 3. *The Journal of biological chemistry*, 278:49495–504, December 2003. ISSN 0021-9258.

Sanna Pasonen-Seppänen, Susanna Karvinen, Kari Törrönen, Juha M T Hyttinen, Tiina Jokela, Mikko J Lammi, Markku I Tammi, and Raija Tammi. Egf upregulates, whereas tgf-beta downregulates, the hyaluronan synthases has2 and has3 in organotypic keratinocyte cultures: correlations with epidermal proliferation and differentiation. *The Journal of investigative dermatology*, 120:1038–44, June 2003. ISSN 0022-202X.

A Jacobson, J Brinck, M J Briskin, A P Spicer, and P Heldin. Expression of human hyaluronan synthases in response to external stimuli. *The Biochemical journal*, 348 Pt 1:29–35, May 2000. ISSN 0264-6021.

W Knudson and B P Toole. Membrane association of the hyaluronate stimulatory factor from lx-1 human lung carcinoma cells. *Journal of cellular biochemistry*, 38:165–77, November 1988. ISSN 0730-2312.

M Edward, C Gillan, D Micha, and R H Tammi. Tumour regulation of fibroblast hyaluronan expression: a mechanism to facilitate tumour growth and invasion. *Carcinogenesis*, 26:1215–23, July 2005. ISSN 0143-3334.

Antoine E Karnoub, Ajeeta B Dash, Annie P Vo, Andrew Sullivan, Mary W Brooks, George W Bell, Andrea L Richardson, Kornelia Polyak, Ross Tubo, and Robert A Weinberg. Mesenchymal stem cells within tumour stroma promote breast cancer metastasis. *Nature*, 449:557–63, October 2007. ISSN 1476-4687.

Naoki Itano and Koji Kimata. Mammalian hyaluronan synthases. *IUBMB life*, 54:195–9, October 2002. ISSN 1521-6543.

R. Stern, A.A. Asari, and K.N. Sugahara. Hyaluronan fragments: an information-rich system. *European journal of cell biology*, 85:699–715, 2006.

R Kosaki, K Watanabe, and Y Yamaguchi. Overproduction of hyaluronan by expression of the hyaluronan synthase has2 enhances anchorage-independent growth and tumorigenicity. *Cancer research*, 59:1141–5, March 1999. ISSN 0008-5472.

N Liu, F Gao, Z Han, X Xu, C B Underhill, and L Zhang. Hyaluronan synthase 3 overexpression promotes the growth of tsu prostate cancer cells. *Cancer research*, 61:5207–14, July 2001. ISSN 0008-5472.

N Itano, T Sawai, O Miyaishi, and K Kimata. Relationship between hyaluronan production and metastatic potential of mouse mammary carcinoma cells. *Cancer research*, 59:2499–504, May 1999b. ISSN 0008-5472.

Hiroshi Koyama, Terumasa Hibi, Zenzo Isogai, Masahiko Yoneda, Minoru Fujimori, Jun Amano, Masatomo Kawakubo, Reiji Kannagi, Koji Kimata, Shun'ichiro Taniguchi, and Naoki Itano. Hyperproduction of hyaluronan in neu-induced mammary tumor accelerates angiogenesis through stromal cell recruitment: possible involvement of versican/pg-m. *The American journal of pathology*, 170:1086–99, March 2007. ISSN 0002-9440.

Alexandra Zoltan-Jones, Lei Huang, Shibnath Ghatak, and Bryan P Toole. Elevated hyaluronan production induces mesenchymal and transformed properties in epithelial cells. *The Journal of biological chemistry*, 278:45801–10, November 2003. ISSN 0021-9258.

Alexis Desmoulière, Christelle Guyot, and Giulio Gabbiani. The stroma reaction myofibroblast: a key player in the control of tumor cell behavior. *The International journal of developmental biology*, 48:509–17, January 2004. ISSN 0214-6282.

M Löhr, C Schmidt, J Ringel, M Kluth, P Müller, H Nizze, and R Jesnowski. Transforming growth factor-beta1 induces desmoplasia in an experimental

model of human pancreatic carcinoma. *Cancer research*, 61:550–5, January 2001. ISSN 0008-5472.

Naoki Itano, Takahiro Sawai, Fukiko Atsumi, Osamu Miyaishi, Shun'ichiro Taniguchi, Reiji Kannagi, Michinari Hamaguchi, and Koji Kimata. Selective expression and functional characteristics of three mammalian hyaluronan synthases in oncogenic malignant transformation. *The Journal of biological chemistry*, 279:18679–87, April 2004. ISSN 0021-9258.

Achilleas D Theocharis, Demitrios H Vynios, Nikoletta Papageorgakopoulou, Spyros S Skandalis, and Dimitrios A Theocharis. Altered content composition and structure of glycosaminoglycans and proteoglycans in gastric carcinoma. *The international journal of biochemistry & cell biology*, 35: 376–90, March 2003. ISSN 1357-2725.

Naoki Itano, Fukiko Atsumi, Takahiro Sawai, Yoichi Yamada, Osamu Miyaishi, Takeshi Senga, Michinari Hamaguchi, and Koji Kimata. Abnormal accumulation of hyaluronan matrix diminishes contact inhibition of cell growth and promotes cell migration. *Proceedings of the National Academy of Sciences of the United States of America*, 99:3609–14, March 2002. ISSN 0027-8424.

Nikki Cheng, Anna Chytil, Yu Shyr, Alison Joly, and Harold L Moses. Enhanced hepatocyte growth factor signaling by type ii transforming growth factor-beta receptor knockout fibroblasts promotes mammary tumorigenesis. *Cancer research*, 67:4869–77, May 2007. ISSN 0008-5472.

P Auvinen, R Tammi, J Parkkinen, M Tammi, U Agren, R Johansson, P Hirvikoski, M Eskelinen, and V M Kosma. Hyaluronan in peritumoral stroma and malignant cells associates with breast cancer spreading and predicts survival. *The American journal of pathology*, 156:529–36, February 2000. ISSN 0002-9440.

K. Ropponen, M. Tammi, J. Parkkinen, M. Eskelinen, R. Tammi, P. Lipponen, U. Agren, E. Alhava, and V.M. Kosma. Tumor cell-associated hyaluronan as an unfavorable prognostic factor in colorectal cancer. *Cancer Research*, 58:342–347, 1998.

P. Lipponen, S. Aaltomaa, R. Tammi, M. Tammi, U. Ågren, and V.M. Kosma. High stromal hyaluronan level is associated with poor differentiation and metastasis in prostate cancer. *European Journal of Cancer*, 37:849–856, 2001.

M.A. Anttila, R.H. Tammi, M.I. Tammi, K.J. Syrjanen, S.V. Saarikoski, and V.M. Kosma. High levels of stromal hyaluronan predict poor disease outcome in epithelial ovarian cancer 1. *Cancer research*, 60:150–155, 2000.

L P Setälä, M I Tammi, R H Tammi, M J Eskelinen, P K Lipponen, U M Agren, J Parkkinen, E M Alhava, and V M Kosma. Hyaluronan expression in gastric cancer cells is associated with local and nodal spread and reduced survival rate. *British journal of cancer*, 79:1133–8, March 1999. ISSN 0007-0920.

S H Hautmann, V B Lokeshwar, G L Schroeder, F Civantos, R C Duncan, R Gnann, M G Friedrich, and M S Soloway. Elevated tissue expression of hyaluronic acid and hyaluronidase validates the ha-haase urine test for bladder cancer. *The Journal of urology*, 165:2068–74, June 2001. ISSN 0022-5347.

R Pirinen, R Tammi, M Tammi, P Hirvikoski, J J Parkkinen, R Johansson, J Böhm, S Hollmén, and V M Kosma. Prognostic value of hyaluronan expression in non-small-cell lung cancer: Increased stromal expression indicates unfavorable outcome in patients with adenocarcinoma. *International journal of cancer. Journal international du cancer*, 95:12–7, January 2001. ISSN 0020-7136.

Supaporn Suwiwat, Carmela Ricciardelli, Raija Tammi, Markku Tammi, Paivi Auvinen, Veli-Matti Kosma, Richard G LeBaron, Wendy A Raymond, Wayne D Tilley, and David J Horsfall. Expression of extracellular matrix components versican, chondroitin sulfate, tenascin, and hyaluronan, and their association with disease outcome in node-negative breast cancer. *Clinical cancer research : an official journal of the American Association for Cancer Research*, 10:2491–8, April 2004. ISSN 1078-0432.

Jan Böhm, Leo Niskanen, Raija Tammi, Markku Tammi, Matti Eskelinen, Risto Pirinen, Sinikka Hollmen, Esko Alhava, and Veli-Matti Kosma. Hyaluronan expression in differentiated thyroid carcinoma. *The Journal of pathology*, 196:180–5, February 2002. ISSN 0022-3417.

Martin Köbel, Wilko Weichert, Katharina Crüwell, Wolfgang D Schmitt, Christine Lautenschläger, and Steffen Hauptmann. Epithelial hyaluronic acid and cd44v6 are mutually involved in invasion of colorectal adenocarcinomas and linked to patient prognosis. *Virchows Archiv : an international journal of pathology*, 445:456–64, November 2004. ISSN 0945-6317.

R T Pirinen, R H Tammi, M I Tammi, P K Pääkkö, J J Parkkinen, U M Agren, R T Johansson, M M Viren, U Törmänen, Y M Soini, and V M Kosma. Expression of hyaluronan in normal and dysplastic bronchial epithelium and in squamous cell carcinoma of the lung. *International journal of cancer. Journal international du cancer*, 79:251–5, June 1998. ISSN 0020-7136.

P Bertrand, N Girard, B Delpech, C Duval, J D'Anjou, and J P Dauce. Hyaluronan (hyaluronic acid) and hyaluronectin in the extracellular matrix of human breast carcinomas: comparison between invasive and non-invasive areas. *International journal of cancer. Journal international du cancer*, 52:1–6, August 1992. ISSN 0020-7136.

J Ponting, Shant Kumar, and D Pye. Co-localisation of hyaluronan and hyaluronectin in normal and neoplastic breast tissues. *International Journal of Oncology*, 2:889–893, 1993.

V B Lokeshwar, D Rubinowicz, G L Schroeder, E Forgacs, J D Minna, N L Block, M Nadji, and B L Lokeshwar. Stromal and epithelial expression of tumor markers hyaluronic acid and hyal1 hyaluronidase in prostate cancer. *The Journal of biological chemistry*, 276:11922–32, April 2001. ISSN 0021-9258.

Alaa M Afify, Sarah Craig, Augusto F G Paulino, and Robert Stern. Expression of hyaluronic acid and its receptors, cd44s and cd44v6, in normal, hyperplastic, and neoplastic endometrium. *Annals of diagnostic pathology*, 9: 312–8, December 2005. ISSN 1092-9134.

S Aaltomaa, P Lipponen, R Tammi, M Tammi, J Viitanen, J-P Kankkunen, and V-M Kosma. Strong stromal hyaluronan expression is associated with psa recurrence in local prostate cancer. *Urologia internationalis*, 69:266–72, January 2002. ISSN 0042-1138.

Sinan Ekici, Wolfgang H Cerwinka, Robert Duncan, Pablo Gomez, Francisco Civantos, Mark S Soloway, and Vinata B Lokeshwar. Comparison of the prognostic potential of hyaluronic acid, hyaluronidase (hyal-1), cd44v6 and microvessel density for prostate cancer. *International journal of cancer. Journal international du cancer*, 112:121–9, October 2004. ISSN 0020-7136.

J Timothy Posey, Mark S Soloway, Sinan Ekici, Mario Sofer, Francisco Civantos, Robert C Duncan, and Vinata B Lokeshwar. Evaluation of the prognostic potential of hyaluronic acid and hyaluronidase (hyal1) for prostate cancer. *Cancer research*, 63:2638–44, May 2003. ISSN 0008-5472.

Essi L J Hiltunen, Maarit Anttila, Anne Kultti, Kirsi Ropponen, Jorma Penttinen, Merja Yliskoski, Arja T Kuronen, Matti Juhola, Raija Tammi, Markku Tammi, and Veli-Matti Kosma. Elevated hyaluronan concentration without hyaluronidase activation in malignant epithelial ovarian tumors. *Cancer research*, 62:6410–3, November 2002. ISSN 0008-5472.

Mario Wernicke, Laura Cecilia Piñeiro, Daniela Caramutti, Vanesa G Dorn, Maria Marta Lopez Raffo, Hector G Guixa, Margarita Telenta, and Ana Alcestes Morandi. Breast cancer stromal myxoid changes are associated with tumor invasion and metastasis: a central role for hyaluronan. *Modern pathology : an official journal of the United States and Canadian Academy of Pathology, Inc*, 16:99–107, February 2003. ISSN 0893-3952.

W J Blot and J K McLaughlin. The changing epidemiology of esophageal cancer. *Seminars in oncology*, 26:2–8, October 1999. ISSN 0093-7754.

D M Parkin, P Pisani, and J Ferlay. Estimates of the worldwide incidence of 25 major cancers in 1990. *International journal of cancer. Journal international du cancer*, 80:827–41, March 1999. ISSN 0020-7136.

R M Gore. Esophageal cancer. clinical and pathologic features. *Radiologic clinics of North America*, 35:243–63, March 1997. ISSN 0033-8389.

U Ribeiro, M C Posner, A V Safatle-Ribeiro, and J C Reynolds. Risk factors for squamous cell carcinoma of the oesophagus. *The British journal of surgery*, 83:1174–85, September 1996. ISSN 0007-1323.

WJ Blot. Epidemiology and genesis of esophageal cancer. *Thoracic oncology. Philadelphia: WB Saunders*, 12:1, 1995.

Christophe Mariette, Laetitia Finzi, Guillaume Piessen, Isabelle Van Seuningen, and Jean Pierre Triboulet. Esophageal carcinoma: prognostic differences between squamous cell carcinoma and adenocarcinoma. *World journal of surgery*, 29:39–45, January 2005. ISSN 0364-2313.

J Rüdiger Siewert and Katja Ott. Are squamous and adenocarcinomas of the esophagus the same disease? *Seminars in radiation oncology*, 17:38–44, January 2007. ISSN 1053-4296.

Rebecca S Holmes and Thomas L Vaughan. Epidemiology and pathogenesis of esophageal cancer. *Seminars in radiation oncology*, 17:2–9, January 2007. ISSN 1053-4296.

H R Wabinga, D M Parkin, F Wabwire-Mangen, and S Nambooze. Trends in cancer incidence in kyadondo county, uganda, 1960-1997. *British journal of cancer*, 82:1585–92, May 2000. ISSN 0007-0920.

Scott Keeney and Thomas L Bauer. Epidemiology of adenocarcinoma of the esophagogastric junction. *Surgical oncology clinics of North America*, 15: 687–96, October 2006. ISSN 1055-3207.

A Paloma Vizcaino, Victor Moreno, Rene Lambert, and D Maxwell Parkin. Time trends incidence of both major histologic types of esophageal carcinomas in selected countries, 1973-1995. *International journal of cancer. Journal international du cancer*, 99:860–8, June 2002. ISSN 0020-7136.

Manuel Pera. Trends in incidence and prevalence of specialized intestinal metaplasia, barrett's esophagus, and adenocarcinoma of the gastroesophageal junction. *World journal of surgery*, 27:999–1008; discussion 1006–8, September 2003. ISSN 0364-2313.

Manuel Pera, Carlos Manterola, Oscar Vidal, and Luis Grande. Epidemiology of esophageal adenocarcinoma. *Journal of surgical oncology*, 92:151–9, December 2005. ISSN 0022-4790.

A Newnham, M J Quinn, P Babb, J Y Kang, and A Majeed. Trends in the subsite and morphology of oesophageal and gastric cancer in england and wales 1971-1998. *Alimentary pharmacology & therapeutics*, 17:665–76, March 2003a. ISSN 0269-2813.

Heiko Pohl and H Gilbert Welch. The role of overdiagnosis and reclassification in the marked increase of esophageal adenocarcinoma incidence. *Journal of the National Cancer Institute*, 97:142–6, January 2005. ISSN 1460-2105.

Nicholas J Shaheen. Advances in barrett's esophagus and esophageal adenocarcinoma. *Gastroenterology*, 128:1554–66, May 2005. ISSN 0016-5085.

J Lagergren. Adenocarcinoma of oesophagus: what exactly is the size of the problem and who is at risk? *Gut*, 54 Suppl 1:i1–5, March 2005. ISSN 0017-5749.

Ai Kubo and Douglas A Corley. Marked regional variation in adenocarcinomas of the esophagus and the gastric cardia in the united states. *Cancer*, 95: 2096–102, November 2002. ISSN 0008-543X.

Ai Kubo and Douglas A Corley. Marked multi-ethnic variation of esophageal and gastric cardia carcinomas within the united states. *The American journal of gastroenterology*, 99:582–8, April 2004. ISSN 0002-9270.

E Bollschweiler, E Wolfgarten, C Gutschow, and A H Hölscher. Demographic variations in the rising incidence of esophageal adenocarcinoma in white males. *Cancer*, 92:549–55, August 2001. ISSN 0008-543X.

R V Lord, M G Law, R L Ward, G G Giles, R J Thomas, and V Thursfield. Rising incidence of oesophageal adenocarcinoma in men in australia. *Journal of gastroenterology and hepatology*, 13:356–62, April 1998. ISSN 0815-9319.

A Newnham, M J Quinn, P Babb, J Y Kang, and A Majeed. Trends in oesophageal and gastric cancer incidence, mortality and survival in england and wales 1971-1998/1999. *Alimentary pharmacology & therapeutics*, 17: 655–64, March 2003b. ISSN 0269-2813.

S S Devesa, W J Blot, and J F Fraumeni. Changing patterns in the incidence of

esophageal and gastric carcinoma in the united states. *Cancer*, 83:2049–53, November 1998. ISSN 0008-543X.

Thames Cancer Registry. *Cancer in South East England 1997*. Thames Cancer Registry, London, 2000.

A A Botterweck, L J Schouten, A Volovics, E Dorant, and P A Van Den Brandt. Trends in incidence of adenocarcinoma of the oesophagus and gastric cardia in ten european countries. *International journal of epidemiology*, 29: 645–54, August 2000. ISSN 0300-5771.

Mohammad Farhadi, Zahra Tahmasebi, Shahin Merat, Farin Kamangar, Dariush Nasrollahzadeh, and Reza Malekzadeh. Human papillomavirus in squamous cell carcinoma of esophagus in a high-risk population. *World journal of gastroenterology : WJG*, 11:1200–3, February 2005. ISSN 1007-9327.

Shahram Bahmanyar and Weimin Ye. Dietary patterns and risk of squamous-cell carcinoma and adenocarcinoma of the esophagus and adenocarcinoma of the gastric cardia: a population-based case-control study in sweden. *Nutrition and cancer*, 54:171–8, January 2006. ISSN 0163-5581.

Heiner Boeing, Thomas Dietrich, Kurt Hoffmann, Tobias Pischon, Pietro Ferrari, Petra H Lahmann, Marie Christine Boutron-Ruault, Francoise Clavel-Chapelon, Naomi Allen, Tim Key, Guri Skeie, Eiliv Lund, Anja Olsen, Anne Tjonneland, Kim Overvad, Majken K Jensen, Sabine Rohrmann, Jakob Linseisen, Antonia Trichopoulou, Christina Bamia, Theodora Psaltopoulou, Lars Weinehall, Ingegerd Johansson, Maria-José Sánchez, Paula Jakszyn, Eva Ardanaz, Pilar Amiano, Maria Dolores Chirlaque, J Ramón Quirós, Elisabet Wirfalt, Göran Berglund, Petra H Peeters, Carla H Van Gils, H Bas Bueno-de Mesquita, Frederike L Büchner, Franco Berrino, Domenico Palli, Carlotta Sacerdote, Rosario Tumino, Salvatore Panico, Sheila Bingham,

Kay-Tee Khaw, Nadia Slimani, Teresa Norat, Mazda Jenab, and Elio Riboli. Intake of fruits and vegetables and risk of cancer of the upper aerodigestive tract: the prospective epic-study. *Cancer causes & control : CCC*, 17:957–69, September 2006. ISSN 0957-5243.

S R DeMeester and T R DeMeester. Columnar mucosa and intestinal metaplasia of the esophagus: fifty years of controversy. *Annals of surgery*, 231: 303–21, March 2000. ISSN 0003-4932.

Steven R DeMeester. Adenocarcinoma of the esophagus and cardia: a review of the disease and its treatment. *Annals of surgical oncology*, 13:12–30, January 2006. ISSN 1068-9265.

J Lagergren, R Bergström, H O Adami, and O Nyrén. Association between medications that relax the lower esophageal sphincter and risk for esophageal adenocarcinoma. *Annals of internal medicine*, 133:165–75, August 2000. ISSN 0003-4819.

Jesper Lagergren and Catarina Jansson. Use of tight belts and risk of esophageal adenocarcinoma. *International journal of cancer. Journal international du cancer*, 119:2464–6, November 2006. ISSN 0020-7136.

J Lagergren, R Bergström, and O Nyrén. Association between body mass and adenocarcinoma of the esophagus and gastric cardia. *Annals of internal medicine*, 130:883–90, June 1999a. ISSN 0003-4819.

M Solaymani-Dodaran, R F A Logan, J West, T Card, and C Coupland. Risk of oesophageal cancer in barrett's oesophagus and gastro-oesophageal reflux. *Gut*, 53:1070–4, August 2004. ISSN 0017-5749.

J Lagergren, R Bergström, A Lindgren, and O Nyrén. Symptomatic gastroesophageal reflux as a risk factor for esophageal adenocarcinoma. *The New England journal of medicine*, 340:825–31, March 1999b. ISSN 0028-4793.

Sjoerd M Lagarde, Fiebo J W Ten Kate, Johannes B Reitsma, Olivier R C Busch, and J Jan B Van Lanschot. Prognostic factors in adenocarcinoma of the esophagus or gastroesophageal junction. *Journal of clinical oncology : official journal of the American Society of Clinical Oncology*, 24:4347–55, September 2006. ISSN 1527-7755.

A Alexandrou, P A Davis, S Law, S Murthy, B P Whooley, and J Wong. Squamous cell carcinoma and adenocarcinoma of the lower third of the esophagus and gastric cardia: similarities and differences. *Diseases of the esophagus : official journal of the International Society for Diseases of the Esophagus / I.S.D.E*, 15:290–5, January 2002. ISSN 1120-8694.

H Abunasra, S Lewis, L Beggs, J Duffy, D Beggs, and E Morgan. Predictors of operative death after oesophagectomy for carcinoma. *The British journal of surgery*, 92:1029–33, August 2005. ISSN 0007-1323.

Guang Dai, Till Freudenberger, Petra Zipper, Ariane Melchior, Susanne Grether-Beck, Berit Rabausch, Jens de Groot, Soren Twarock, Helmut Hanenberg, Bernhard Homey, Jean Krutmann, Julia Reifenberger, and Jens W Fischer. Chronic ultraviolet b irradiation causes loss of hyaluronic acid from mouse dermis because of down-regulation of hyaluronic acid synthases. *Am J Pathol*, 171(5):1451–1461, 2007. ISSN 0002-9440 (Print). doi: 10.2353/ajpath.2007.070136.

Thomas S Wilkinson, Steven L Bressler, Stephen P Evanko, Kathleen R Braun, and Thomas N Wight. Overexpression of hyaluronan synthases alters vascular smooth muscle cell phenotype and promotes monocyte adhesion. *J Cell Physiol*, 206(2):378–385, 2006. ISSN 0021-9541 (Print). doi: 10.1002/jcp.20468.

Zhetcho Kyossev and Paul H Weigel. An enzyme capture assay for analysis

of active hyaluronan synthases. *Anal Biochem*, 371(1):62–70, 2007. ISSN 0003-2697 (Print). doi: 10.1016/j.ab.2007.08.025.

K Furukawa and H Terayama. Isolation and identification of glycosaminoglycans associated with purified nuclei from rat liver. *Biochim Biophys Acta*, 499(2): 278–289, 1977. ISSN 0006-3002 (Print).

K Furukawa and H Terayama. Pattern of glycosaminoglycans and glycoproteins associated with nuclei of regenerating liver of rat. *Biochim Biophys Acta*, 585(4):575–588, 1979. ISSN 0006-3002 (Print).

J A Ripellino, R U Margolis, and R K Margolis. Immunoelectron microscopic localization of hyaluronic acid-binding region and link protein epitopes in brain. *J Cell Biol*, 108(5):1899–1907, 1989. ISSN 0021-9525 (Print).

Vincent C Hascall, Alana K Majors, Carol a De La Motte, Stephen P Evanko, Aimin Wang, Judith a Drazba, Scott a Strong, and Thomas N Wight. Intracellular hyaluronan: a new frontier for inflammation? *Biochimica et biophysica acta*, 1673:3–12, July 2004. ISSN 0006-3002.

Stephen P Evanko, W Tony Parks, and Thomas N Wight. Intracellular hyaluronan in arterial smooth muscle cells: association with microtubules, rhamm, and the mitotic spindle. *J Histochem Cytochem*, 52(12):1525–1535, 2004. ISSN 0022-1554 (Print). doi: 10.1369/jhc.4A6356.2004.

T B Deb and K Datta. Molecular cloning of human fibroblast hyaluronic acid-binding protein confirms its identity with p-32, a protein co-purified with splicing factor sf2. hyaluronic acid-binding protein as p-32 protein, co-purified with splicing factor sf2. *J Biol Chem*, 271(4):2206–2212, 1996. ISSN 0021-9258 (Print).

S Zhang, M C Chang, D Zylka, S Turley, R Harrison, and E A Turley. The hyaluronan receptor rhamm regulates extracellular-regulated kinase. *J Biol Chem*, 273(18):11342–11348, 1998. ISSN 0021-9258 (Print).

Robert D Finn, John Tate, Jaina Mistry, Penny C Coggill, Stephen John Sammut, Hans-Rudolf Hotz, Goran Ceric, Kristoffer Forslund, Sean R Eddy, Erik L L Sonnhammer, and Alex Bateman. The pfam protein families database. *Nucleic Acids Res*, 36(Database issue):D281–8, 2008. ISSN 1362-4962 (Electronic). doi: 10.1093/nar/gkm960.

Paul H Weigel and Paul L DeAngelis. Hyaluronan synthases: a decade-plus of novel glycosyltransferases. *J Biol Chem*, 282(51):36777–36781, 2007. ISSN 0021-9258 (Print). doi: 10.1074/jbc.R700036200.

Johannes Soding. Protein homology detection by hmm-hmm comparison. *Bioinformatics*, 21(7):951–960, 2005. ISSN 1367-4803 (Print). doi: 10.1093/bioinformatics/bti125.

Johannes Soding, Andreas Biegert, and Andrei N Lupas. The hhpred interactive server for protein homology detection and structure prediction. *Nucleic Acids Res*, 33(Web Server issue):W244–8, 2005. ISSN 1362-4962 (Electronic). doi: 10.1093/nar/gki408.

J Schultz, F Milpetz, P Bork, and C P Ponting. Smart, a simple modular architecture research tool: identification of signaling domains. *Proc Natl Acad Sci U S A*, 95(11):5857–5864, 1998. ISSN 0027-8424 (Print).

C P Ponting, J Schultz, F Milpetz, and P Bork. Smart: identification and annotation of domains from signalling and extracellular protein sequences. *Nucleic Acids Res*, 27(1):229–232, 1999. ISSN 0305-1048 (Print).

Ivica Letunic, Tobias Doerks, and Peer Bork. Smart 6: recent updates and new developments. *Nucleic Acids Res*, 37(Database issue):D229–32, 2009. ISSN 1362-4962 (Electronic). doi: 10.1093/nar/gkn808.

Maria D Corte, L O Gonzalez, M Luz Lamelas, Ana Alvarez, Sara Junquera, M Teresa Allende, Jose L Garcia-Muniz, Juan Arguelles, and Francisco J

Vizoso. Expression and clinical signification of cytosolic hyaluronan levels in invasive breast cancer. *Breast Cancer Res Treat*, 97(3):329–337, 2006. ISSN 0167-6806 (Print). doi: 10.1007/s10549-005-9130-7.

F J Vizoso, J M del Casar, M D Corte, I Garcia, M G Corte, A Alvarez, and J L Garcia-Muniz. Significance of cytosolic hyaluronan levels in gastric cancer. *Eur J Surg Oncol*, 30(3):318–324, 2004. ISSN 0748-7983 (Print). doi: 10.1016/j.ejso.2003.11.007.

A Ruibal, M I Nunez, J Rodriguez, L Jimenez, M C del Rio, and J Zapatero. Cytosolic levels of neuron-specific enolase in squamous cell carcinomas of the lung. *Int J Biol Markers*, 18(3):188–194, 2003. ISSN 0393-6155 (Print).

Walter Nickel. Unconventional secretory routes: direct protein export across the plasma membrane of mammalian cells. *Traffic*, 6(8):607–614, 2005. ISSN 1398-9219 (Print). doi: 10.1111/j.1600-0854.2005.00302.x.

Igor Prudovsky, Francesca Tarantini, Matteo Landriscina, David Neivandt, Raffaella Soldi, Aleksandr Kirov, Deena Small, Karuppanan Muthusamy Kathir, Dakshinamurthy Rajalingam, and Thallapuranam Krishnaswamy Suresh Kumar. Secretion without golgi. *J Cell Biochem*, 103(5):1327–1343, 2008 Apr 1. ISSN 1097-4644 (Electronic). doi: 10.1002/jcb.21513.

Derek C Radisky, Yohei Hirai, and Mina J Bissell. Delivering the message: epimorphin and mammary epithelial morphogenesis. *Trends Cell Biol*, 13 (8):426–434, 2003. ISSN 0962-8924 (Print).

David L Daleke. Regulation of transbilayer plasma membrane phospholipid asymmetry. *J Lipid Res*, 44(2):233–242, 2003. ISSN 0022-2275 (Print). doi: 10.1194/jlr.R200019-JLR200.

Jenny Paupert, Stephanie Dauvillier, Bernard Salles, and Catherine Muller. Transport of the leaderless protein ku on the cell surface of activated mono-

cytes regulates their migratory abilities. *EMBO Rep*, 8(6):583–588, 2007. ISSN 1469-221X (Print). doi: 10.1038/sj.embor.7400976.

J Huot, F Houle, S Rousseau, R G Deschesnes, G M Shah, and J Landry. Sapk2/p38-dependent f-actin reorganization regulates early membrane blebbing during stress-induced apoptosis. *J Cell Biol*, 143(5):1361–1373, 1998. ISSN 0021-9525 (Print).

Christopher Alan Maxwell, James McCarthy, and Eva Turley. Cell-surface and mitotic-spindle rhamm: moonlighting or dual oncogenic functions? *J Cell Sci*, 121(Pt 7):925–932, 2008. ISSN 0021-9533 (Print). doi: 10.1242/jcs.022038.

Yetrib Hathout. Approaches to the study of the cell secretome. *Expert Rev Proteomics*, 4(2):239–248, 2007. ISSN 1744-8387 (Electronic). doi: 10.1586/14789450.4.2.239.

Jeremy C Simpson, Alvaro Mateos, and Rainer Pepperkok. Maturation of the mammalian secretome. *Genome Biol*, 8(4):211, 2007. ISSN 1465-6914 (Electronic). doi: 10.1186/gb-2007-8-4-211.

Stephen Chivasa, John M Hamilton, Richard S Pringle, Bongani K Ndimba, William J Simon, Keith Lindsey, and Antoni R Slabas. Proteomic analysis of differentially expressed proteins in fungal elicitor-treated arabidopsis cell cultures. *J Exp Bot*, 57(7):1553–1562, 2006. ISSN 0022-0957 (Print). doi: 10.1093/jxb/erj149.

Stephen Chivasa, William J Simon, Xiao-Lan Yu, Nasser Yalpani, and Antoni R Slabas. Pathogen elicitor-induced changes in the maize extracellular matrix proteome. *Proteomics*, 5(18):4894–4904, 2005. ISSN 1615-9853 (Print). doi: 10.1002/pmic.200500047.

Harold Tjalsma, Wendy Pluk, Lambert P van den Heuvel, Wilbert H M Peters, Rian Roelofs, and Dorine W Swinkels. Proteomic inventory of "anchorless" proteins on the colon adenocarcinoma cell surface. *Biochim Biophys Acta*, 1764(10):1607–1617, 2006. ISSN 0006-3002 (Print). doi: 10.1016/j.bbapap.2006.09.002.

Mei Sun, Lanfeng Ma, Linda Xu, Jia Li, Wei Zhang, Gyorgy Petrovics, Mazen Makarem, Isabell Sesterhenn, Mei Zhang, E Joan Blanchette-Mackie, Judd Moul, Shiv Srivastava, and Zhiqiang Zou. A human novel gene derpc on 16q22.1 inhibits prostate tumor cell growth and its expression is decreased in prostate and renal tumors. *Mol Med*, 8(10):655–663, 2002. ISSN 1076-1551 (Print).

Andrew R Green, Sophie Krivinskas, Peter Young, Emad A Rakha, E Claire Paish, Desmond G Powe, and Ian O Ellis. Loss of expression of chromosome 16q genes dpep1 and ctcf in lobular carcinoma in situ of the breast. *Breast Cancer Res Treat*, 113(1):59–66, 2009. ISSN 1573-7217 (Electronic). doi: 10.1007/s10549-008-9905-8.

Andreas Werner, Mark Carlile, and Daniel Swan. What do natural antisense transcripts regulate? *RNA Biol*, 6(1):43–48, 2009. ISSN 1555-8584 (Electronic).

Elizabeth S Henson and Spencer B Gibson. Surviving cell death through epidermal growth factor (egf) signal transduction pathways: implications for cancer therapy. *Cell Signal*, 18(12):2089–2097, 2006. ISSN 0898-6568 (Print). doi: 10.1016/j.cellsig.2006.05.015.

Hongtao Zhang, Alan Berezov, Qiang Wang, Geng Zhang, Jeffrey Drebin, Ramachandran Murali, and Mark I Greene. Erbb receptors: from oncogenes to targeted cancer therapies. *J Clin Invest*, 117(8):2051–2058, 2007. ISSN 0021-9738 (Print). doi: 10.1172/JCI32278.

Y Yarden. The egfr family and its ligands in human cancer. signalling mechanisms and therapeutic opportunities. *Eur J Cancer*, 37 Suppl 4:S3–8, 2001. ISSN 0959-8049 (Print).

Robert N Jorissen, Francesca Walker, Normand Pouliot, Thomas P J Garrett, Colin W Ward, and Antony W Burgess. Epidermal growth factor receptor: mechanisms of activation and signalling. *Exp Cell Res*, 284(1):31–53, 2003. ISSN 0014-4827 (Print).

T Kisseleva, S Bhattacharya, J Braunstein, and C W Schindler. Signaling through the jak/stat pathway, recent advances and future challenges. *Gene*, 285(1-2):1–24, 2002. ISSN 0378-1119 (Print).

Eric Van Cutsem, Claus-Henning Kohne, Erika Hitre, Jerzy Zaluski, Chung-Rong Chang Chien, Anatoly Makhson, Geert D'Haens, Tamas Pinter, Robert Lim, Gyorgy Bodoky, Jae Kyung Roh, Gunnar Folprecht, Paul Ruff, Christopher Stroh, Sabine Tejpar, Michael Schlichting, Johannes Nippgen, and Philippe Rougier. Cetuximab and chemotherapy as initial treatment for metastatic colorectal cancer. *N Engl J Med*, 360(14):1408–1417, 2009. ISSN 1533-4406 (Electronic). doi: 10.1056/NEJMoa0805019.

Ann Marie Egloff and Jennifer Rubin Grandis. Improving response rates to egfr-targeted therapies for head and neck squamous cell carcinoma: Candidate predictive biomarkers and combination treatment with src inhibitors. *J Oncol*, 2009:896407, 2009. ISSN 1687-8450 (Print). doi: 10.1155/2009/896407.

Appendix A

Publications

Chronic ultraviolet B irradiation causes loss of hyaluronic acid from mouse dermis because of down-regulation of hyaluronic acid synthases.

Dai G, Freudenberger T, Zipper P, Melchior A, Grether-Beck S, Rabausch B, de Groot J, Twarock S, Hanenberg H, Homey B, Krutmann J, Reifenberger J, Fischer JW.

Am J Pathol. 2007 Nov;171(5):1451-61.

Appendix B

Ackowledgement

First of all, I want to thank Prof. Jens W. Fischer for giving me the opportunity to work on this highly interesting research topic in his lab and also providing me extraordinary supports throughout the whole project. His organization and encouragement for our group is truly the basis of this work.

I would like to extend my gratitude to our colarborition partners: Dr. Christian Mielke and Prof. Boege for the pMC vector and instructions for stably expression cell line construction; Dr. Stöcklein for patients' biopsies and PT1590 cells; Prof. Hanenberg for lentiviral expression system; Prof. Reifenberger for skin fibroblasts; Prof. Ehrmann, Dr. Sonja Hasenbein and Dr. Michael Meltzer for the help of *in silico* analysis.

Furthermore, I would like to thank all my great colleagues from our group. It was so lucky for me to work with you guys.

Especially, I would like to thank Kirsten for all the experimental supports. It is such a nice experience to work with you!

For Annika and Annette, thanks a lot for the help in immunohistochemistry.

I thank Ariane for her instruction on many techniques and the kind help regarding to the HAS enzymatic capture assay.

To Till, a continual source of support and friendship, I owe a great deal.

Also, I would like to thank Ms. Sieberg and Ms. Görtz for the institute organization.

I express my enduring love and thanks to my parents who have always been there to encourage and support me.

Finally, I would like to thank my wife, Guwa Gegen, for her continual encouragement and support. You have been there through it all.

Appendix C

Abbreviations

bHAbp	BIOTINLYATED HA BINDING PROTEIN
Da	DALTON
ECM	EXTRACELLULAR MATRIX
ERK	EXTRACELLULAR-SIGNAL REGULATED KINASE
EGF	EPIDERMAL GROWTH FACTOR
EGFR	EPIDERMAL GROWTH FACTOR RECEPTOR
FACS	FLUORESCENCE ACTIVATED CELL SORTER
FAK	FOCAL ADHESION KINASE
FGF	FIBROBLAST GROWTH FACTOR
GAG	GLYCOSAMINOGLYCAN
GlcA	GLUCURONIC ACID
GlcNAc	N-ACETYLGLUCOSAMINE
HA	HYALURONAN
HAbp	HA BINDING PROTEIN
HAS	HYALURONAN SYNTHASE
HYAL	HYALURONIDASE
IαI	INTER-ALPHA-INHIBITOR
IHABP	INTRACELLULAR HA BINDING PROTEIN
IL-1β	INTERLEUKIN-1 BETA
KB	KILLOBASE
MAP	MITOGEN ACTIVATED PROTEIN
MAPK	MITOGEN ACTIVATED PROTEIN KINASE
MEK	MITOGEN ACTIVATED EXTRACELLULAR RESPONSE KINASE
MEKK-1	MAPK/ERK KINASE KINASE
MMP	MATRIX METALLOPROTEINASE
NFκB	NUCLEAR FACTOR KAPPA-B
PDGF	PLATELET DERIVED GROWTH FACTOR
PI3K	PHOSPHOINOSITIDE 3-KINASE
PKC	PROTEIN KINASE C
RHAMM	RECEPTOR FOR HYALURONIC ACID MEDIATED MOTILITY
TLR	TOLL-LIKE RECEPTOR

Appendix D

Curriculum Vitae

Personal Information

Name:	Guang Dai
Date of Birth:	July 25^{th}, 1978
Place of Birth:	Shenyang, Liaoning Province
Nationality:	China
Family status:	married (Guwa Gegen) since August 2005
Address:	Overbeckstr. 16, 45147, Essen

Education

2006.01 - now	Dusseldorf University / Duisburg Essen University *Ph.D Thesis*
2002.10 - 2004.10	Dresden University of Technology *Master's Degree in Molecular Bioengineering*
1996 - 2000	Liaoning University in China *Bachelor's Degree in Biotechnology*

Essen, October 10, 2009

(*Guang Dai*)

Appendix E

Erklärung

Erklärung:

Hiermit erkläre ich, gem. §6 Abs. 2, Nr. 8 der Promotionsordnung der Math.-Nat.- Fachbereiche zur Erlangung der Dr. rer. nat., dass ich das Arbeitgebiet, dem das Thema "Functional analysis of human hyaluronan synthase 3 splicing variant 2" zuzuordnen ist, in Forschung und Lehre vertrete und den Antrag von Herrn Guang Dai befürworte.

Essen, den 12.10.2009 _____

(Prof. Jens W. Fischer)

Erklärung:

Hiermit erkläre ich, gem. §6 Abs. 2, Nr. 6 der Promotionsordnung der Math.-Nat.- Fachbereiche zur Erlangung des Dr. rer. nat., dass ich die vorliegende Dissertation selbständig verfasst und mich keiner anderen als der angegebenen Hilfsmittel bedient habe.

Essen, den 12.10.2009 _____

(Guang Dai)

Erklärung:

Hiermit erkläre ich, gem. §6 Abs. 2, Nr. 7 der Promotionsordnung der Math.-Nat.- Fachbereiche zur Erlangung des Dr. rer. nat., dass ich keine anderen Promotionen bzw. Promotionsversuche in der Vergangenheit durchgeführt habe und dass diese Arbeit von keiner anderen Fakultät abgelehnt worden ist.

Essen, den 12.10.2009 _____

(Guang Dai)